2004-06

The numerical weather prediction system at the Italian Air Force Weather Service impact of non-conventional observations and increased resolution

Torrisi, Lucio.

Monterey California. Naval Postgraduate School

NAVAL POSTGRADUATE SCHOOL

MONTEREY, CALIFORNIA

THESIS

THE NUMERICAL WEATHER PREDICTION SYSTEM AT THE ITALIAN AIR FORCE WEATHER SERVICE: IMPACT OF NON-CONVENTIONAL OBSERVATIONS AND INCREASED RESOLUTION

by

Lucio Torrisi

June 2004

Thesis Advisor: Roger T. Williams
Second Reader: Carlyle H. Wash

Approved for Public Release; Distribution is Unlimited

THIS PAGE INTENTIONALLY LEFT BLANK

REPORT DOCUMENTATION PAGE			Form Approved OMB No. 0704-0188
Public reporting burden for this collection of information is estimated to average 1 hour per response, including the time for reviewing instruction, searching existing data sources, gathering and maintaining the data needed, and completing and reviewing the collection of information. Send comments regarding this burden estimate or any other aspect of this collection of information, including suggestions for reducing this burden, to Washington headquarters Services, Directorate for Information Operations and Reports, 1215 Jefferson Davis Highway, Suite 1204, Arlington, VA 22202-4302, and to the Office of Management and Budget, Paperwork Reduction Project (0704-0188) Washington DC 20503.			
1. AGENCY USE ONLY *(Leave blank)*	**2. REPORT DATE** June 2004	**3. REPORT TYPE AND DATES COVERED** Master's Thesis	
4. TITLE AND SUBTITLE The Numerical Weather Prediction System at the Italian Air Force Weather Service: Impact of Non-Conventional Observations and Increased Resolution			**5. FUNDING NUMBERS**
6. AUTHOR(S) Lucio Torrisi			
7. PERFORMING ORGANIZATION NAME(S) AND ADDRESS(ES) Naval Postgraduate School Monterey, CA 93943-5000			**8. PERFORMING ORGANIZATION REPORT NUMBER**
9. SPONSORING /MONITORING AGENCY NAME(S) AND ADDRESS(ES) N/A			**10. SPONSORING/MONITORING AGENCY REPORT NUMBER**
11. SUPPLEMENTARY NOTES The views expressed in this thesis are those of the author and do not reflect the official policy or position of the Department of Defense or the U.S. Government.			
12a. DISTRIBUTION / AVAILABILITY STATEMENT Approved for public release; distribution is unlimited			**12b. DISTRIBUTION CODE**

13. ABSTRACT ***(maximum 200 words)***

The impact of non-conventional observations and increased horizontal resolution on the numerical weather prediction (NWP) system of the National Center for Aeronautic Meteorology and Climatology of the Italian Air Force (CNMCA) has been investigated. The present study is part of ongoing research activities whose goal is the improvement of CNMCA's operational numerical weather prediction capabilities through the assimilation of non-conventional observations. Additional data derived from satellite observations, such as 10 m wind retrieved from Quikscat polar-orbit satellite, atmospheric motion vectors (AMVs) from Meteosat geostationary satellites and manual and automated aircraft observations were used. The NWP system, which is in operational use, is based on an "observation space" version of the 3D-Var method for the objective analysis component (3D-PSAS), while the prognostic component is based on the High Resolution Regional Model (HRM) of the German Meteorological Service (DWD). The analysis and forecast fields derived from the NWP system were objectively evaluated through comparisons with radiosonde and conventional surface observations. Comparisons with parallel runs of the HRM model starting from the 3D-Var operational analysis have showed that each of those observations have a measurable positive impact on forecast skill.

14. SUBJECT TERMS Meteorology, Objective Analysis, Data Assimilation, Meteorological Observation, Observing System Experiment, Impact Study			**15. NUMBER OF PAGES** 115
			16. PRICE CODE
17. SECURITY CLASSIFICATION OF REPORT Unclassified	**18. SECURITY CLASSIFICATION OF THIS PAGE** Unclassified	**19. SECURITY CLASSIFICATION OF ABSTRACT** Unclassified	**20. LIMITATION OF ABSTRACT** UL

NSN 7540-01-280-5500 Standard Form 298 (Rev. 2-89)
Prescribed by ANSI Std. 239-18

THIS PAGE INTENTIONALLY LEFT BLANK

Approved for public release; distribution is unlimited

THE NUMERICAL WEATHER PREDICTION SYSTEM AT THE ITALIAN AIR FORCE WEATHER SERVICE: IMPACT OF NON-CONVENTIONAL OBSERVATIONS AND INCREASED RESOLUTION

Lucio Torrisi
Captain, Italian Air Force
M.S., University of Catania, 1992

Submitted in partial fulfillment of the
requirements for the degree of

MASTER OF SCIENCE IN METEOROLOGY

from the

NAVAL POSTGRADUATE SCHOOL
June 2004

Author: Lucio Torrisi

Approved by:

Thesis Advisor
Roger T. Williams

Second Reader
Carlyle H. Wash

Carlyle H. Wash
Chairman, Department of Meteorology

THIS PAGE INTENTIONALLY LEFT BLANK

ABSTRACT

The impact of non-conventional observations and increased horizontal resolution on the numerical weather prediction (NWP) system of the National Center for Aeronautic Meteorology and Climatology of the Italian Air Force (CNMCA) has been investigated. The present study is part of ongoing research activities whose goal is the improvement of CNMCA's operational numerical weather prediction capabilities through the assimilation of non-conventional observations. Additional data derived from satellite observations, such as 10 m wind retrieved from Quikscat polar-orbit satellite, atmospheric motion vectors (AMVs) from Meteosat geostationary satellites and manual and automated aircraft observations were used. The NWP system, which is in operational use, is based on an "observation space" version of the 3D-Var method for the objective analysis component (3D-PSAS), while the prognostic component is based on the High Resolution Regional Model (HRM) of the German Meteorological Service (DWD). The analysis and forecast fields derived from the NWP system were objectively evaluated through comparisons with radiosonde and conventional surface observations. Comparisons with parallel runs of the HRM model starting from the 3D-Var operational analysis have showed that each of those observations have a measurable positive impact on forecast skill.

THIS PAGE INTENTIONALLY LEFT BLANK

TABLE OF CONTENTS

THIS PAGE INTENTIONALLY LEFT BLANK

LIST OF FIGURES

THIS PAGE INTENTIONALLY LEFT BLANK

LIST OF TABLES

THIS PAGE INTENTIONALLY LEFT BLANK

ACKNOWLEDGMENTS

The author would like to acknowledge and express gratitude to Col. Massimo Capaldo, Prof. Carlyle Wash, Col. (ret) Gary Roser and Ms Annamaria Munno for giving him the opportunity to attend the Naval Postgraduate School and for establishing a course of studies tailored to his specific needs.

The author would like to offer his sincerest appreciation to Prof. Roger T. Williams and Prof. Carlyle Wash for their careful review of the manuscript and many helpful suggestions. It was a privilege to work with them.

The author is indebted to: Col. Massimo Capaldo and Lt. Col. Massimo Ferri for their encouragement and support of this work; Capt Massimo Bonavita for his valuable contribute to improve and test the analysis algorithms used in this thesis.

Sincere appreciation is due to my wife Giovanna and my child Luca for their love and support.

THIS PAGE INTENTIONALLY LEFT BLANK

I. INTRODUCTION

Numerical weather prediction (NWP) is an "initial/boundary condition problem," given an estimate of the present state of the atmosphere and appropriate surface and lateral boundary conditions, the model simulates the atmospheric evolution. A NWP system is based on three main components:

1. observing component;
2. diagnostic or analysis component;
3. prognostic component.

A worldwide network of in-situ and satellite-based observing systems nowadays composes the observing component. The diagnostic component of the forecasting system is responsible for producing an estimate of the "true" state of the atmosphere (initial conditions) over a regular spatial grid at a given time. The "primitive" equations governing the evolution of the atmosphere are integrated forward in time starting from the initial state, in order to produce an estimate of the state of the atmosphere at some future time (prognostic component).

The ability to make a skillful forecast requires that the initial conditions be known accurately. The determination of the initial conditions for a forecast model is a complex and important problem. Currently, operational NWP centers produce initial conditions through a statistical combination of observations and short-range forecasts. This approach is known as data assimilation, whose purpose is to use all the available observations, in order to determine as accurately as possible the initial state of all the important geophysical variables within the domain of the forecast model and at its boundaries.

In a NWP system some variables are more important than others; the variables describing the mass and the wind fields are of primary importance (wind, temperature and surface pressure), next there is the humidity field and then the variables affecting the surface fluxes. An enormous quantity of the available observations of temperature and wind are irregularly distributed in space and taken at different and "asynoptic" times. The

so-called “non-conventional observations” include data coming from aircraft and satellite systems and they are particularly helpful to describe the atmospheric flow in data sparse regions.

Observing system experiments have to be performed, in order to gauge the relative impact on a NWP system of each new source of data. Observations of easier exploitation in the context of NWP are those related to model prognostic variables by simple observations operators, such as aircraft reports, Quikscat surface winds and Meteosat winds.

The main subject of the present thesis is the impact of these non-conventional observations and increased resolution on the CNMCA forecasting system objectively evaluated through comparisons of forecast fields with radiosoundings and conventional surface observations. Also a description of the data assimilation system including the 3D-Var analysis algorithm will be given, together with a discussion of the non-conventional observations used in this study and an overview of the others relevant to NWP.

II. ATMOSPHERIC DATA ASSIMILATION

The diagnostic component or data assimilation system can be thought of as having four main subcomponents (Daley, 1991):

1. data quality control;
2. objective analysis;
3. initialization of the analyzed fields;
4. short range run of the prognostic model in order to produce an initial estimate of the atmospheric state for the successive analysis step (background fields).

A schematic representation of the 6-hour intermittent data assimilation system of CNMCA is given in Fig. 2.1 and discussed in this chapter. In such a system the observations of a variable within a certain time interval are processed to compute a correction to a background forecast. In this way the assimilation cycle produces a series of corrections (or analysis increments) for each analysis time, which keeps the sequence of background forecasts close to the observations.

A. DATA QUALITY CONTROL

The data quality control step is of fundamental importance in order to prevent erroneous data to be fed to the objective analysis step with deleterious results to the performance of the NWP system. At CNMCA the data quality control of the observations is performed in two distinct steps:

1. observation pre-processing;
2. observation screening.

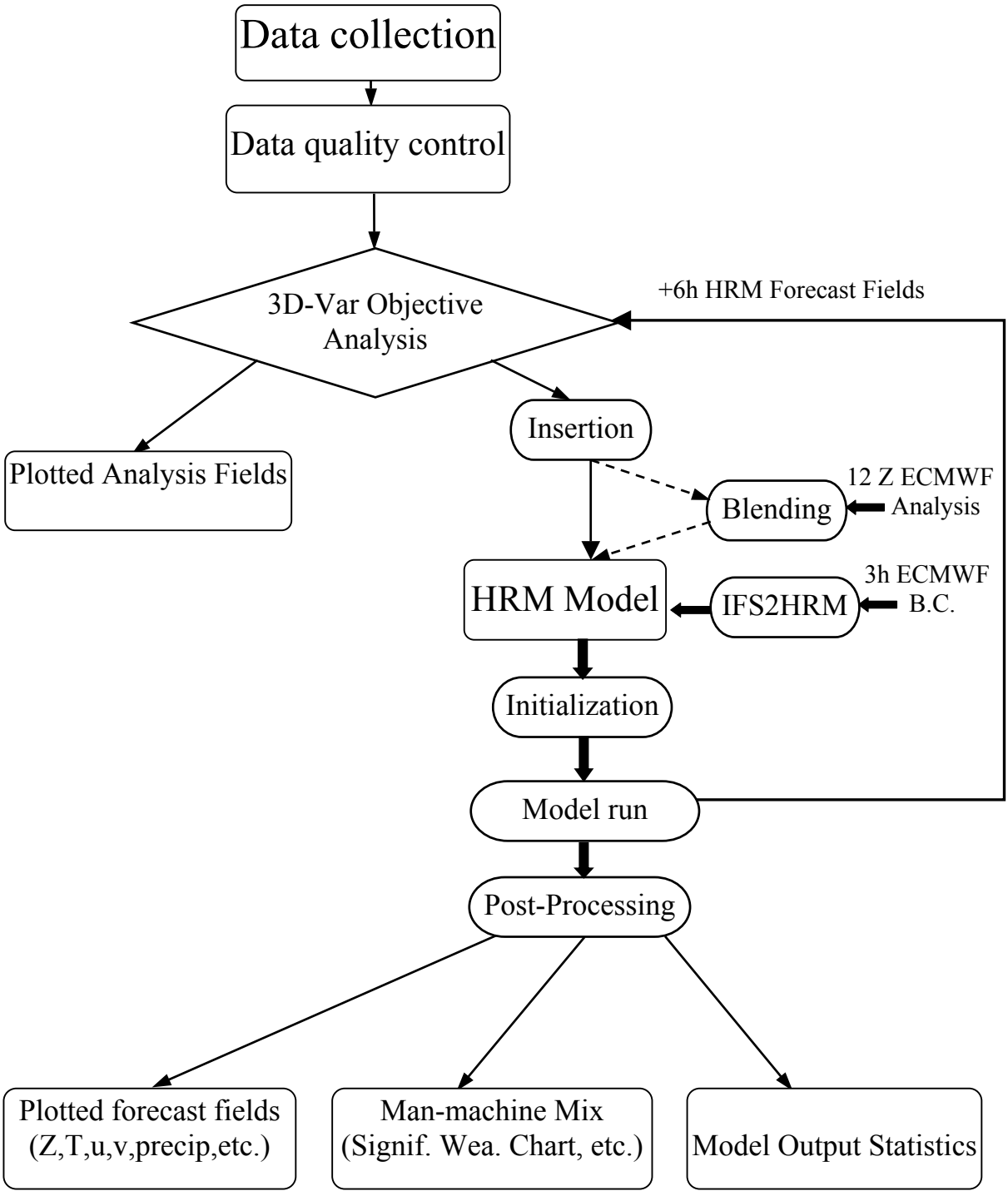

Figure 2.1 Data assimilation cycle at CNMCA.

1. Observation Pre-Processing

The observation pre-processing has the purpose of assigning a degree of confidence to each reported datum. The observations arrive at CNMCA through GTS (Global Telecommunications System) and are stored in a decoded format in the GWDB (Global Weather Data Base). Prior to the data assimilation the observations undergo some rudimentary quality control, such as:

1. observation format checks;
2. climatological and hydrostatic gross limit checks;
3. internal consistency checks (for example between reported and recomputed heights in TEMP messages);
4. temporal and spatial consistency checks for observations from moving platforms (for example SHIP messages).

More details can be found in Norris (1990). Each observation and associated confidence level are encoded in BUFR format for all available data. Then an observation file suitable for assimilation (ASCII format) is created. This entails format conversions, change of some observed variables, as well as assignment of observation error statistics. The resulting file contains all the observational information from the data window (currently three hours) and is an input for the observation screening module.

2. Observation Screening

The observation screening module selects the best quality and unique observations. The screening time window extends over the whole assimilation time window.

The observation screening begins with a preliminary check of the completeness of the reports. For instance, also the reporting practice for SYNOP and TEMP mass observations (surface pressure and geopotential height) is checked. Moreover, observations whose confidence level (computed by the pre-processing module) is below the 70% mark are discarded.

Next the observations are scanned through for blacklisting. An orographic rejection limit is applied in the case of the observation being too deep inside the model orography. Moreover, a monthly monitoring blacklist is applied for discarding the stations that have recently been reporting in an excessively noisy or biased manner as compared with the background fields.

The duplicated levels are removed from the reports. The removal of duplicated reports is performed by searching pairs of co-located reports of the same observation types and then checking the content of these reports. It may, for instance, happen that an aircraft report (AIREP) is duplicated having only a slightly different station identifier but the observed variables inside these reports are exactly the same ones, or partially duplicated. The pair-wise checking of duplicates results in a rejection of some or all of the content of one of the reports.

To reduce redundancy of information and prevent possible numerical problems in the subsequent solution of the analysis equations, same kind of observations (with the highest confidence level) whose relative distance is less than the average grid spacing of the numerical model grid are averaged together and combined in a "Super-Observation" (Lorenc, 1981).

A horizontal thinning is performed for all observation types before the assimilation to avoid potential imbalances between data types with different densities (Jarvinen and Unden, 1997). The horizontal thinning of observations means that a predefined minimum horizontal distance between the nearby observations is enforced. In practice the horizontal thinning is performed mostly for aircraft and satellite winds, since they may be very close to each other. In the vicinity of a radiosounding station precedence is given to the TEMP observation with respect to aircraft descending/ascending profiles. In this removal of redundant reports the best quality data is retained.

Finally the decision on whether to accept for ingestion the observations that survived the previous step is taken. At the moment the decision is based solely on the normalized distance of the observations with respect to the background field (background quality control). For this procedure the model counterparts for all the observations are calculated through the observation operators. The screening time window extends over

the whole assimilation time window. Currently closeness to the middle of the data window is preferred as the background is not interpolated to the exact time of the observation.

Although this method is statistically accurate, it can lead to rejection of good data in cases of rapidly evolving and poorly forecasted weather situations. Work is under progress on a buddy-check type of algorithm for gauging the accuracy of marginal observations.

B. VARIATIONAL OBJECTIVE ANALYSIS

The variational analysis consists of combining the background fields with the observations, assuming that both sources of information contain errors and these are well characterized, to get an analysis field, which is spatially consistent and meteorologically balanced.

1. Overview of the Algorithm

A short description of the variational objective analysis algorithm of CNMCA, with a focus on operational considerations, is given here. A more complete account can be found in Bonavita and Torrisi (2004). The following notation conventions are used:

$\boldsymbol{y}$ column vector containing p observations at the analysis time;

$\boldsymbol{x_t}$ column vector of the true values of the state (prognostic) variables at the same time at the n model grid points;

$\boldsymbol{x_a}$ column vector of the analyzed fields;

$\boldsymbol{x_b}$ column vector of the background fields;

$\boldsymbol{e_b} = \boldsymbol{x_b} - \boldsymbol{x_t}$ forecast error vector;

$\boldsymbol{e_o} = \boldsymbol{y} - H(\boldsymbol{x_t})$ observation error vector;

$\boldsymbol{P_b} = < \boldsymbol{e_b}\, \boldsymbol{e_b}^T >$ forecast error covariance matrix;

$\boldsymbol{R} = < \boldsymbol{e_o}\, \boldsymbol{e_o}^T >$ observation error covariance matrix;

where H is the observation (or forward) operator, i.e. the operator that performs the transformation from the state variables on grid points to the observed variables at the observing locations. Under the usual assumptions that these error vectors, $\boldsymbol{e_b}$ and $\boldsymbol{e_o}$ have normal distribution functions with zero mean (i.e.: no bias) and are mutually uncorrelated, it can be shown (Daley, 1991, Chap.2) that the maximum likelihood estimate of the state of the atmospheric system is the one the minimizes the following cost function:

$$J(\boldsymbol{x}) = 0.5[\boldsymbol{y} - H(\boldsymbol{x})]^T \boldsymbol{R}^{-1} [\boldsymbol{y} - H(\boldsymbol{x})] + 0.5[\boldsymbol{x} - \boldsymbol{x_b}]^T \boldsymbol{P}_b^{-1} [\boldsymbol{x} - \boldsymbol{x_b}] \qquad (2.1)$$

i.e., minimize a scalar distance in L_2 of the analysis fields from both the observations and the first guess fields based on their respective perceived accuracies.

The minimum of the cost function (2.1) is found by setting $\nabla J = 0$, which yields, after some manipulation:

$$\boldsymbol{x}_a - \boldsymbol{x}_b = \boldsymbol{P}_b \boldsymbol{H}^T (\boldsymbol{H}\, \boldsymbol{P}_b\, \boldsymbol{H}^T + \boldsymbol{R})^{-1} [\boldsymbol{y} - H(\boldsymbol{x}_b)] \qquad (2.2)$$

where the Jacobian matrix $\boldsymbol{H}$ of the observation operator was introduced:

$$\boldsymbol{H} \equiv \partial(H)/\partial \boldsymbol{x}|_{x=xb} \qquad (2.3)$$

The assumption here is that the analysis fields are only first order corrections to the first guess fields so that the so-called "*Tangent Linear*" approximation can be invoked:

$$H(\boldsymbol{x}_a) = H(\boldsymbol{x}_b + (\boldsymbol{x}_a - \boldsymbol{x}_b)) \cong H(\boldsymbol{x}_b) + \boldsymbol{H}(\boldsymbol{x}_a - \boldsymbol{x}_b) \qquad (2.4)$$

This formulation of the variational problem, proposed by Lorenc (1986), is the one used in the CNMCA assimilation system. In operational environments, it was first implemented in the NASA/Goddard Data Assimilation Office "Physical Space Statistical

Analysis System - PSAS" (Cohn et al., 1998) and, more recently, in the NAVDAS assimilation system of NRL Monterey (Daley and Barker, 2000).

A possible extension of (2.2) to observations non-linearly related to the state variables (such as radiances, wind speeds, total column water content, etc., where H depends on the model state x) is conceptually straightforward (Lorenc, 1988), and, in the present case, it is documented in Bonavita and Torrisi (2004).

From inspection of (2.2), it is clear that this is an observation space algorithm: $\boldsymbol{R}$ is defined in observation space while $\boldsymbol{P}_b$ is projected into it by means of the observation operator $\boldsymbol{H}$. Taking into account the average number of observations currently entering into the CNMCA assimilation system ($O(10^4)$) and the dimension of the state vector ($O(10^6)$), the current approach (PSAS) allows a considerable reduction of the computational and storage load on the computing facilities, beside allowing a simpler and cleaner modeling of the correlation functions. In the PSAS approach, the system of equations (2.2) is solved in two steps. First solution of the linear $p \; x \; p$ system in the unknown vector $\boldsymbol{z}$:

$$(\boldsymbol{H}\,\boldsymbol{P}_b\,\boldsymbol{H}^T + \boldsymbol{R})\,\boldsymbol{z} = \boldsymbol{y} - H(\boldsymbol{x}_b) \tag{2.5}$$

Secondly, projection of the solution on grid space via:

$$\boldsymbol{x}_a - \boldsymbol{x}_b = \boldsymbol{P}_b\,\boldsymbol{H}^T\boldsymbol{z} \tag{2.6}$$

The first step involves the solution of a large, sparse, symmetric and positive definite linear system. This step is mathematically equivalent to finding the minimum of the following cost function (Golub and van Loan, 1996):

$$F(\boldsymbol{z}) = 1/2\boldsymbol{z}^T(\boldsymbol{H}\,\boldsymbol{P}_b\,\boldsymbol{H}^T + \boldsymbol{R})\boldsymbol{z} - \boldsymbol{z}^T\,(\boldsymbol{y} - H(\boldsymbol{x}_b)) \tag{2.7}$$

which can be done using a standard preconditioned Conjugate Gradient (CG) algorithm. The computational cost of the minimization step is $O(p*p*N_{cvg})$, where N_{cvg} is the number of iterations needed for achieving convergence, while the projection step has a cost of $O(n*p)$. While n, in the current integration domain, is two orders of magnitude larger than p, N_{cvg} is also O(100) making the two steps roughly equivalent in terms of

required CPU time. On the other hand, it is to be remarked that the cost of the minimization step is quadratic in p, thus becoming quickly dominant as the number of ingested observations increase.

An efficient parallel (MPI) minimization of the cost function (2.7) has been achieved through a CG algorithm with block jacobi preconditioning which makes use of routines adapted from the Portable Extensible Toolkit for Scientific Computation (PETSc) mathematical library (Balay et al., 2002). An attractive feature of the PETSc library implementation of the CG algorithm is the possibility of computing and storing matrix elements of $(\boldsymbol{H P_b H^T + R})$ locally on each processor, thus avoiding the need for the expensive passing of matrix elements between different processors.

The second step amounts to performing a matrix-vector product between the [p,n] matrix $\boldsymbol{P_b H^T}$ and the p vector $\boldsymbol{z}$, which can be computed efficiently in Fortran90 code. Once the p-size vector $\boldsymbol{z}$ has been computed, it is passed to all available processors. From this point onwards the computation is completely parallel. In the present implementation the analysis grid may be divided up in boxes corresponding to horizontal and vertical sub-domains, which are then assigned to the available processors.

2. Background Error Covariances

The most important element in the objective analysis algorithm is the background error covariance matrix (Daley, 1991). From the inspection of (2.2), the form of this matrix governs the resulting objective analysis: the larger the background covariance compared with the observation error covariance, the larger the correction to the first guess.

The derivation follows the main ideas of Bergman (1979), Thiebaux et al. (1986), Thiebaux at al. (1990), Tillmann (1999). Its main features are:

1. the separable formulation of the temperature-wind cross correlations in spherical coordinates on isobaric surfaces, using the thermal wind relationship as a constraint;

2. the derivation of the covariances (expected first guess error variances and correlation lengths) through a statistical analysis of observation-minus-first guess differences from all available radiosounding sites over the model integration domain for the summer and winter months. Isobaric observation increments were fitted with gaussian (and its 5^{th} order piecewise rational function approximation: see Gaspari and Cohn, 1999) and SOAR type functions: eventually the SOAR function has been selected due to its ability to give slightly better fits to the observed increments ("Observation method", Rutherford, 1972; Hollingsworth and Lönnberg, 1986; for details of the method presently employed see Vocino, 2002).

The need to express the auto and cross-correlations in spherical coordinates instead of using a local plane projection arises from the fact that, for the correlation model and correlation lengths used, one has non negligible correlation values at distances comparable to the Earth's radius. Taking into account the narrower structure shown by the background vertical correlations of temperature with respect to those of geopotential and the weaker vertical correlation of radiosondes' temperature measurements with respect to geopotential observations, the choice was made to adopt the following analysis variables: temperature (T), zonal (u) and meridional (v) components of wind, surface pressure (ps) and relative humidity (RH).

The vertical and quasi-horizontal correlations used are shown in Fig. 2.2 and Fig. 2.3 respectively. Details of the derivation are presented in Bonavita and Torrisi (2004). The surface analysis covariances used in the objective analyses of the surface pressure (ps), mean sea level pressure (MSLP) and 10-meter wind fields (10u, 10v) are a simplified version of the models used in the upper air analysis.

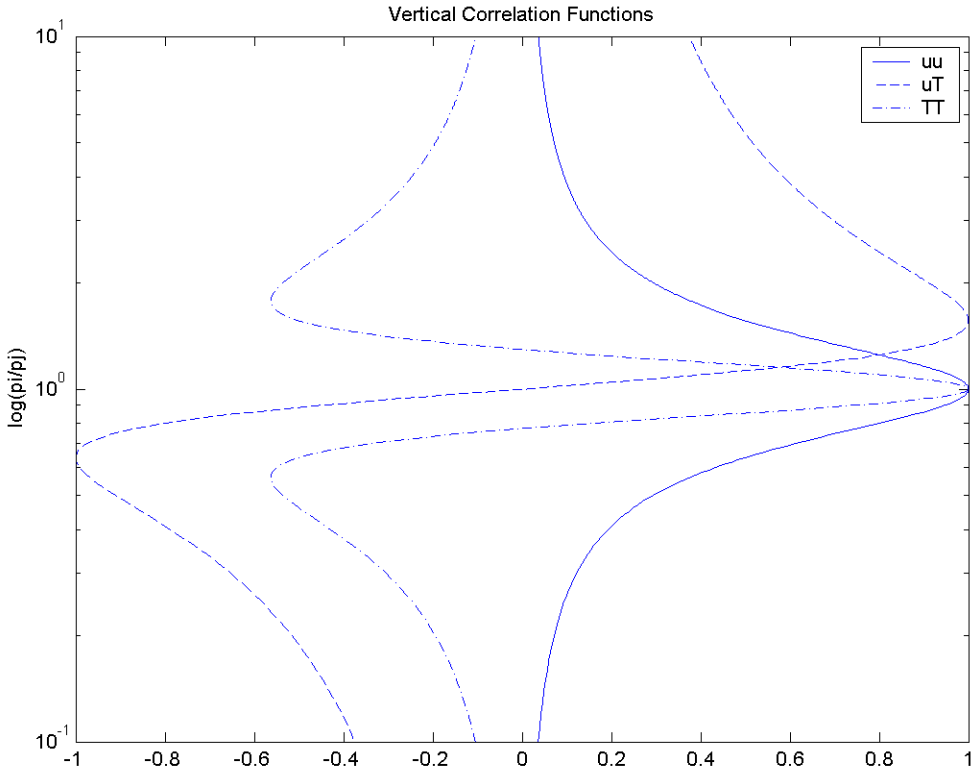

Figure 2.2 Vertical correlation functions.

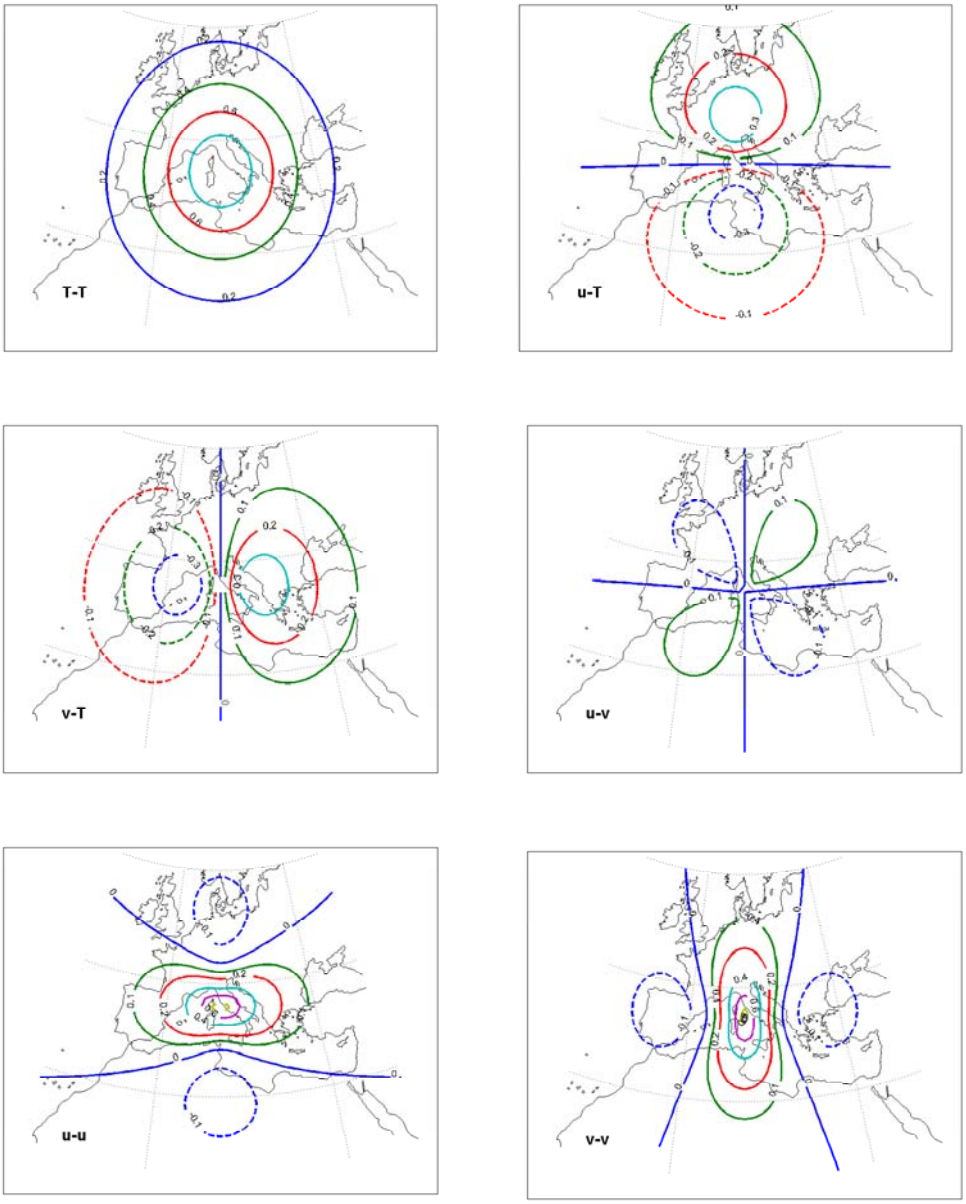

Figure 2.3 Isobaric correlation functions in equidistant conical projection.

3. Observation Errors

Most meteorological measurements contain a contribution from motion (or from thermal and humidity structures) on spatial and temporal scales too small to be resolved by NWP models. A radiosonde wind observation, for example, comprises a contribution from the synoptic-scale flow which can be resolved and a contribution from local gustiness (scale of order 100 m) which cannot be resolved. Theoretically the smallest scale, which can be resolved on a model grid, is given by twice the grid length. The small scale "roughness" which is sampled by the observations, but which the model is incapable of representing, is referred to as the representativeness error. Such errors also apply to the vertical which may be more important than the horizontal when discussing multi-level observations (soundings). The issue of representativeness error can also arise from not being able to represent small temporal scales. For most observations, the assimilation deals with the representativeness error (which can be estimated) by incorporating it into the overall observation error (i.e. observation error = instrument error + representativeness error) and weighting the impact of the observation in proportion to the inverse of the observation error. However, in some cases the representativeness error is considered so large that it is impracticable to use the observation. For example, surface winds over land are subject to local unresolved orographic effects and they are not used in the larger scale models.

A summary of the use of the conventional and non-conventional observations in the CNMCA data assimilation system is given in Table 2.1.

Mandatory and significant level radiosonde observations of temperature (T), dew point (Td) and wind are assimilated: observations at levels not coincident with isobaric analysis levels are vertically (linearly in *log(p)*) interpolated. From the statistical analysis of observation increments (Vocino, 2002), the assumed accuracy (Root Mean Square Error) of the temperature observations from radiosoundings have been set to 1.2 ºC; no radiative corrections are employed. For relative humidity the assumed accuracy has been set to 5%. Perceived winds accuracy varies from 2.1 m/s in the lower levels to 3.5 m/s in the stratosphere.

PILOT weather balloons (Pibals) wind reports and wind profiler data are also routinely analyzed, with expected observation errors somewhat greater than those assigned to radiosonde reports.

Atmospheric motion vectors (AMVs) are assigned errors starting from 4 m/s in the lower troposphere to 6 m/s in the stratosphere. AMVs are used at a resolution less than that one of the model (≈120 km), since they are generally correlated data (Bormann, Saarinen et al., 2002).

Automated aircraft reports (Aircraft Meteorological Data Reporting - AMDAR) are assigned errors of around 1.5 ºC for temperature and 2.5 m/s for wind components, slightly larger values for manual reports (AIREP). Aircraft data are assumed to be spatially uncorrelated enabling the data to be used at a resolution similar to that of the model (≈40 km).

Conventional surface observations, both over land (SYNOP) and over the sea (SHIP, BUOY) are also routinely analyzed. For the upper air analysis only temperature innovations are used.

Surface fields (surface pressure, mean sea level pressure, 10m wind) are analyzed through a two-dimensional, multivariate version of the algorithm. Winds are only assimilated over sea. At the moment geostrophy is not strictly enforced, using a geostrophic coupling parameter μ=0.8. Quikscat winds are assigned errors of 3 m/s, while for BUOY observation 4 m/s. An accuracy of 1.2 hPa is assumed for SHIP and BUOY pressure observations, while for SYNOP its value is 0.8 hPa.

MSLP is well defined over the sea but, over land, is more of a visual aid for forecasters than a real meteorological field. However it is felt to be important that the analyzed MSLP field closely draws to the accepted MSLP and surface wind observations. To accomplish this, it has been found necessary to objectively analyze the MSLP and surface wind departures: reduction of surface pressure (ps) analysis to mean sea level did not give satisfactory results, mainly because of the differences between model and observed temperatures.

Table 2.1 Use of the observations in the CNMCA NWP system.

Observation type	Description	Variables used	Number of obs.
SYNOP	Surface weather observations over land	MSLP, ps, 2T, 2Td	1985
SHIP	Surface weather observations on the sea	MSLP, ps, 2T	280
BUOYS	Observations from moored/ drifting buoys	MSLP, ps, 10u, 10v	80
TEMP	Upper air radiosonde observations	T, u, v, Td	245
PILOT	Upper air balloon observations	u, v	20
WIND PROFILER	Surface based Doppler radar upper air wind observations	u, v	10
QUIKSCAT	Polar satellite backscatter measurements over the sea	10u, 10v	520
AMV	Atmospheric motion winds from geostationary satellite imagery	u, v	950
AMDAR	Automatic observations from aircraft	T, u, v	1110
AIREP	Manual observations from aircraft	T, u, v	115

C. INITIALIZATION

The objective analysis procedures do not provide fields of mass and motion that are in optimal form to initiate the integration of a primitive equation model. The main reason for this lies in the fact that the imposed balance between the wind and mass observation increments are linear simplified conditions (approx. geostrophic, non-divergent), while the background fields implicitly satisfy the multivariate nonlinear conditions of the numerical model. As a result, the integration of non-initialized fields would cause the model to go through a geostrophic adjustment process with the excitation of inertia-gravity waves and the consequent degradation and noisiness of the forecast fields in the first 6-12 hours.

To avoid these undesirable effects, the "Adiabatic Implicit Normal Mode Initialization" technique is used. A detailed explanation can be found in Temperton, 1988, but the main ideas can be summarized as follows. The analyzed fields are projected over the normal modes of a linearised version of the model equations. These normal modes can be classified (at least in the extra-tropics) based on their respective frequencies or propagation velocities: "fast" modes, corresponding to inertia-gravity waves, "slow" modes, corresponding to meteorological Rossby waves. The result of the projection operation is two sets of ordinary differential equations whose integration in time gives the time evolution of the amplitudes of the normal modes. The imposition of appropriate conditions (so called Machenauer conditions) on the time tendencies of the amplitudes of the normal modes lead to an effective filtering of the high-frequency modes and removal of spurious numerical noise (Haltiner & Williams, 1980, pp.377-385).

D. PROGNOSTIC MODEL

The numerical model used to produce the first guess fields used in the objective analysis step and in the long-range run is the High-Resolution Regional Model (HRM) of CNMCA. The HRM is a modified version of the Deutscher Wetterdienst EM/DM hydrostatic model (Majewski, 2003), improved and adapted to run on HP Alpha and IBM servers.

The prognostic variables are: temperature (T), zonal and meridional wind component (u,v), surface pressure (ps), specific humidity (q_v), cloud liquid water content (q_c) and cloud ice water content (q_i). A rotated latitude/longitude grid is chosen such that the rotated equator runs through the centre of the model domain and the geographic North pole moves to a new position. This has the advantage of a rather small variation of the scale factor across the model domain compared to normal geographic coordinates. The forecast computation can thus use larger time steps. The vertical coordinate is the so called η system. Above a certain level p_t the η system is identical to a pure p system. From p_t on downwards to ps (surface pressure) the η system slowly approaches the σ system (σ=p/ps) which is mainly determined by the orographic structure (Simmons et al.,

1981). The lateral boundary formulation is due to Davies (1976).

The main numerical and physical features of this hydrostatic primitive equation model are summarized in Table 2.2.

Table 2.2 Characteristics of the HRM model.

Basic equations	hydrostatic primitive
Prognostic variables	u, v, T, q_v, q_c, q_i, ps
Horizontal coordinates	rotated geographical **(λ,φ)**
Vertical coordinate	generalized terrain-following
Horizontal grid	Arakawa C
Vertical grid	Lorenz staggering
Space discretization	2^{nd} order centered
Time integration	split semi-implicit (Burridge, 1975)
Numerical smoothing	linear 4^{th} order horizontal diffusion
Grid-scale clouds and precipitation	Hydci and Hydor (Doms et al., 2003)
Subgrid scale clouds	based on relative humidity and height
Moist convection	mass flux scheme (Tiedtke, 1989)
Radiation	δ-two stream (Ritter and Geleyn, 1992)
Vertical diffusion	K closure lev. 2 with Louis scheme at surf.
Soil processes	Two-level soil (Jacobsen and Heise, 1982)

The area of model integration is shown in Fig. 2.4 (EURO-HRM domain). In this configuration the grid spacing is 0.5° (operational run) or 0.25° (experimental runs), the number of vertical layers is 31 and the rotated North pole is at 32.5 N 170 W.

Three hourly forecast fields from the 3D-Var suite of the ECMWF model give the boundary conditions for the EURO-HRM model. The IFS2HRM software package is used to interpolate and adapt the ECMWF boundary fields to HRM grid and prognostic variables and to accomplish a daily blending of CNMCA 12Z analysis fields with ECMWF 12Z analysis fields (Fig. 2.1). The interface between the objective analysis step

and the prognostic model is completed by a spline interpolation of analyzed fields from the analysis 30 pressure levels (10, 20, 30, 50, 70, 100, 150, 200, 250, 300, 350, 400, 450, 500, 550, 600, 650, 700, 750, 800, 850, 900, 925, 950, 970, 985, 1000, 1007, 1013 and 1020 hPa) to 31 hybrid coordinate model levels (Insertion software package). Post-processing is performed for both forecast and analysis fields.

At this stage, the assimilation cycle is run operationally on one Compaq ES45 server, with a 3-h data window around the analysis nominal time. Conventional data including observations of pressure, temperature and wind coming from surface-based (SYNOP, SHIP, BUOY, WIND PROFILER) and balloon radiosonde (TEMP, PILOT) are operationally assimilated. Experiments with AMDAR/AIREP reports, Meteosat Atmospheric Motion Vectors (AMVs) and Quikscat surface winds have been performed.

The run time for an average number of independent observations (only conventional ones) entering the analysis algorithm (~7000) is around 45 minutes, which, considering the time necessary for the post-processing elaborations, leads to the availability of the analyzed fields less than three hours after the analysis nominal time. Twice daily (at 00Z and 12 Z), an extended run (+72h) of the EURO-HRM model based on the assimilation cycle analysis is performed.

The EURO-HRM domain with 0.25° grid spacing has been used to perform the impact studies of no-conventional observations. The data assimilation cycles and the EURO-HRM runs have been implemented on the ECMWF IBM supercomputer, where a large amount of computational time is available for each member states.

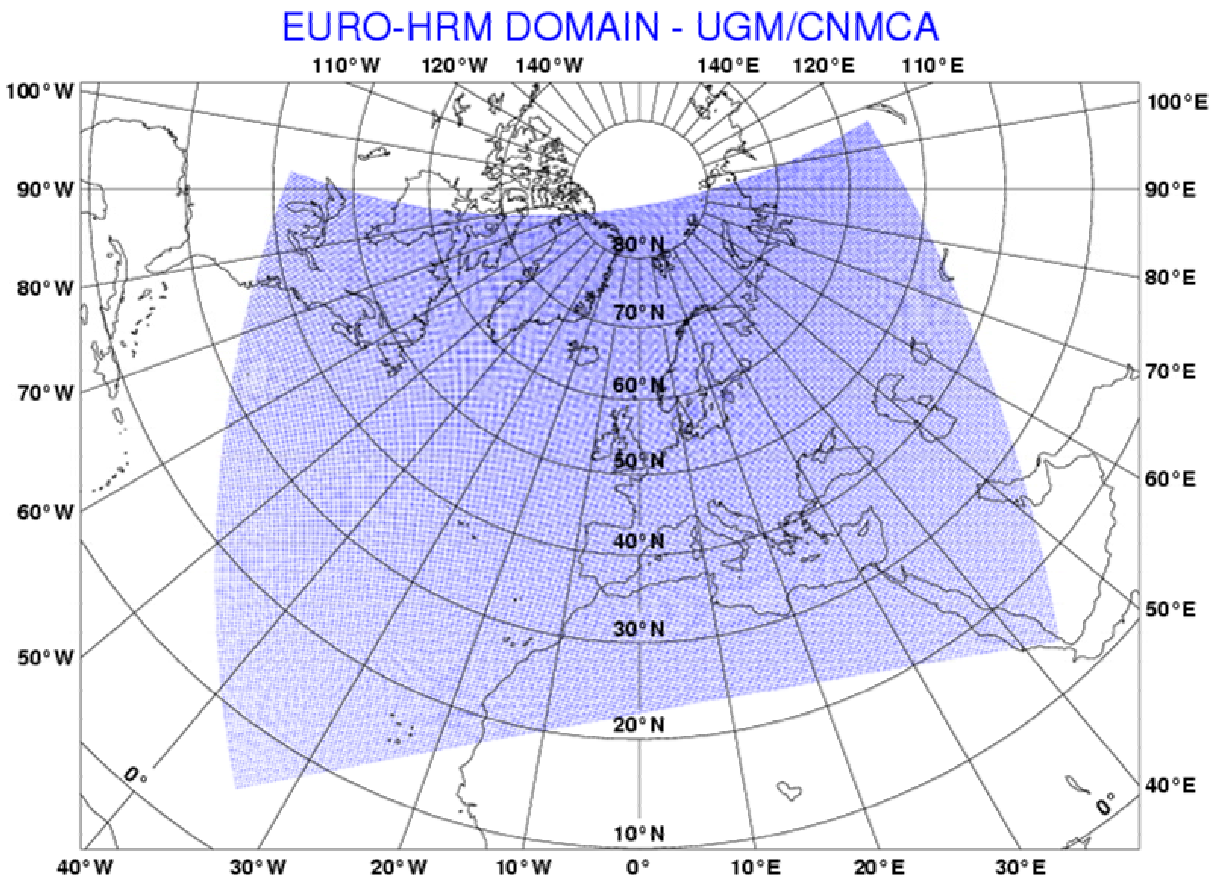

Figure 2.4 Regional model (EURO-HRM) domain of integration.

III. NON-CONVENTIONAL OBSERVATIONS

The Global Telecommunication System (GTS) is distributing the meteorological observations of the Global Observing System (GOS) in a timely manner for many meteorological applications. The GTS conventional data include observations of pressure, temperature, humidity, wind and other parameters coming from the surface-based (ground stations, buoys, ships, etc.) and balloon radiosonde observations. These conventional data are not enough to describe the atmospheric flow in sufficient detail. Over land, there is a lack of observations in the poorly populated and/or undeveloped regions of the world. Over the oceans, the lack of observations is a more acute problem.

Planes cover limited regions of the global ocean (only traffic routes) at irregular intervals of time and space, but unfortunately they tend to avoid the worst weather. Satellites offer an effective way to provide meteorological information in these otherwise data sparse regions, but the satellite data processing and assimilation into operational NWP models is more complex than for aircraft or conventional observations (Simmons, 2000 and Thepaut, 2003).

There are three types of remote sensing instrument technologies (Eyre, 2000) relevant to NWP used onboard satellites: passive, active and GPS (Global Positioning Satellite). The passive instruments measure the electromagnetic radiation coming from the Earth surface and/or its surrounding atmosphere. The active instruments emit electromagnetic radiation towards the Earth and measure the properties of the signal that comes back to the instrument, after the absorption, reflection or scattering by the Earth's surface or its atmosphere. GPS meteorology makes use of signals emitted from global positioning satellites and measured by instruments either on the ground or on low Earth-orbiting satellite.

This chapter provides a discussion about the aircraft based observations, the Quikscat surface winds (active measurement) and Meteosat atmospheric motion winds (passive measurement) assimilated in the CNMCA data assimilation system and an overview of the other satellite observations relevant to the NWP.

A. AIRCRAFT BASED OBSERVATION

Meteorological aircraft based observations are manual or automatic.

Weather information collected by pilot or flight crew during a flight are called Air Reports (AIREPs) or Pilot Reports (PIREPs). These reports deal with aviation hazards, such as turbulence and icing conditions, but they often provide a direct measure of the temperature and wind at flight level.

Automatic aircraft observations (wind and temperature) are recorded by instruments onboard commercial aircrafts, both at cruise level and during ascent and descent at airports. The data are collected by means of aeronautical telecommunications networks and distributed around the world via the GTS. The aircraft data have increased in numbers and coverage very substantially in recent years, with coordination provided by World Meteorological Organization (WMO) and European Composite Observing System (EUCOS) programs. The predominant sources of automated aviation data have been from ASDARs (Aircraft to Satellite Data Relay), and more recently ACARS (Aircraft Communication Addressing and Reporting System) equipped aircraft (WMO, 2003).

ASDAR data are transmitted from the host aircraft via the International Data Collection System (IDCS) on board the Meteorological Geosynchronous Satellite System (Meteosat, GOES E, GOES W, GMS). Ground stations are located in the USA, Japan and Europe where the received data are encoded into WMO AMDAR code and injected into the GTS.

ACARS systems, route data back via general purpose information processing and transmitting systems (VHF, HF and satellite communication systems) now fitted to many commercial aircraft. Experience with both systems (ASDAR, ACARS) has led to the conclusion that ACARS are preferred, based on ease implementation, worldwide applicability and overall cost (Stickland, 2001).

The various systems (ASDAR, ACARS) are collectively named Aircraft Meteorological Data Reporting (AMDAR) systems and are making an increasingly important contribution to the observational database of the World Weather Watch of the World Meteorological Organization (WMO, 1996). It is envisaged that AMDAR data

will inevitably supersede manual air reporting (AIREP). In recent years the WMO AMDAR Program has been set up to maximize the cost/benefit ratio of AMDAR systems by reducing the number of redundant data at the main airports and in heavy air traffic routes, while improving the reporting in data sparse areas.

AMDAR systems operate on aircraft, which are equipped with sophisticated navigation and other sensing systems. There are sensors for measuring air speed, air temperature and air pressure. Other data relating to aircraft position, acceleration, and orientation are available from the aircraft navigation system. The aircraft also carry airborne computers for the flight management and navigation systems, by which navigation and meteorological data are computed continuously and made available to the aircrew at the flight deck. In AMDAR systems they are further processed and fed automatically to the aircraft communication system for transmission to the ground, or alternatively a dedicated processing package can be used on the aircraft to access raw data from the aircraft systems and independently derive the meteorological variables. In AMDAR systems these facilities are used to compile and transmit meteorological reports in real time (BUFR format in Europe and North-America). Two global software standards are currently in use: ACARS Aircraft AMDAR (AAA) and Aeronautical Radio Incorporated (ARINC) 620 Meteorological Report. Work is been done to meet one common specification reflecting the operational requirements of the global meteorological community.

AMDAR reports are often produced at the specified frequency of one report per seven minutes at cruise level, with additional reports at wind maxima. During ascent, reporting is typically at 10 hPa intervals vertically for the first 100 hPa in the lower part of the profile and every 50 hPa above that layer to top of climb (near 20000 feet) with the reverse applying during the descent phase. The AMDAR system thus provides data at altitude roughly every 70 - 100 km along the flight path as well as detailed profiles in the near vicinity of airports. Consequently, AMDAR observations, where made, can meet the resolution and accuracy requirements for NWP. On the other hand, representativeness can be a problem with aircraft reports, particularly in the vertical. Planes flying in the direction of the wind tend to seek the jet core, which is of limited vertical extent and thus may be sampling part of the atmosphere, which is not fully resolved by the model (where

typically the vertical resolution may be only 30 hPa). It should also be noted that AMDAR reports are not made at standard times and thus significant gaps in observations arise due to the normal flight scheduling. The messages contain wind speed and direction, air temperature, altitude (flight or pressure level), a measure of turbulence and the aircraft position.

The source data for meteorological observations require significant correction and complex processing to yield meteorological measurements representative of the free air stream in the vicinity of the aircraft. Although the data processing involved it quite complex, errors in reported wind and temperatures are comparable with those of radiosounding systems. Thus AMDAR observations can provide high quality single level data. The traditional AIREP measurements are of lower quality than AMDAR measurements.

B. QUIKSCAT DATA

Severe storms that hit Europe often originate over the North Atlantic Ocean, where sparse meteorological observations are available. As a consequence, the initial stage of severe storms is often poorly analyzed and their development poorly predicted. Wind data from polar-orbit satellite scatterometers, such as SeaWinds on Quikscat (NASA satellite), can be assimilated in operational numerical models, since they provide accurate sea-surface wind vector information with a high coverage compared to conventional data. The Quikscat data coverage is such that developing storms are likely hit, thus depicting their position and amplitude.

1. Scatterometer

The scatterometer is a monostatic (transmitter and receiver use the same antenna) non-nadir looking real aperture radar for which a combination of range and angle resolution techniques is used to get a spatial resolution of typically 25-50 km. The normalized radar cross-section σ^o on the ocean surface roughness is measured by a scatterometer. Since the sea-surface roughness is driven by the wind, the latter can be inferred from radar data. The gravity-capillary (Bragg) waves are the dominant

contribution to the radar backscatter. The wind-to-backscatter relationship is generally referred to as the geophysical model function (GMF). The empirically derived forward model function (GMF), which relates the state variables (10 m wind speed and wind direction) to the observations (radar backscatter), is generally defined as:

$$\sigma^o = B_0[1 + B_1 \cos(\Phi) + B_2 \cos(2\Phi)]^z \qquad (3.1)$$

where Φ is the 10 m wind direction (Φ=0 blowing towards the radar); B_0, B_1, and B_2 are coefficients depending on the 10 m wind speed, the local incidence angle, and the polarization and frequency of the radar beam, the z is a coefficient that depends on the tuning performed for each GMF. It is important to realize that any effect that relates to the mean vector at 10 m height is incorporated in the backscatter-to-wind relationship. As such, air stability, the appearance of surface slicks, and the amplitude of gravity or longer ocean waves depend to some degree on the strength of the wind and may, to the same degree, be fitted by a GMF.

The SeaWinds on Quikscat mission from the NASA is a quick-recovery mission to fill the gap created by the loss of data from the NASA Scatterometer (NSCAT) after the ADEOS-1 satellite lost power in June 1997. Quikscat was launched from Vandenberg Air Force Base (USA) in June 1999.

The SeaWinds instrument is a conically scanning pencil-beam Ku-band scatterometer. It uses a rotating 1-meter dish antenna with two spot beams of about 25 km size on the ground, a horizontal polarization beam (HH) and a vertical polarization beam (VV) at incidence angles of 46˚ and 54˚, respectively, that sweep the surface in a circular pattern (Fig. 3.1). Due to the conical scanning, a wind vector cell (WVC) is generally viewed when looking forward (fore) and a second time when looking aft. As such, up to four measurement classes emerge: HH fore, HH aft, VV fore, and VV aft, in each WVC. The 1800-km-wide swath covers 90% of the ocean surface 24 hours. In comparison with the NSCAT side-looking scatterometer, the SeaWinds has the following advantages: higher signal-to-noise ratio, smaller footprint size, and superior coverage. On the other hand, the wind retrieval from SeaWinds data is not trivial, since the number of views and their azimuthal angles vary with the subsatellite cross-track location. More information

on the Quikscat instrument and data can be found in Spencer et al. (1997), JPL (2001), and Leidner et al (2000).

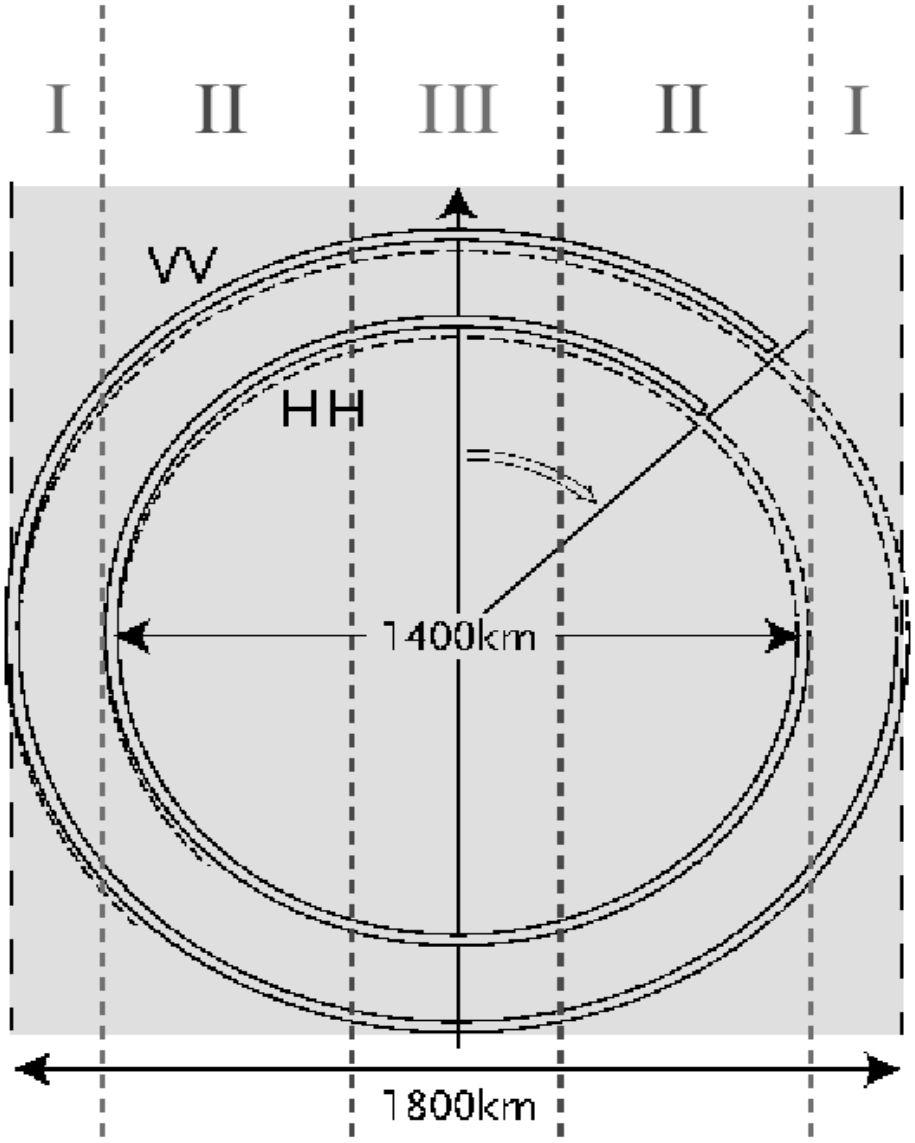

Figure 3.1 Schematic illustration of the illumination pattern of the SeaWinds scatterometer (from Portabella, 2002).

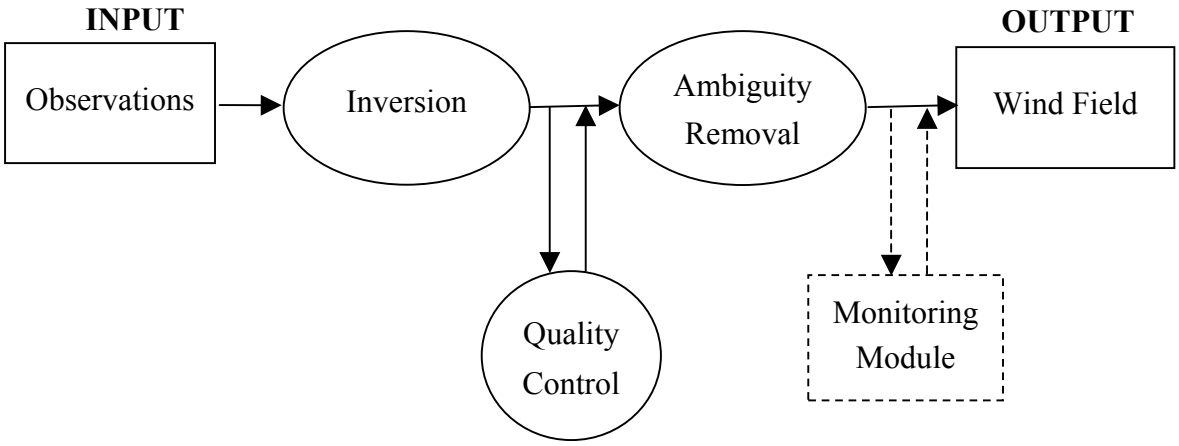

Figure 3.2 Schematic illustration of the scatterometer wind retrieval process (from Portabella, 2002).

2. Wind Retrieval

The wind retrieval procedure for scatterometer data is schematically illustrated in Fig. 3.2. A set of radar backscatter measurements in each cell (WVC) is inverted into a set of ambiguous wind solutions. The inversion output is then used, together with some additional information (typically from NWP models) and spatial consistency constraints, to select one of the ambiguous wind solutions as the observed wind for every WVC. This is called ambiguity removal (AR), and in contrast with the inversion, that is performed on a WVC-by-WVC basis, the AR procedure is spatially filtering many neighbouring WVCs at once. An important aspect of the wind retrieval is the quality control (QC). The goal of the QC is to detect and reject poor-quality retrieved winds. As illustrated in Fig. 3.2, the output from inversion can be used for QC purposes prior to AR. Finally, a monitoring module of the backscatter data quality and wind products is included in the wind retrieval procedure. A detailed discussion of the wind retrieval problem can be found in Portabella (2002).

a. Inversion

The SeaWinds swath is divided into 76 equidistant 25 km-by-25 km WVCs, numbered from left to right when looking along the satellite propagation direction. Quikscat has an antenna illumination pattern that is dependent on cross-track-location or node number, due to its circular scans on the ocean. As a consequence, the number of views, the polarization and the azimuth diversity are dependent on the node number, where azimuth diversity is defined as the spread of the azimuth looks among the measurements in the wind vector cell (WVC).

The number of independent σ^o values from the same area (WVC) is therefore of particular importance for a successful inversion of the unknowns in the GMF. Two backscatter measurements with different azimuth angles (20˚-160˚ separation), that is two views, should be enough to derive a unique wind-vector solution since the inversion problem should resolve two unknowns. However, because of the high non linearity of the GMF in the wind direction domain, up to four equally likely (ambiguous) solutions are possible, with varying wind speeds and very different wind directions. This is illustrated in Fig. 3.3, where the wind solutions (circles) correspond to the intersections of the two individual solution curves (one for each σ^o) and the arrow points to the true solution.

If the views are too far or too close in azimuth the problem is underdetermined. In the case of three or more views and good azimuth diversity, the problem is over-determined. In reality, the measurement noise will almost always produce two equally likely ambiguous solutions. For poor azimuth diversity, the wind retrieval accuracy depends on the speed and direction of the true wind with respect to the azimuth views.

In summary, the skill of the wind retrieval algorithm depends very much on the number of measurements and their polarization and azimuth diversity. The nadir region has fore and aft looks of both beams (HH and VV) nearly 180˚ apart. At the edges of the swath (outer region), the outer VV beam fore and aft looks are nearly in the same direction and no inner HH beam information is available. In both areas, the skill of the

wind retrieval algorithm is decreased with respect to the rest of the swath (called the sweet zone) where there are four measurements (fore-HH, fore-VV, aft-HH, and aft-VV) with enough azimuth diversity.

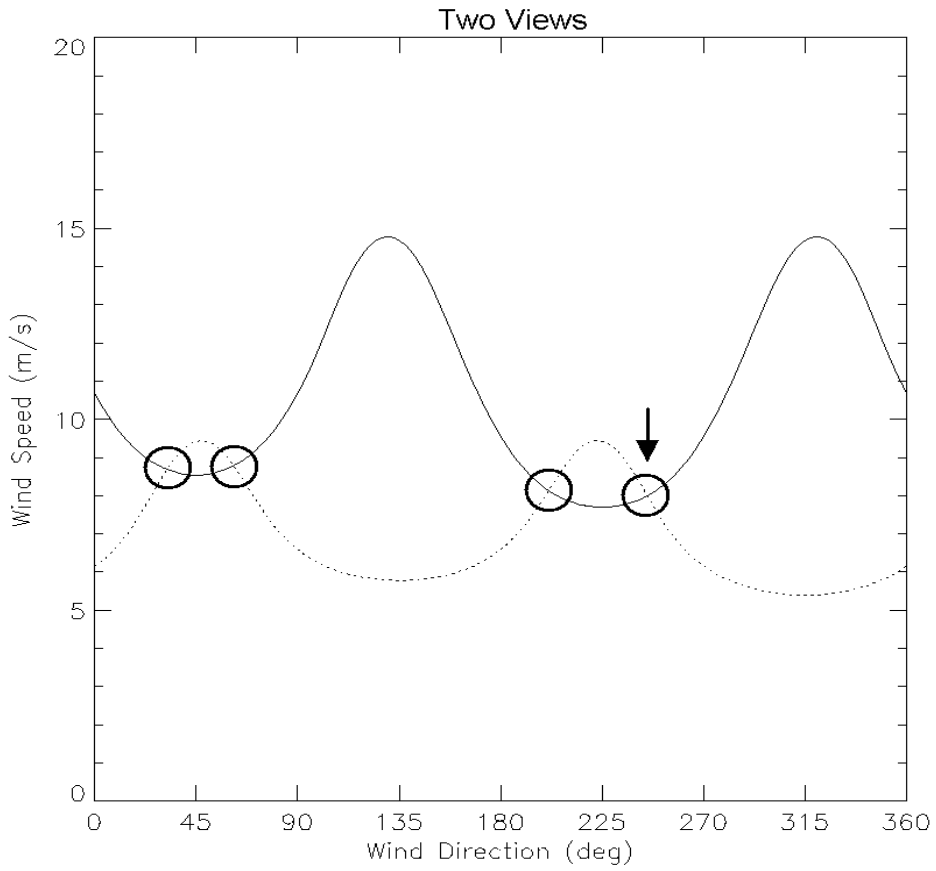

Figure 3.3 Curves represent set of wind speed and direction values, which satisfy the GMF for a σ^o measurement with two views having different azimuth angles (from Portabella, 2002).

For two or more independent σ^o views, a technique called Maximum Likelihood Estimation (MLE) is used to invert winds. The MLE is an optimization technique derived from Bayes theory, which maximizes the probability of the true wind by minimizing the so-called MLE cost function. The shape of the latter can in turn be used to examine the inversion problem since it provides information on the relative probability of every point (wind solution) of the cost function. In this respect, the poor azimuth diversity in the views of the Quikscat nadir region produces broad minima in the

MLE cost function, indicating a decrease in the level of determination of the problem, compared to the steep and well defined minima of the Quikscat sweet regions. The MLE is defined by:

$$J = \frac{1}{N}\sum_{i=1}^{N}\frac{(\sigma_{oi}^{o} - \sigma_{mi}^{o})^2}{Var(\sigma_{mi}^{o})} \tag{3.2}$$

where N is the number of measurements, σ_{oi} are the backscatter measurements, σ_{mi} are the model backscatter values corresponding to the measurements, and $Var(\sigma_{mi})$ are the measurement error variances (noise).

The scatterometer standard wind retrieval procedure consist of considering the MLE cost function minima (inversion residual) as the potential (ambiguous) wind solutions that are used by the AR procedure to select the observed wind. In particular, the MLE cost function can be normalized to remove some unwanted dependencies to certain parameters (node number, wind condition, etc) mainly caused by the measurement noise. It can be then transformed into a probability of the true wind by experimentally finding the relation between the MLE and the probability of the true wind.

In the Quikscat nadir region and the edges of the outer swaths, where the cost function minima are broad, the use of the standard procedure results in inaccurate and unrealistic wind fields. A multiple solution scheme (MSS), which takes into account the information on the shape of the MLE cost function, allows more ambiguous wind solutions (not constrained to only the cost function minima). This scheme was proposed by Portabella and Stoffelen (2004) to overcome the inversion limitations in the nadir region.

b. Quality Control

Space-borne scatterometers with extended coverage are able to provide accurate winds over the ocean surface and can potentially contribute to improve the situation for tropical and extratropical cyclone prediction. However the impact of observations on weather forecast often critically depends on the QC applied. For example, Rohn et al. (1998) show a positive impact of cloud motion winds on ECMWF model after QC, while the impact is negative without QC. The goal of QC is to detect and

reject poor-quality WVCs. Several geophysical phenomena other than wind can contaminate the scatterometer observation and in turn decrease the quality of the retrieved winds.

1. A WVC partially or totally covered by other surfaces than water, such as land or sea ice, will contain poor or no wind information. Consequently, it is important to identify and remove such WVCs from the wind retrieval process. In contrast with the coastal lines, for which a precise description is available, the sea ice edge information is less accurate since the sea ice is continuously changing. The information used to identify sea ice areas in the radar data processing chain is often derived from satellite data, which is often insufficient for an accurate and up-to-date monitoring of the sea ice sheet changes. Therefore, WVCs at high latitudes, can be ice-contaminated, which have not been flagged as such in the data product.

2. In cases of confused sea state, such as in the vicinity of the center of a low-pressure system or along atmospheric front lines where the sea is clearly not in equilibrium with the local wind, the wind retrieval is of poor quality. In such cases, different wind fields can be present in the same WVC (e.g., imagine a front line, which separates two different wind fields, crossing the WVC), which decreases in turn the quality of the retrievals.

3. Rain is known to both attenuate and backscatter the microwave signal. Raindrops are small compared to radar wavelengths and cause Rayleigh scattering (inversely proportional to wavelength to the fourth power). Large drops are relatively more important in the scattering and smaller wavelengths are more sensitive. As the rain rate increases, the spaceborne instrument sees less and less of the radiation emitted by the surface, and increasingly sees the rainy layer that becomes optically thick due to the volumetric Rayleigh scattering. In particular as SeaWinds operates at high incidence angles and therefore the radiation must travel a long path through the atmosphere, the problem of rain becomes acute. For example,

a dense rain cloud results in a radar cross section corresponding to 15-20 m/s wind. In addition to these effects, there is a splashing effect. The roughness of the sea surface is increased because of splashing due to raindrops. This may increase the measured σ^o, which in turn will affect the quality of wind speed (positive bias due to σ^o increase) and direction (loss of anisotropy in the backscatter signal) retrievals.

c. Ambiguity Removal

The ambiguity removal is the process of selecting a unique wind vector out of a set of ambiguous wind vectors at each WVC. The AR is not computed in a WVC-by-WVC basis but over many neighbouring WVCs at once. There are two AR techniques: spatial filters, e.g., median filter and variational analysis.

The median filter is used in the Jet Propulsion Laboratory – NOAA for Quikscat AR (JPL, 2001). The wind field over an entire revolution of scatterometer data is initialized with the help of a NWP model (vector solution closer to the NWP field). The median vector for the center of a certain (7x7) filter window is compared with the ambiguities in that WVC. The closest ambiguity is selected for use in the next iteration. The entire revolution is filtered in that way. The process continues until it converges (no replacement of vectors).

A 2D variational analysis (2D-Var) scheme was developed at the Dutch Meteorological Institute - KNMI (Stoffelen et al., 2000). It attempts to minimize the cost function:

$$J(\delta x) = J_b + J_o^{scat} \tag{3.3}$$

where J_b is the background term and J_o^{scat} is the observation term. It uses an incremental formulation with the control variable of wind increments, $\delta x = x - x_b$, defined on a rectangular equidistant grid. The reference variable x_b is the background field, which in 2D-Var is a NWP model forecast. The forecast is also used as first guess making the control variable equal to the null vector at the start of the minimization. The J_b is a quadratic term that contains the inverse of the background error covariance matrix; it

penalizes the deviation from the background field. The J_o^{scat} expresses the misfit between the ambiguous wind vector solutions and the control variable at each observation point. The contribution of the wind solutions in each observation point is weighted by the solution probability obtained in the inversion procedure. In order to solve the minimization problem, a conjugate gradients method is used, which also requires the gradient of the cost function. After convergence, the control variable vector of wind increments is added to the background field to obtain the wind analysis. Finally the wind solution closest to the analyzed wind is selected.

3. KNMI Product

KNMI has a near real time 100 km resolution Quikscat wind product (BUFR format) developed for assimilation in numerical weather prediction models, which includes inversion, QC and ambiguity removal (outer swath not processed). The original NOAA QuikSCAT products have a resolution of 25 km. Stoffelen et al. (2000) showed that the 25 km Quikscat winds are often too noisy, especially at low winds and in the nadir region. They also showed that the averaging of the radar backscatter information, and therefore the reduction of the spatial resolution, significantly reduces the noise of the inverted winds. For application such as mesoscale NWP data assimilation, where the effective resolution of the models is never lower than 100 km, the use of reduced resolution Quikscat simplifies the representativeness problem. A 100-km WVC consists of sixteen (4x4) 25-km cells. If half of them contain valid HH and VV, and, fore and aft backscatter data (i.e. 4 kinds), then the inversion is performed. A standard inversion procedure is used, but with some extensions to the JPL-NOAA procedure (JPL, 2001) described in Stoffelen et al. (2000):

1. the use of the measured noise in the expression of the MLE, rather than the estimated noise; in this way the number of ambiguous solutions per WVC decreases, but without detrimental effects on verification;

2. the NSCAT-2 Geophysical Model Function (Wentz and Smith, 1999), rather than later versions, since this GMF proves less ambiguous after

inversion than later versions; also high speeds are less exaggerated in this version of the GMF;

3. the normalization of the inversion residual (MLE) and its use as a quality indicator in the QC (including JPL-NOAA rain screening).

The 2D-VAR AR uses a T+24h NCEP wind forecast at 1000 hPa as background field. The so-called "Index of selection" is encoded in the Quikscat wind BUFR files, in order to flag the wind vector solution extracted by the 2D-Var AR.

C. ATMOSPHERIC MOTION VECTORS

Geostationary satellites provide an almost continuous view of the same part of the Earth. The high temporal resolution of the geostationary satellites makes them essentially suitable for nowcasting applications, but also for NWP systems through the provision of Atmospheric Motion Vectors (AMVs).

Atmospheric Motion Vectors are winds derived from sequences of well navigated and calibrated geostationary satellite images (infrared - IR, visible - Vis and water vapor - WV) by the tracking of clouds or other constituents (e.g. water vapor and ozone) with cross correlation methods. The use of water vapor images to calculate winds (AMVs) means that information can be obtained in clear (tracking humidity features), as well as in cloudy, regions of the atmosphere.

1. General Characteristics

The AMVs derivation is mostly an automatic procedure based on the following main components:

1. target extraction
2. tracking
3. height assignment

4. quality control

This procedure measures the displacement of cloud patterns (for infrared, visible and cloudy sky water vapor winds) and gradients in water vapor concentration (for clear sky water vapor winds) between usually three consecutive images (typically taken at half hourly intervals) and through this displacement computes the wind vectors.

The AMVs are available within the useful field of view of the satellite, usually up to 60 degrees from the sub satellite point; these provide the main source of remotely sensed winds for NWP. Typically the AMV extraction frequency is between 1.5 to 6 hours and the horizontal density is of synoptic scale (100 km or worse). The AMV quality control in the data assimilation system is necessary to decide what data are acceptable for the inclusion in the NWP model. In certain cases, tracer motion may not equate to the wind. For instance, cloud tracers in tropical regions are often convectively driven and do not follow the mean winds, and orographic cloud remains tied to land features.

AMVs provide data similar to an aircraft wind report. There are, however, several important differences. The height level of the vector needs to be assigned and this can be derived by compare, for example, the measured cloud-top temperature with external information such as a forecast model temperature profile. The height assignment methods rely on a number of assumptions, and if these are not satisfied the resulting product will have dubious quality. Different height assignment schemes for AMV data show root mean square errors of 60-110 hPa and mean differences of 30 hPa (Nieman et al., 1993). It is important to realize that AMVs are not a direct measurement of the wind field, therefore, may possess properties that compromise their use as a single observation of the wind field. First, clouds are not always passive tracers. Second the location of cloud occurrence may not always be in areas of the strongest wind speed. Cloud motion may also represent a layer mean flow rather than a wind vector at a specific level.

The representativeness problems are usually not as severe as those associated with aircraft data, since the observing technique implies that a volume measurement that is comparable to model resolution is provided. In jets, however there is a tendency to under-

report the wind speed, either because the volume measurement is too large or the tracer is not moving with the wind (Hasler et al., 1979).

2. EUMETSAT Product

AMVs from Meteosat image data are produced routinely by the EUMETSAT operational Meteorological Product Extraction Facility (MPEF) in Germany (Schmetz et al., 1993, Buhler and Holmlund, 1993, Holmlund 2002).

The first basic step in the extraction component is the selection, specific to the spectral channel, of the tracer for each segment in the middle image. In the case of the infrared images, the selection is done by taking the coldest cluster classified as cloud. For the visible channel the cloud cluster with the highest entrophy is selected usually for the low level clouds. In case of the water vapor channel the coldest cluster corresponding to medium and the high level tracers is chosen. Multilayered cloud situations and coastal regions are avoided, as they might have an impact on the tracking.

The second operation in the extraction component is the definition of the target area and the search area, according to the selected tracers. These areas are the parts of the images on which the tracking component is applied (cross correlation method). Each wind derivation cycle requires a triplet of consecutive images as basic input data. A target area (segment) of 32x32 pixels (16x16 pixels for high resolution water vapor winds) is taken from the central image of the three consecutive images. The search area of 96x96 pixels is centered on the location of the target area in the other image (the previous or succeeding one).

The third step is the enhancement procedure, which is applied in the same way to the target and search areas. The goal of this enhancement is to facilitate the task of the tracking component (obtaining higher and sharper correlation peaks) by increasing the contrast within the tracer and/or by reducing the contrast elsewhere. This enhancement is based on the tracer cluster statistics and it includes the definition of masked pixels ignored by the correlation computation. In addition an image filtering, that uses a spatial coherency method (Hoffman, 1990), is applied to extract cloud pixels belonging to the highest cloud layer.

In the tracking component the selected tracer is tracked in the previous and next image by the calculation of cross-correlations coefficients. The computed winds of the backward and forward mode are then combined into one wind vector. The tracking of the targets is generally the task that uses the largest amount of computer resources in any AMV extraction scheme. A two step approach is used in the MPEF AMV tracking scheme, where a reduced resolution correlation surface is first calculated by the preprocessed arrays of pixels for the target and search areas. Then a refined location is extracted around the three most significant peaks in the reduced surface. It has been shown that the results are agreeing up to 97% of a full matching surface (Nuret and Schmetz, 1988). The volume of computation is further reduced by using forecast wind information to start the peak search. Such peaks correspond to the most likely displacements. For each of these displacement vectors, the corresponding wind vector is computed via the geographical coordinates and converted to m/s and orientation. A slightly different algorithm (Fast Fourier Transform surface correlation) is used for the high resolution water vapor product.

Each extracted vector is then assigned to a particular height. The height of AMVs is defined by the temperature of the tracer and converted to a pressure level via the temperature-to-pressure ECMWF forecast profile. Large errors in the height assignment occur for subpixel or semitransparent cloud tracers, since the satellite observed infrared radiance contains contributions from below the cloud. A correction method, known as semitransparency correction, is applied operationally in the Meteosat AMV extraction. This method employs two simultaneous radiance observations in both WV and IR channels where one pair of radiances is from the transparent cloud and a second pair from an adjacent cloud-free area. In addition, the relationship between the IR and WV radiances for opaque clouds at different levels in a given atmosphere is computed with radiative forward calculations using the ECMWF temperature and humidity forecasts. The height assignment of AMVs is currently the most challenging task in the AMV extraction schemes. Broken clouds, multi-layered cloud targets, low level targets and height assignment of clear sky targets, do all require their special attention.

The AMVs undergo quality control before being disseminated on the GTS in BUFR or SATOB format. The automatic quality control (Holmlund, 1998) calculates a

number of consistency indicators for the extracted wind, and combines these as a weighted mean into an overall reliability indicator, the so-called quality indicator (QI). The indicators are based on a set of some tests for consistency: e.g. checking direction, speed, vector consistencies between the two AMV components, a spatial test checking the consistency with neighboring vectors and a forecast test checking the consistency with the used forecast. Additionally, the QI scheme also involves an inter-channel consistency check. This check compares low level infrared and visible winds to collocated clear sky water vapor winds. Based on the notion that the infrared and visible low level winds should describe completely different motion than the clear sky water vapor winds, low level winds that are similar to the clear sky water vapor winds are removed. This test has proven to be important in removing vectors related to extremely thin cirrus that have remained unidentified in the image analysis and are therefore erroneously assigned to a low level.

There are different wind products, depending on channel, resolution, quality and type of encoding. Redundant wind measurements are produced by observing the same tracer in different spectral channels. In most of the cases, high level wind from the WV channel and low level winds from the Vis channel are better than the corresponding winds from the IR channels. Brief descriptions of each of the MPEF AMV products are given in the Table 3. A typical product distributed in BUFR code contains up to 2000 winds together with the associated QI and the product is generated every 1.5 hours during daytime. A SATOB code product includes only the best wind determined from the QI value (up to 750 winds per channel). The current baseline channels for AMV extraction is presented in Table 3.2, where HLC, MLC and LLC refer to high, medium and low level clouds, respectively. The AMV are also available from the Meteosat Second Generation (MSG) satellite.

Table 3.1 Meteosat AMV product suite (after Holmlund, 2002).

Product type	Product information	Format type
Cloud Motion Winds	Only best wind above 995 hPa in the segment. WV winds only above 400 hPa. Minimum speed 2.5 m/s.	SATOB
Expanded Low Resolution Winds	Only IR channel at 160 km resolution at sub satellite point.	BUFR
High Resolution Visible	Vis winds at 80 km resolution at sub satellite point.	BUFR
Clear Sky Water Vapor Winds	Only clear sky targets (160 km)	BUFR
High Resolution Water Vapor Winds	Only cloudy sky targets (80 km)	BUFR

Table 3.2 Baseline channels for Meteosat AMV extraction (after Holmlund, 2002).

Band	Central wavelength	Prime targets
IR	10.8 μm	Clouds
IR	6.2 μm	HLC/Moisture
IR	7.3 μm	HLC/MLC/Moisture
Vis	0.6 μm	LLC over sea
Vis	0.8 μm	LLC over land

D. OTHER OBSERVATIONS

The other non-conventional observations relevant to the NWP are mainly obtained by satellite measurements. The advantage of the satellite data is that they provide a uniform spatial and temporal coverage of the atmosphere. This advantage is however balanced by a general poor vertical solution of the instruments currently used, and the difficulty to handle clouds, precipitations and surface contributions to the information content of the data. A better handling of new observing techniques (radio-occultation, passive limb soundings, active sensors) in data assimilation schemes may overcome some of these limitations.

An overview of satellite instrument technologies under the general headings of passive, active and GPS is provided in this section, as reported in Eyre (2000).

1. Passive Remote Sensing

The best known satellite data come from visible and infrared imaging radiometers on all operational geostationary satellites and the Advanced Very High Resolution Radiometer (AVHRR) instrument on the NOAA polar orbiters sensing in atmospheric window regions. Clear sky water vapor radiances from a geostationary platform are assimilated in NWP system to improve the quality of the upper tropospheric humidity. Also post-processed products, as atmospheric motion vectors (above considered) and sea surface temperatures derived from infrared imagery play an important role in NWP. New wind products in the polar region are derived by tracking in consecutive swaths from the Moderate-resolution Imaging Spectro-radiometer (MODIS) instrument onboard the NASA's Terra satellite. In mesoscale NWP, cloud imagery is used to initialize the cloud field in the model, but overall imagery data are far from fully exploited in NWP.

Another class of instrument is the nadir infrared sounding radiometer (vertical measurements through the atmosphere). These sense primarily in gaseous absorption bands and measure the radiation emitted by molecules of these gases in the atmosphere. Instruments in this class include filter radiometers such as High-resolution Infrared Radiation Sounder (HIRS) on the NOAA satellites and the sounders on the GOES geostationary satellites Radiance measurements from the polar-orbiting satellites provide

a potentially valuable source of temperature information, in data sparse regions. The assimilation process currently requires a transformation from radiance to temperatures. This is an under-determined problem without the additional information provided by way of a first guess (usually from a model forecast). The radiance measurements at a particular frequency also derive from a rather broad vertical extent of the atmosphere and this implies rather poor vertical resolution (typically ≈3km). The resolution is improved (to about 1km) in the advanced spectrometer Advanced Infrared Sounder (HIRS) on NASA's Aqua satellite and in the interferometer Infrared Atmospheric Sounding Interferometer (IASI) on the EUMETSAT's METOP satellite (to be launched in 2005). These instruments provide information on the profiles of temperature, humidity and ozone profiles, and on surface temperature, but they are fundamentally limited by the presence of cloud. Limb infrared sounders (horizontal measurements through the atmosphere) detect emission at tangent altitudes in the upper troposphere and stratosphere (5-150 km) providing information on temperature and constituent concentration (water vapor, ozone, etc.) vertical profiles. Limb sounders provide good vertical resolution (1-3 km), but they have poor horizontal resolution (100s km) and cloud sensitivity. An instrument of this type is the Michelson Interferometer for Passive Atmospheric Sounding (MIPAS) on ENVISAT satellite of the European Space Agency (ESA).

For NWP, it is important to obtain information on atmospheric temperature and humidity in areas that are predominantly cloudy, as these regions are usually the most meteorologically active. For this reasons, microwave sounding radiometers are highly complementary to their infrared counterparts, as microwave radiation is much more weakly attenuated by the presence of cloud (except where precipitation is present or cloud liquid water amounts are very high). Instruments of this type include the Advanced Microwave Sounding Unit (AMSU) on the NOAA satellites and the Special Sensor Microwave Imager/Sounder (SSMIS) on forthcoming DMSP satellites. It is well known that the ATOVS (Advanced TIROS Operational Vertical Sounder) soundings (HIRS and AMSU) have a substantial beneficial impact on the quality of numerical forecasts, especially on the southern hemisphere.

Microwave imaging radiometers sense radiation mainly in atmospheric window regions, emitted mainly by the surface and/or clouds. Over the ocean they provide

information on surface wind speed, through its effect on the roughness and hence the emissivity of the sea surface, and on sea-ice cover. They also provide information on cloud liquid water (total column), precipitation and water vapor (total column). Instruments in this class include: Special Sensor Microwave/Imager (SSM/I) on DMSP satellites, information and TRMM (Tropical Rainfall Monitoring Mission) Precipitation Radar (TMI) on the TRMM satellite. SSM/I (total column water vapor and near surface wind) instruments provide an important source of data for assimilation.

The ultraviolet region of the spectrum is currently exploited to obtain information on ozone profiles. Instruments in this class include: Solar Backscatter Ultra-Violet Instrument (SBUV) on the NOAA satellites and Global Ozone Monitoring Experiment (GOME) on ERS (of ESA) and METOP satellites. Other instruments to obtain ozone information are the Global Ozone Monitoring by Occultation of Stars (GOMOS - sounder) and the Scanning Imaging Absorption Spectrometer for Atmospheric Chartography (SCIAMACHY - nadir and limb sounder) on the ENVISAT satellite.

2. Active Remote Sensing

The active instruments emit electromagnetic radiation towards the Earth and measure the properties of the signal that comes back to the instrument, after the absorption, reflection or scattering by the Earth's surface or its atmosphere. The most widely used of such data in NWP come from scatterometers above considered (microwave wavelengths). Other instruments in this class are: altimeters, which through measurement of the time delay and the shape of the return signal, provide information on the sea surface height, the wave height and the wind; and synthetic aperture radars (SARs), which provide information on wave spectra. A precipitation radar works at higher frequency than a SAR; one is present in the TRMM satellite.

Another class of active instruments is based on lidars, which operate at visible or infrared wavelengths. Simple lidars measure only the intensity of the return signal as a function of the delay. They can provide information on the cloud top height (for thick cloud) and on the cloud profile (for thin cloud), and also on aerosol profile. Doppler lidars (DWL) measure in addition the Doppler shift of the return signal, which provides

information on the speed of the reflecting object along the line of sight, and hence on the wind speed.

3. GPS

The Global Positioning System (GPS) was deployed primarily as a positioning system for a range of civil and military applications. Applications in meteorology are a fortuitous product. There are two types of observations.

1. A GPS receiver on a on a low Earth-orbiting satellite, such as the GRAS (Global Navigation Satellite Systems Radio Occultation Receiver for Atmospheric Sounding) instrument on board METOP, can measure the additional delay (or Doppler shift) of a GPS signal which has been refracted on passing along an atmospheric limb path (radio-occultation technique). The refraction is caused by refractive gradients along the limb path. Over a period of about a minute, a series of such measurements provides information, via the retrieved refractivity profile, on the temperature profile (stratosphere and upper troposphere), the humidity profile (lower troposphere) and possibly also the surface pressure. This observation technique has high vertical resolution but low horizontal resolution (due to its limb-sounding geometry). GPS receivers on polar-orbiting satellites can provide global coverage and all-weather measurements.

2. A GPS receiver on the Earth's surface can measure the total delay of GPS signal caused by the atmosphere. This provides information of the total column water vapor above the receiver. It is only a local measurement, but can be made at high temporal frequency, and thus has potential for improving humidity analyses in regional NWP models.

THIS PAGE INTENTIONALLY LEFT BLANK

IV. IMPACT STUDIES

The effective use of observations is essential for the production of NWP forecasts. It is thus important to carry out studies that assess the impact of the Global Observing System (GOS), or a component of it. An effective way of doing this is by performing Observing System Experiments (OSEs), in which the data assimilation and forecast cycles are repeated using different combinations of the observing system (Bouttier and Kelly, 2001 and Dumelow, 2003).

OSEs offer precise measures of impact, although interpretation of the results requires care. Due to resources limitations, experiments are typically run for only one or a small of periods which may not sample the full range of synoptic variability on which observing system impact can depend. The impact of a particular observing system will depend on whether all other observing systems are used or whether some other observing systems are also withheld. The impact of an observing system will depend on how well its particular type of observation is handled by the data assimilation system used, and may not be indicative of that which would apply in the assimilation system of another forecasting centre. As a consequence a quantitative measure of the importance of particular components of the observing system is dependent on many factors.

In this study the impact of one observing system (Quikscat, AMV and aircraft observations) at a time on the same assimilation system configuration has been evaluated. Also experiments using all these observing systems and an AMV bias correction scheme have been performed. Moreover, an experiment to evaluate the impact of the resolution on the CNMCA NWP system has been realized. Details of these experiments will be given below, together with a discussion of the results obtained.

A. METHOD OF VERIFICATION

There are two ways through which the quality of the objectively analyzed and forecast fields can be gauged:

1. A subjective, "synoptic" evaluation of the charts produced by the numerical weather system from a forecaster's perspective, assessing the adherence to the observations (especially those not used in the analysis scheme, such as satellite imagery) and the degree of enforcement of "physical" balance properties;

2. A statistical, "objective" verification through comparison of forecasts produced from the analyzed fields with other forecasts started from independent data assimilation cycles or with radiosonde and surface station observations.

The objective approach using radiosonde and surface station observations has been taken in this study. An accuracy measure, such as the root mean square error (RMSE) has been calculated, in order to evaluate the typical magnitude for forecast errors. The root mean square error is given by (Wilkes, 1995):

$$RMSE=(1/n\ \Sigma_{i=1,n}\ (f_i - o_i)^2\ )^{1/2} \tag{4.1}$$

where $(f_i\ ,\ o_i)$ is the ith on n pairs of forecasts and observations. The nearest grid point to the observation position is usually used to define the forecast value. The wind vector RMSE is defined as:

$$\text{WV-}RMSE=(1/n\ \Sigma_{i=1,n}\ (u^{f}_{i} - u^{o}_{i})^2+(v^{f}_{i} - v^{o}_{i})^2\ )^{1/2} \tag{4.2}$$

where $(u^{f}_{i}\ ,u^{o}_{i})$ and $(v^{f}_{i}\ ,v^{o}_{i})$ are the ith on n pairs of wind component (zonal and meridional) forecasts and observations.

A measure of the bias of forecasts, such as the mean error (ME), has been also calculated. It is defined as:

$$ME=1/n\ \Sigma_{i=1,n}\ (f_i - o_i) \tag{4.3}$$

The mean error is simply the difference between the average forecast and average observation.

The impact of the increased resolution in the CNMCA NWP system has been evaluated only for the prognostic component. Two parallel runs of the HRM model have been setup with different resolutions starting from the ECMWF initial conditions.

In order to assess the impact of an observing system in the NWP system on the forecast fields in an objective manner, two parallel data assimilation cycles with a run of the HRM model running at 00UTC every day up to T+48h have been used. Both systems assimilate the conventional observations (TEMP, PILOT, SYNOP, BUOY, SHIP and WIND PROFILER), while the "new" observations are included only in one of the two NWP systems. Apart from the initial conditions, all the other features of the two model integrations are equal (boundary conditions, resolution, etc.): this should guarantee that any difference in the subsequent forecast fields should be traced back to differences in the initial conditions.

Forecasts fields have been verified against observations from the European upper air network and surface synoptic observations covering the whole integration domain (Fig. 4.1). Only land stations having height lower than 700 m and height mismatch with nearest grid point height lower than 100 m have been retained. Mean error and RMSE of surface variables (two meter temperature, ten meter wind, mean sea level pressure), as a function of forecast time (every 6 hours), have been computed. Temperature and wind vertical profiles of mean error and RMSE at the standard pressure levels for 12, 24, 36, 48h forecast steps have been also calculated and plotted. A typical plot shows the vertical profile of the ME, the RMSE and the number of forecast-observation pairs used for their calculation (sample number).

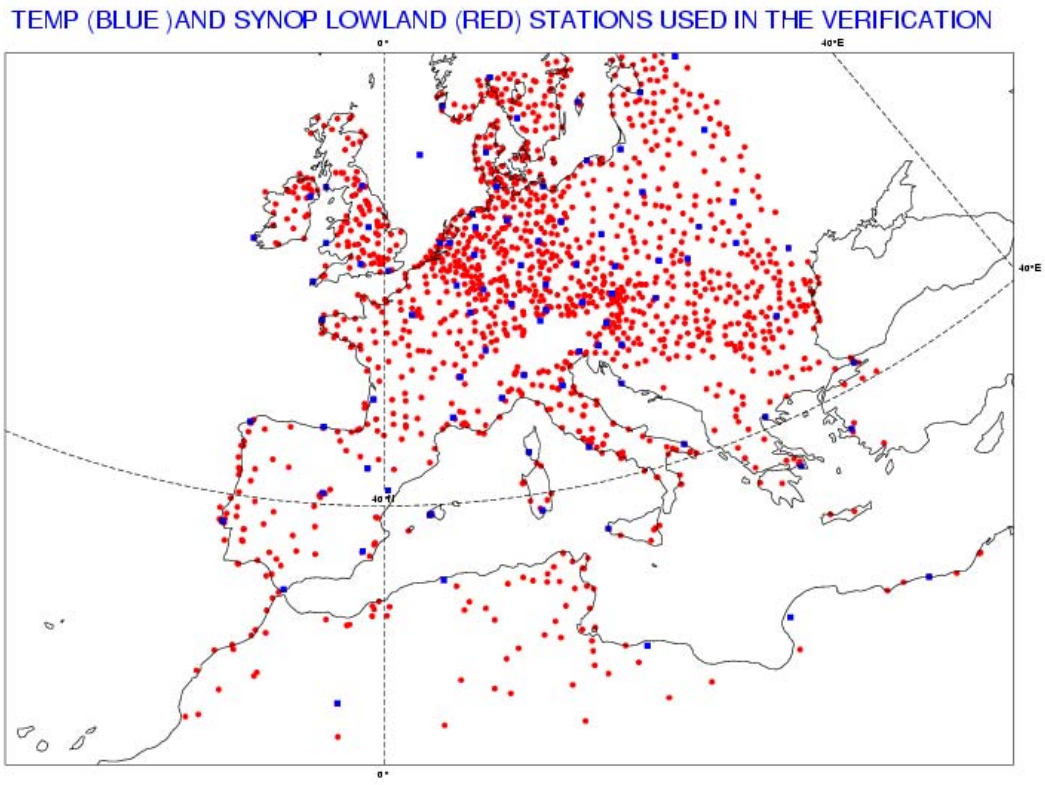

Figure 4.1 TEMP (blue) and SYNOP lowland (red) stations used for verification.

B. VERIFICATION RESULTS

1. Increased Resolution

The impact study has been performed for forecast fields of two parallel 00 UTC EURO-HRM model runs having different grid spacing: 0.5˚ and 0.25˚ (until T+48h). The period of investigation was: 16 December 2003 - 23 January 2004.

The ME and RMSE vertical profiles of temperature and wind for forecasts T+12h, T+24h, T+36h and T+48h are plotted in Fig. 4.2-4.5. Blue and red lines represent scores for the 0.5˚ and 0.25˚ runs, respectively. From the inspection of the plots, the increased resolution run has a small positive impact in the temperature accuracy below 850 hPa becoming less significant, but extended up to 500 hPa, for the T+48h forecast. A reduction of the cold bias below 300 hPa is another improvement obtained by higher

resolution run. A small positive impact of the increased resolution is also evident in the accuracy of the wind vector below 700 hPa. It tends to decrease as the forecast range increases. The negative bias at the jet levels and the positive bias near the surface of the wind speed are reduced, but a bias increase at the other levels is also found. A very slight deterioration is found in the accuracy of temperature (and marginally in the wind vector) at the stratosphere levels. This deterioration is mainly due to small scale features induced by topography (like hydrostatic mountain waves) which show up also in the stratosphere but do not verify well due to their small scale and low predictability.

In this experiment the resolution is only doubled, as a consequence no great improvement was expected in the model performance. The increased resolution of the model topography makes the resolution impact more significant near the surface.

RMSE and ME of temperature, wind speed and mean sea level pressure, as a function of the forecast range, are plotted in Fig. 4.6 and Fig. 4.7. A clear improvement is found for the mean sea level pressure and the 10m wind speed of the increased resolution run. Verification results for the 2m temperature show a slight deterioration in the accuracy and an increased cold bias, except for 12 UTC. This result may be related to the higher evaporation from the ground in the higher resolution model, which cools the model too much during winter. Other experiments (Majeski, personal communication) have showed that an improvement is obtained lowering the height of the lowest vertical layer. The temperature bias is reduced considerably, because the evaporation is less in stable conditions with the lowest model level at 10 m.

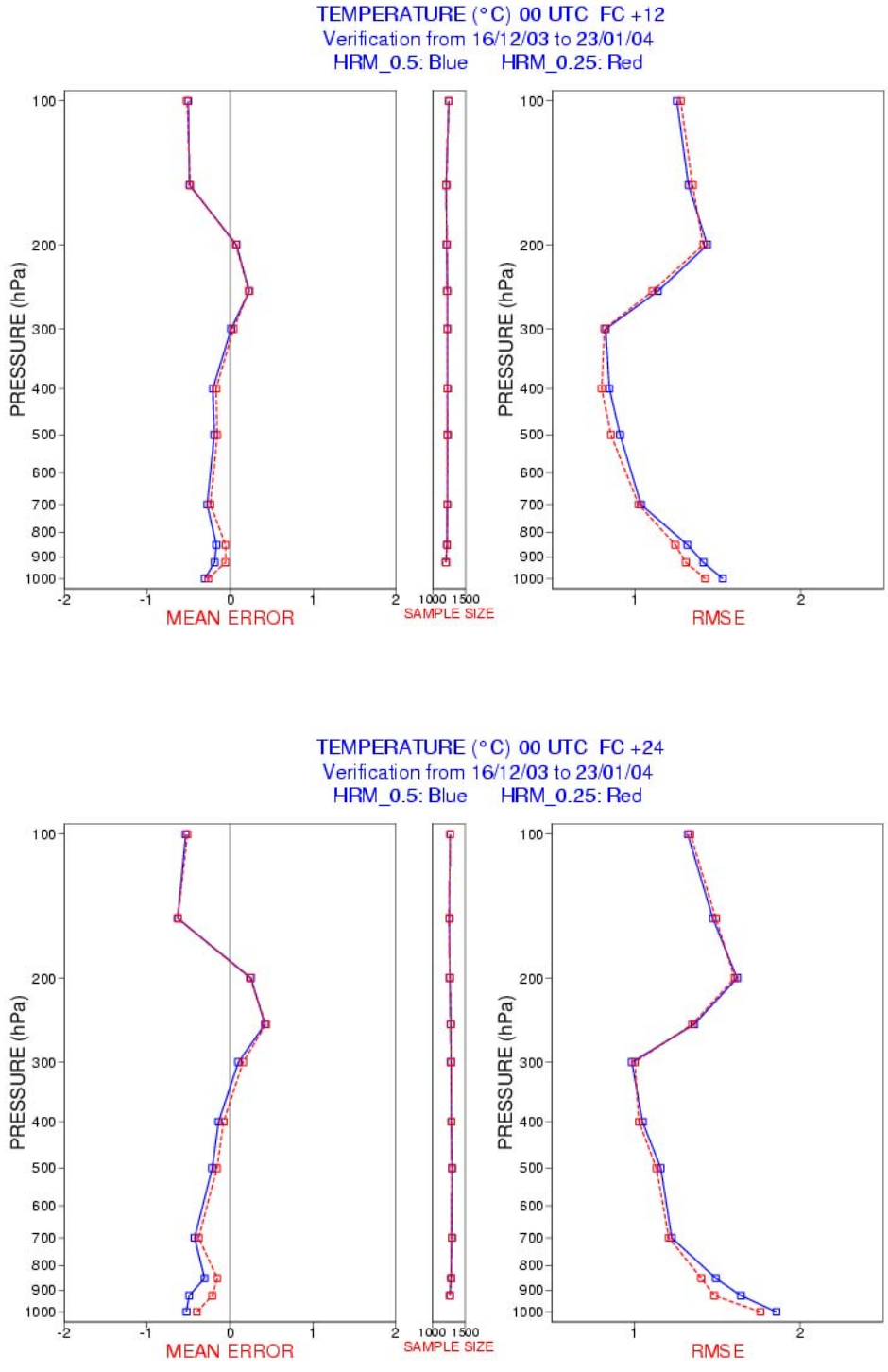

Figure 4.2 Temperature ME and RMSE of EUROHRM forecasts with 0.5˚ (blue) and 0.25˚ (red) resolution verified against radiosoundings: T+12h (top) and T+24h (bottom).

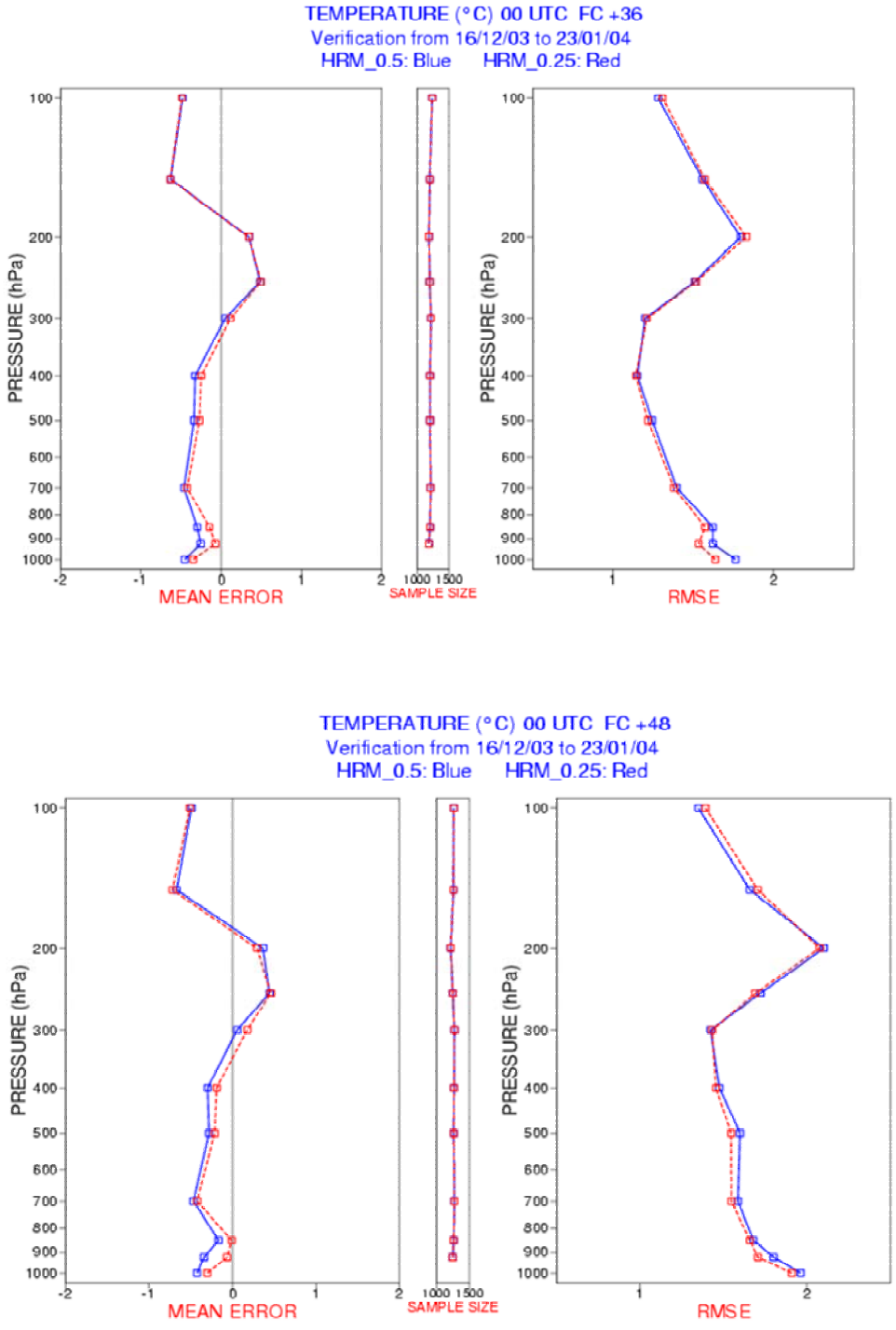

Figure 4.3 Temperature ME and RMSE of EUROHRM forecasts with 0.5˚ (blue) and 0.25˚ (red) resolution verified against radiosoundings: T+36h (top) and T+48h (bottom).

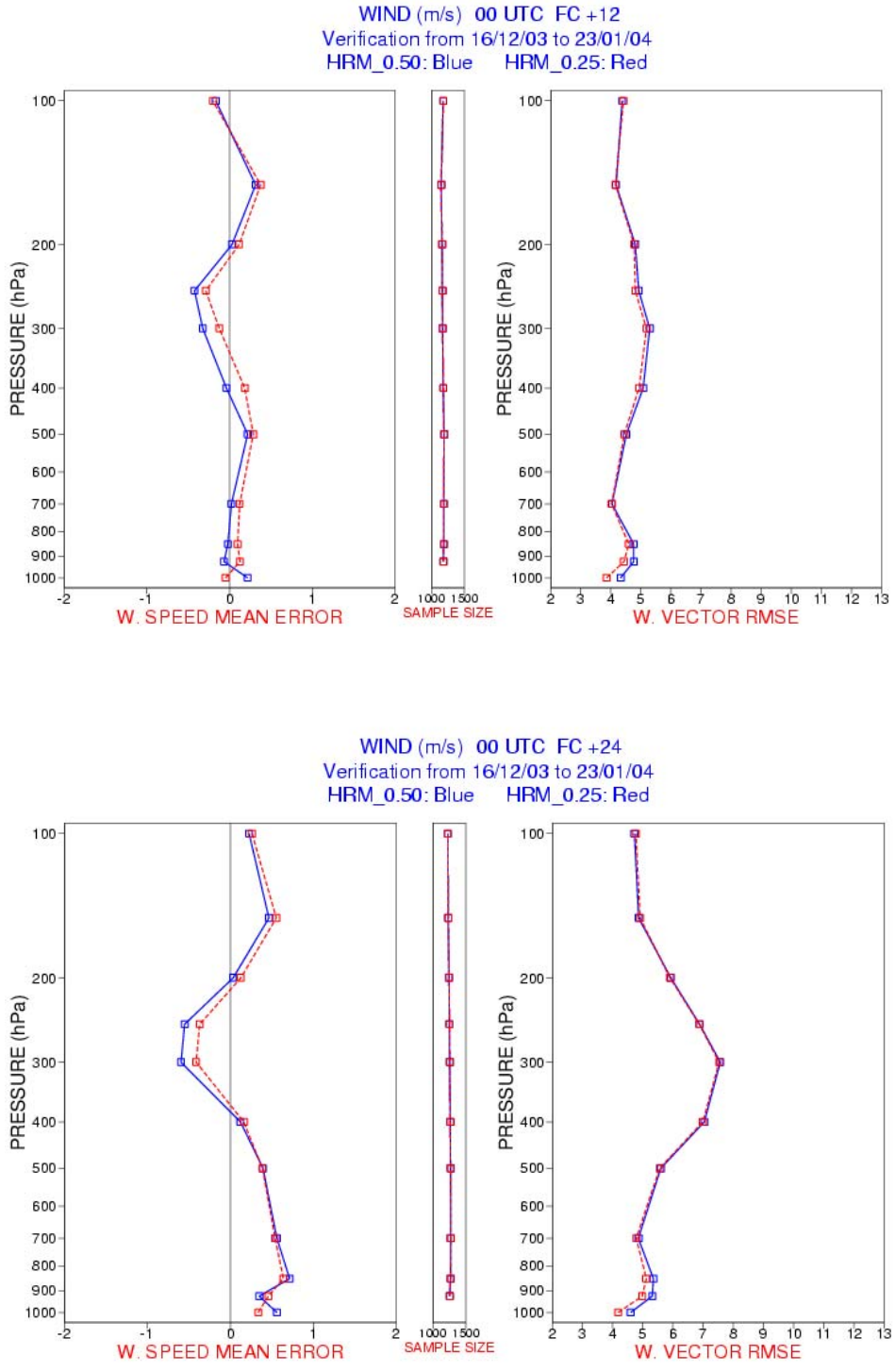

Figure 4.4 Wind speed ME and wind vector RMSE of EUROHRM forecasts with 0.5˚ (blue) and 0.25˚ (red) resolution verified against radiosoundings: T+12h (top) and T+24h (bottom).

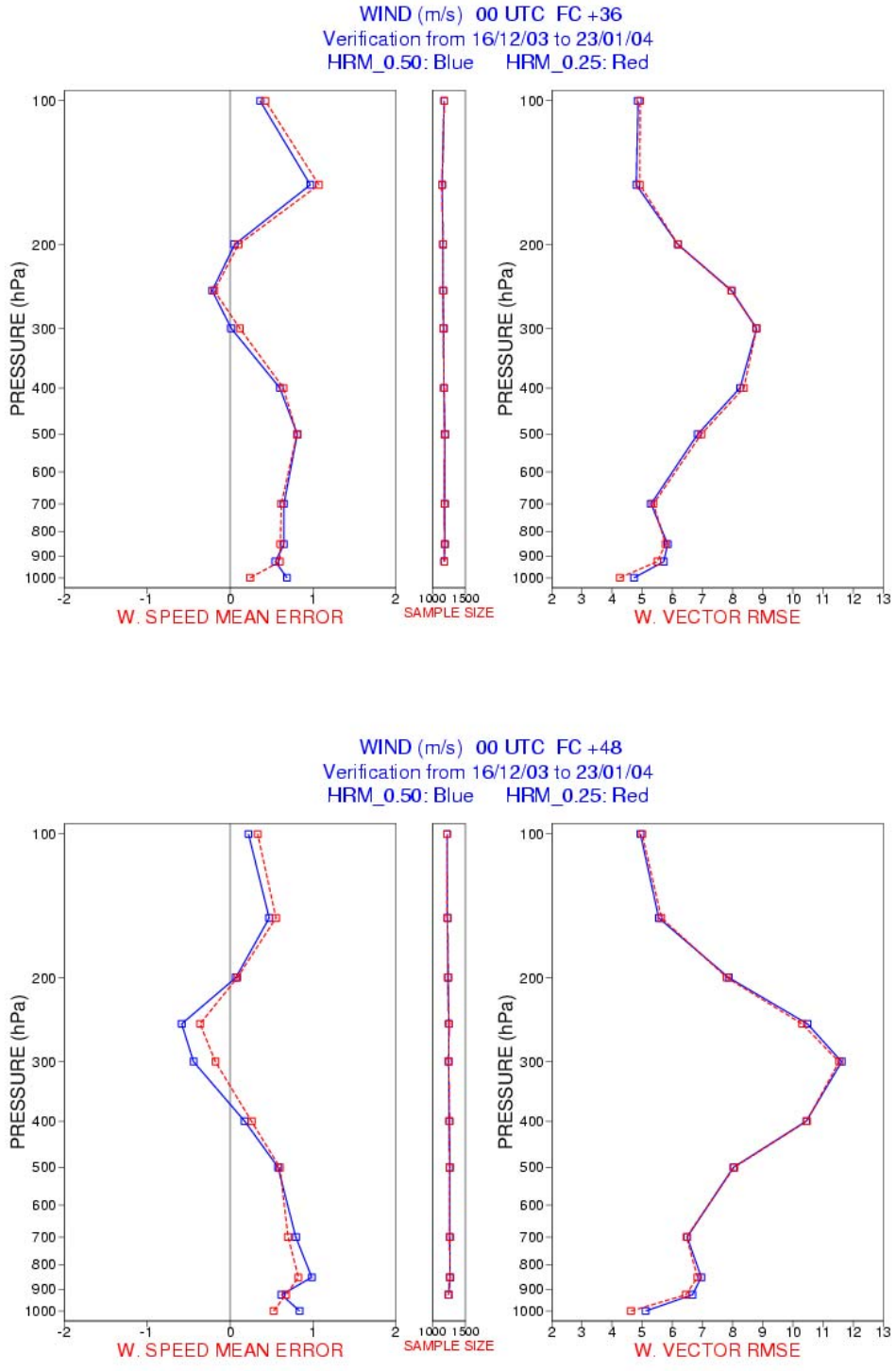

Figure 4.5 Wind speed ME and wind vector RMSE of EUROHRM forecasts from 0.5˚ (blue) and 0.25˚ (red) resolution verified against radiosoundings: T+36h (top) and T+48h (bottom).

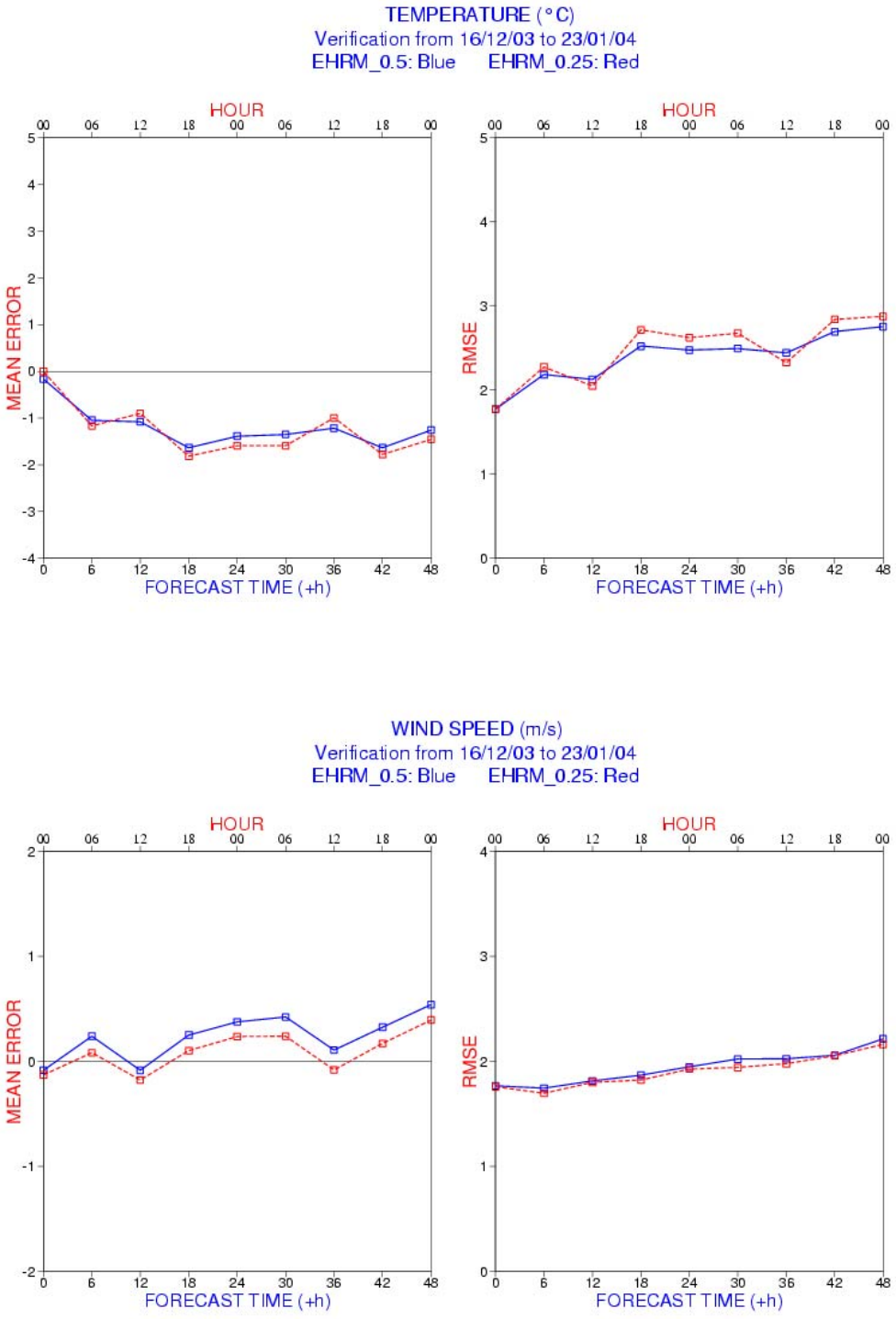

Figure 4.6 ME and RMSE of EUROHRM forecasts with 0.5˚ (blue) and 0.25˚ (red) resolution verified against lowland SYNOP observations: 2m temperature (top) and 10m wind speed (bottom).

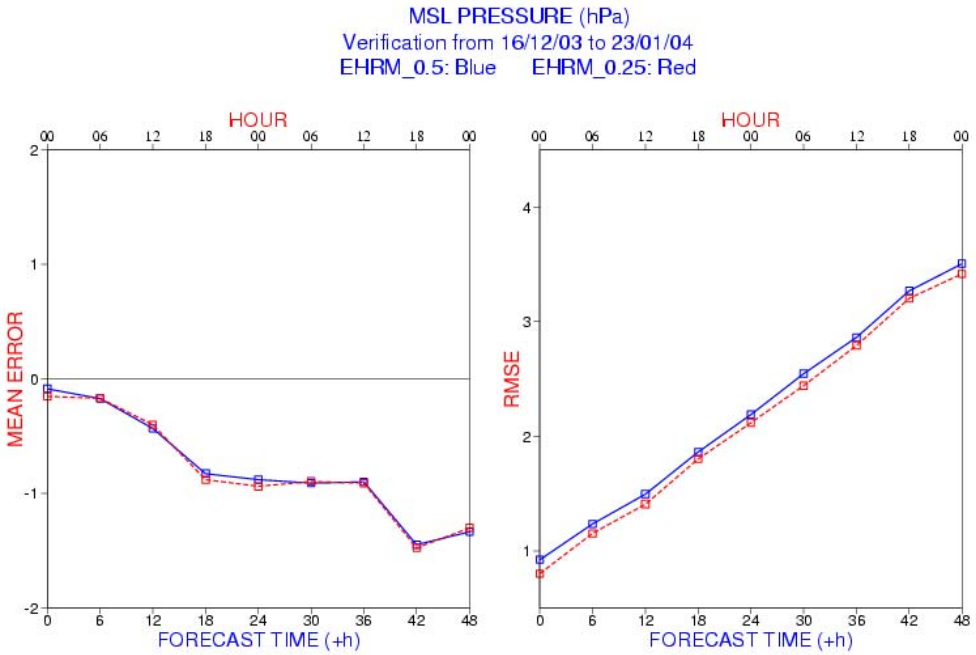

Figure 4.7 Mean sea level pressure ME and RMSE of EUROHRM forecasts with 0.5˚ (blue) and 0.25˚ (red) resolution verified against lowland SYNOP observations.

2. Quikscat Wind Data Assimilation

Quikscat retrieved 10m winds from KNMI are used in the multivariate (surface pressure and wind vectors) 2D-Var objective analysis of the surface pressure field. KNMI winds have a resolution of 100 km covering the eastern part of the Atlantic at around 6 and 18 UTC (Fig. 4.8). These data have been considered as conventional surface wind observations: the observation operator consists of a spatial interpolator of the post-processed surface wind forecast field of the HRM model.

Results from a statistical comparison in the period 08 December 2003 – 24 January 2004 are plotted in Fig. 4.9-4.12. Blue and red lines represent scores for the runs without and with the ingestion of Quikscat winds, respectively. No significant differences

are evident in the RMSE and ME vertical profiles of temperature and wind forecasts at T+12h, T+24h, T+36h and T+48h.

A slight positive impact in the surface parameters (Fig. 4.13-4.14) is found for the mean sea level pressure starting from T+18h onwards. This is understandable in view of the fact that the improvement of the model representation of oceanic weather system can be gauged only when they cross a dense synoptic land networks (about 24 hours later the assimilation). Though the absolute value of the forecast skill is small (≈ 0.1 hPa), it must be considered that the conventional surface network in place in the analysis domain is relatively dense. That the Quikscat winds, which are mostly available over the analysis domain only twice a day, are able to provide even marginal positive impact is remarkable and a clear indication of their potential in more sparsely observed oceanic areas.

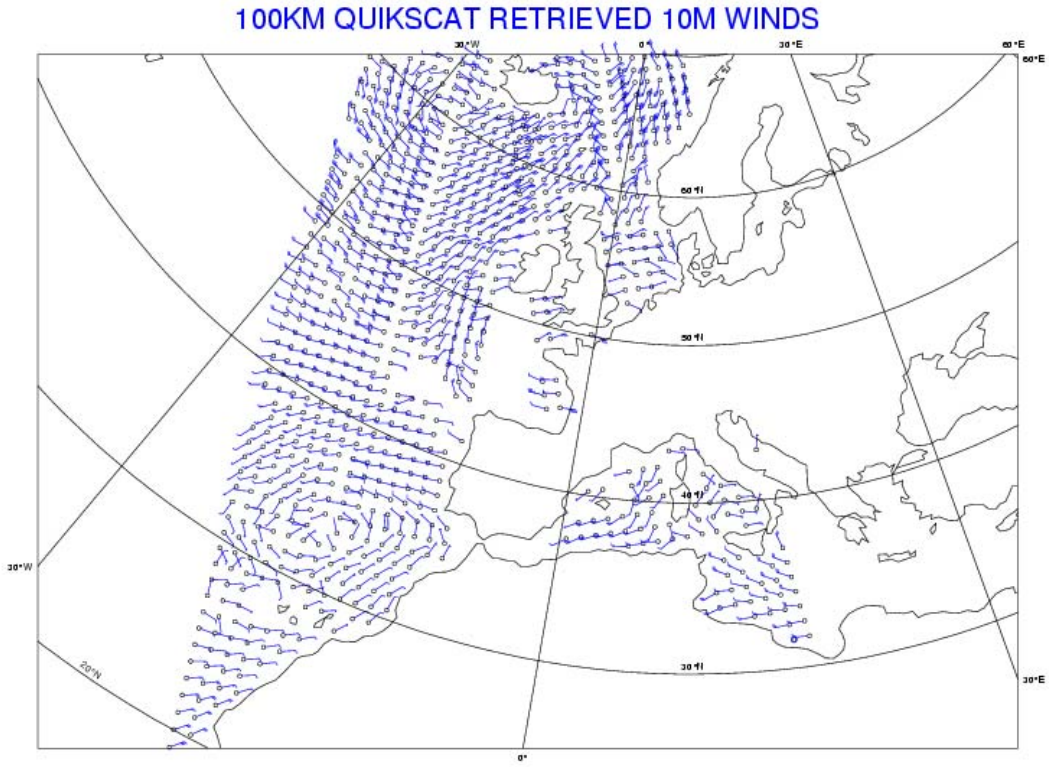

Figure 4.8 Typical coverage of KNMI 100 km Quikscat retrieved winds at 18 UTC.

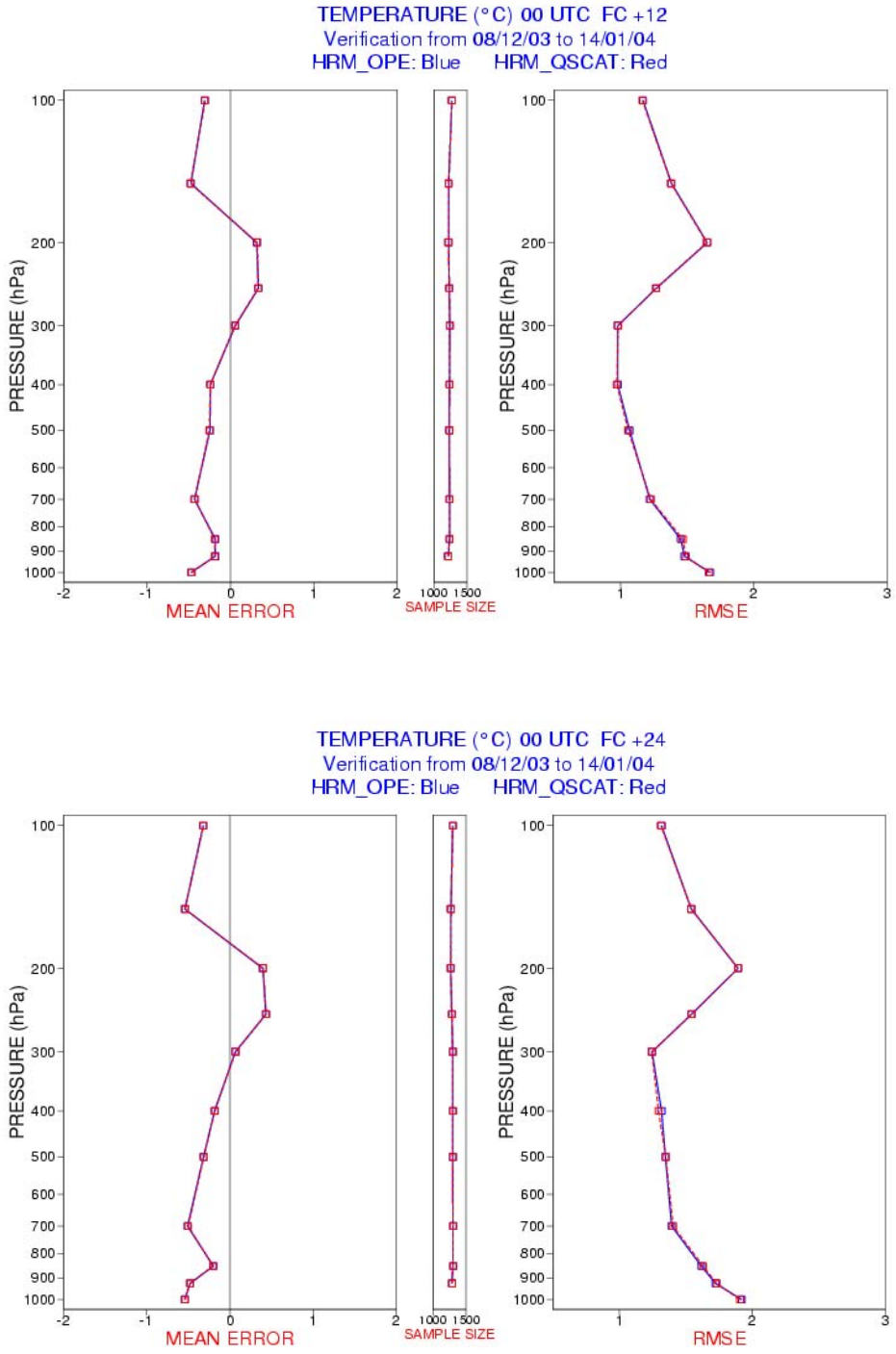

Figure 4.9 Temperature ME and RMSE of EUROHRM forecasts from CNMCA 3DVar analysis with (blue) and without (red) the ingestion of Quikscat retrieved winds verified against radiosoundings: T+12h (top) and T+24h (bottom).

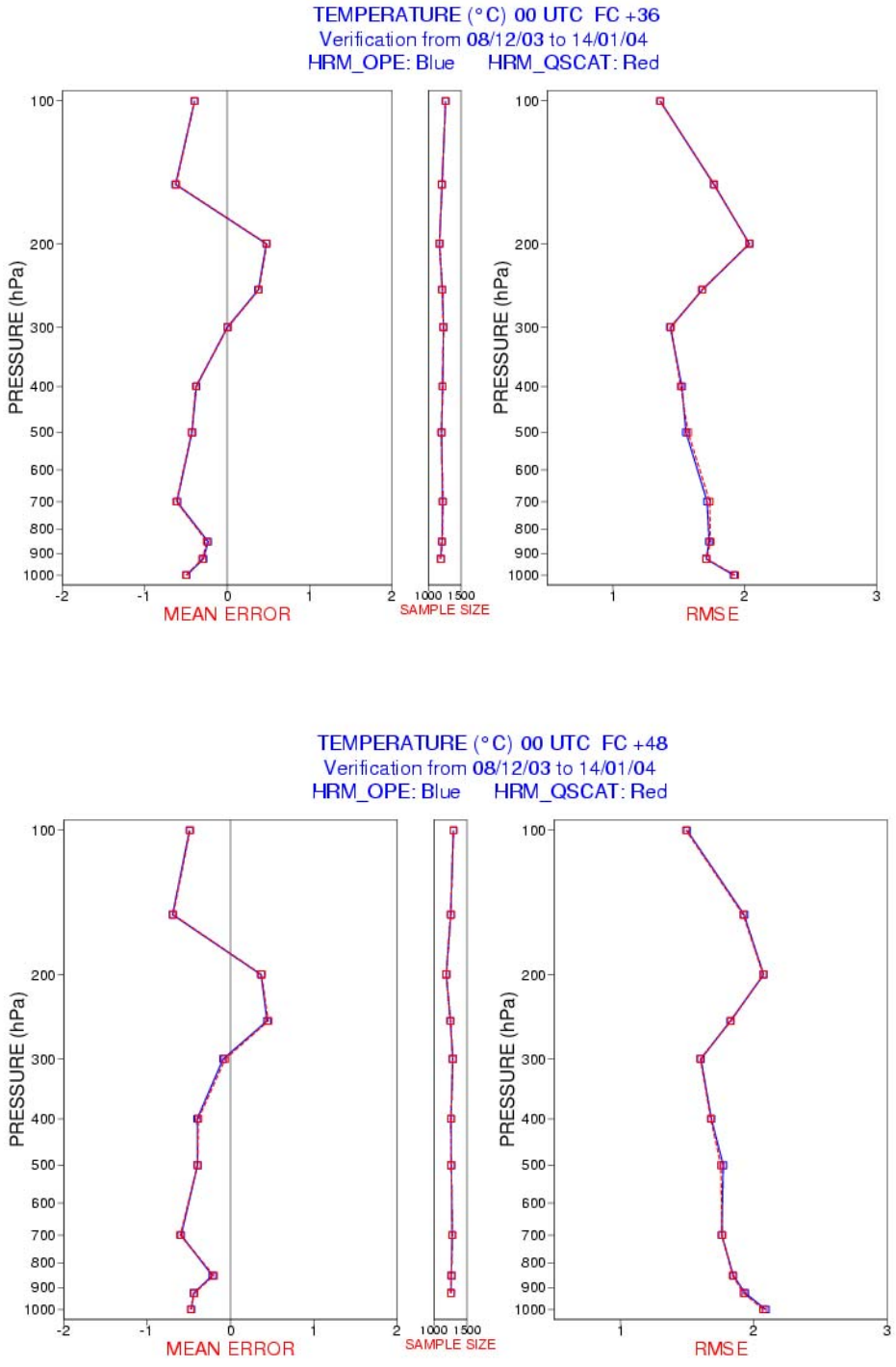

Figure 4.10 Temperature ME and RMSE of EUROHRM forecasts from CNMCA 3DVar analysis with (blue) and without (red) the ingestion of Quikscat retrieved winds verified against radiosoundings: T+36h (top) and T+48h (bottom).

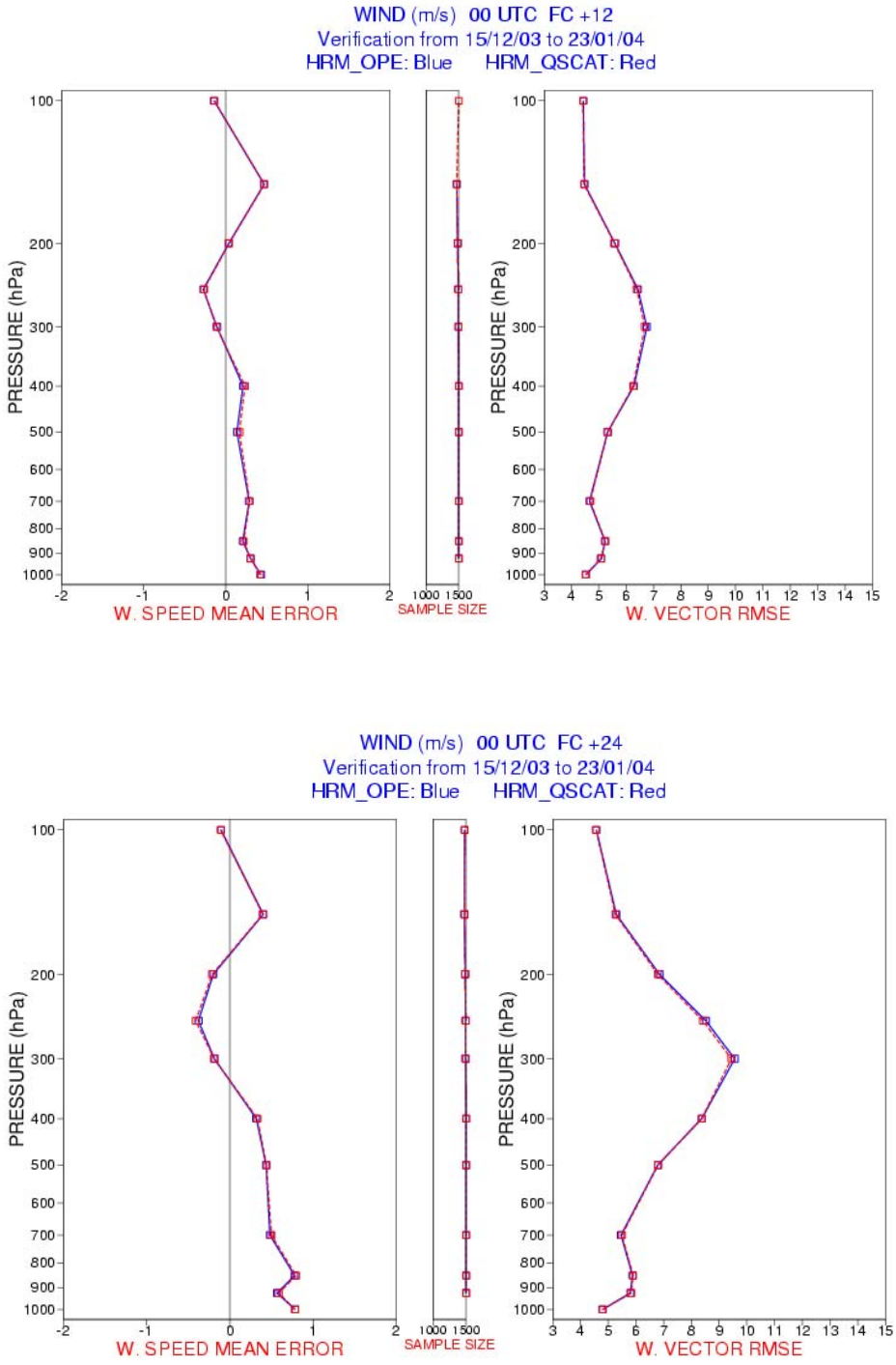

Figure 4.11 Wind speed ME and wind vector RMSE of EUROHRM forecasts from CNMCA 3DVar analysis with (blue) and without (red) the ingestion of Quikscat retrieved winds verified against radiosoundings: T+12h (top) and T+24h (bottom).

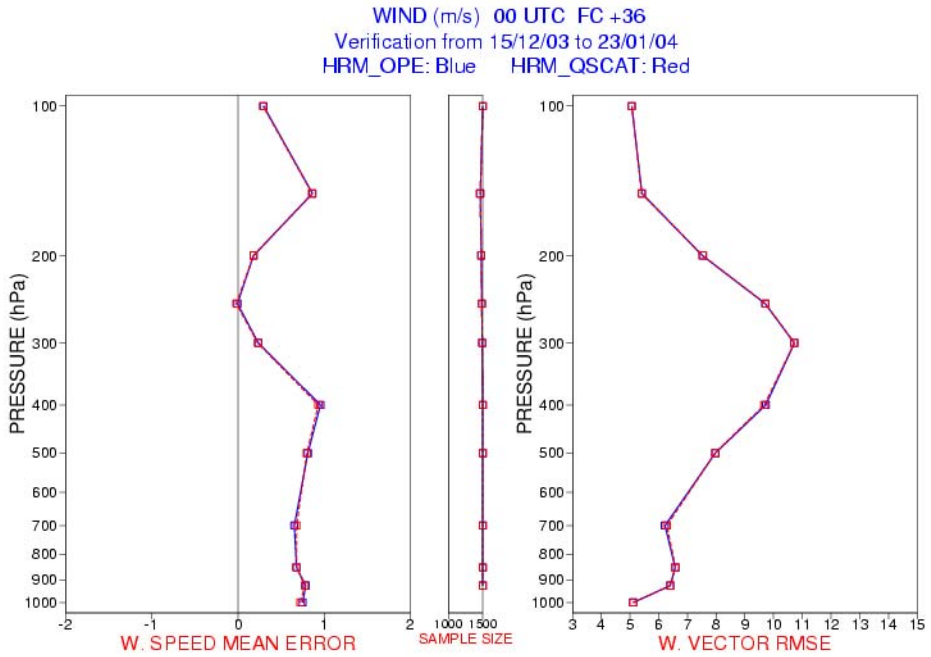

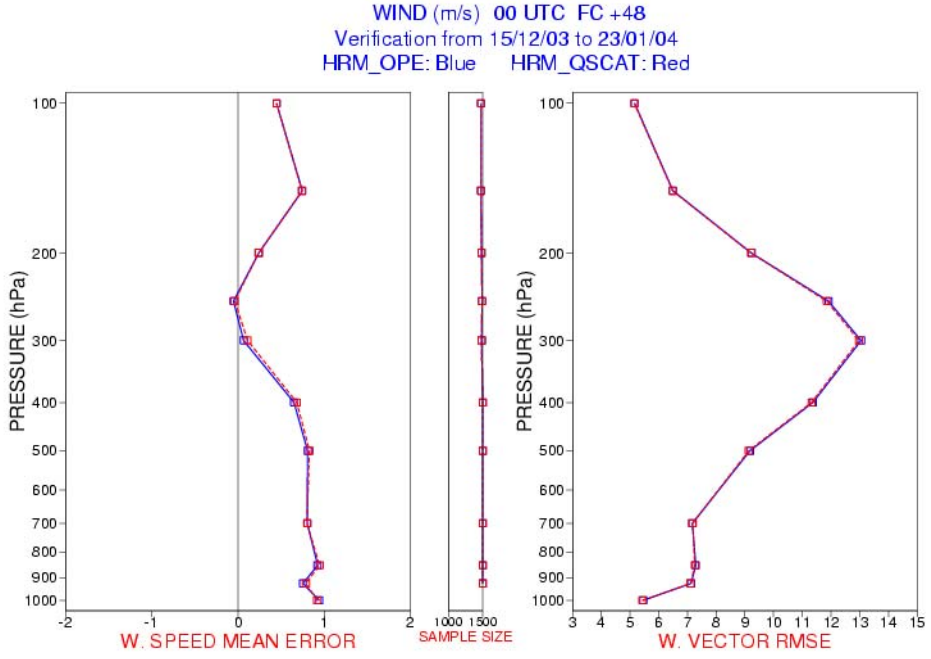

Figure 4.12 Wind speed ME and wind vector RMSE of EUROHRM forecasts from CNMCA 3DVar analysis with (blue) and without (red) the ingestion of Quikscat retrieved winds verified against radiosoundings: T+36h (top) and T+48h (bottom).

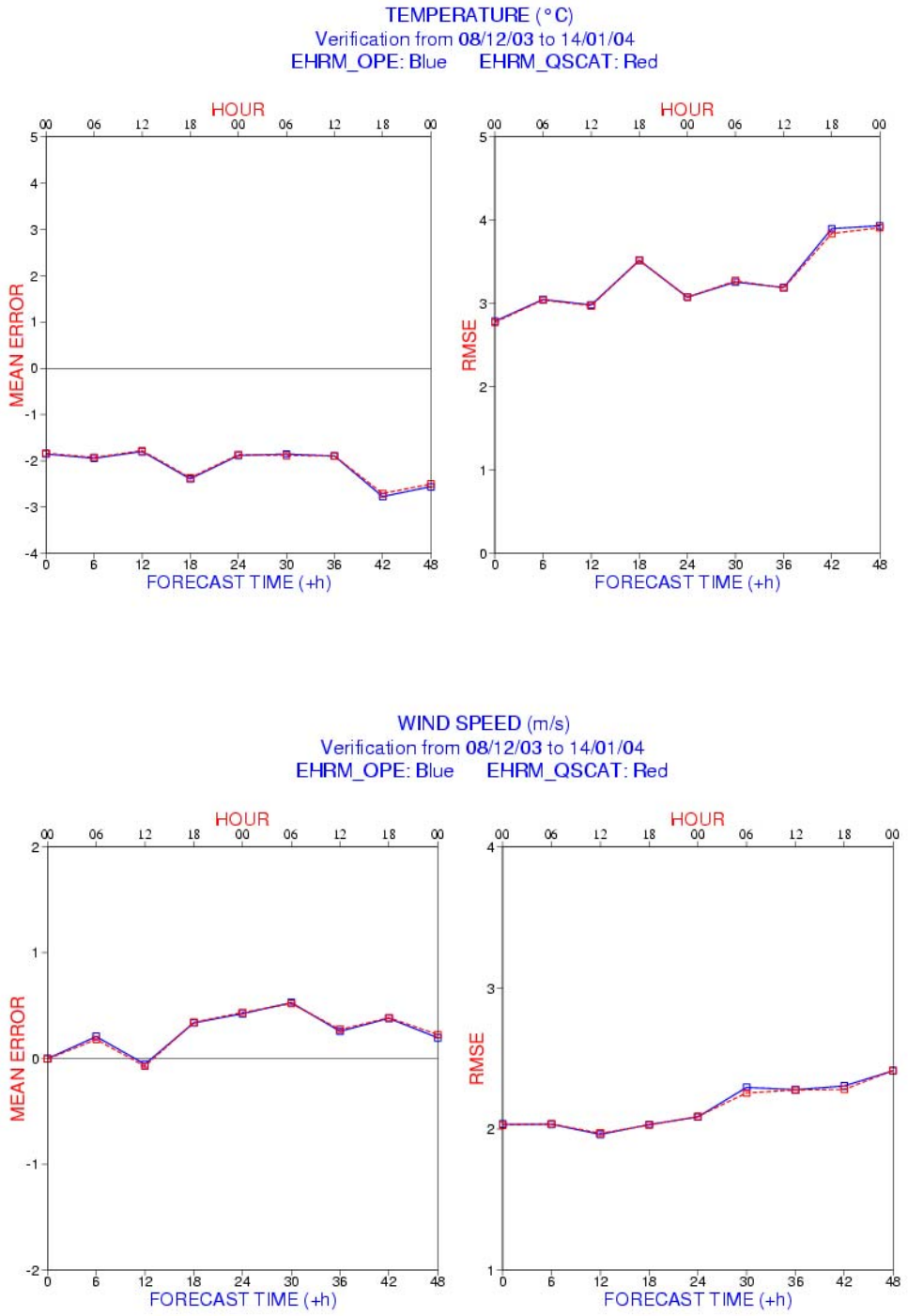

Figure 4.13 ME and RMSE of EUROHRM forecasts from CNMCA 3DVar analysis with (blue) and without (red) ingestion of Quikscat retrieved winds verified against lowland SYNOP observations: 2m temperature (top) and 10m wind speed (bottom).

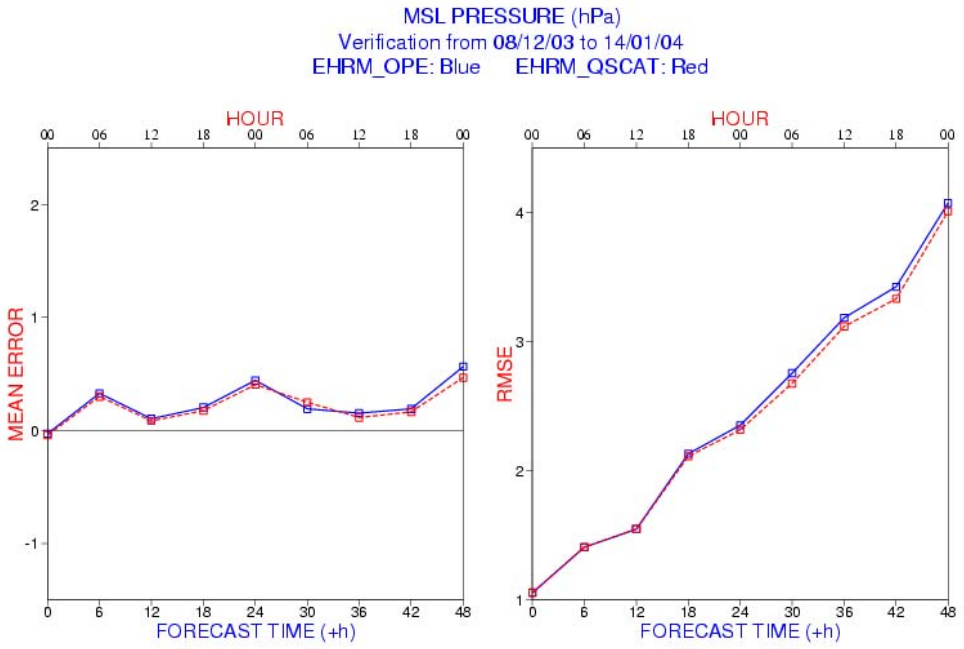

Figure 4.14 Mean sea level pressure ME and RMSE of EUROHRM forecasts from CNMCA 3DVar analysis with (blue) and without (red) ingestion of Quikscat retrieved winds verified against lowland SYNOP observations.

3. Aircraft Data Assimilation

Aircraft based observations (AMDAR and AIREP) available within the time window are assimilated in the CNMCA data assimilation system. Horizontal (40 km) and vertical (30 hPa) observational thinning is also performed. A typical coverage of aircraft based observations in 11-13 UTC time window is showed in Fig.4.15.

The statistical evaluation of the impact of aircraft data in the CNMCA NWP system was performed during the period 05 January 2004 – 21 February 2004. The ME and RMSE vertical profiles of temperature and wind forecasts at T+12h, +24h, +36h and +48h are plotted in Fig. 4.16-4.19. Green and red lines represent scores for runs without and with the ingestion of aircraft data, respectively.

The aircraft data have a positive impact in the temperature and wind vector accuracy in layer 200 - 850 hPa, where the most of these data are collocated. From the

T+36h the improvement extends also above and below this layer. A significant impact is found on the wind speed ME, which is reduced in the 100 – 850 hPa layer.

Verification results for the surface parameters are plotted in Fig. 4.20-4.21. A clear and positive impact is found on the mean sea level pressure from the T+18h to the T+48h. No significant differences are found in the 2m temperature, while the accuracy of the 10m wind speed is slightly reduced after T+24h.

4. AMV Data Assimilation

An example of the coverage of AMVs in the layer 300-700 hPa at 12UTC is showed in Fig.4.22. Meteosat AMVs are used in the CNMCA NWP system after a selection procedure to blacklist unwanted data. The selection rules applied in this procedure are listed below:

1. time window: only analysis time;
2. derivation method: high resolution visible, high resolution and clear sky water vapor;
3. land mask: over ocean, over land only if south of 35N and above 600 hPa, in order to allow their usage over North Africa;
4. quality indicator: MPEF QI above 0.8 in case of water vapor winds or above 0.6 in case of visible winds;
5. wind speed: above 2.5 m/s;
6. thinning: within a box of 120 km (horizontal) and 20 hPa (vertical), priority to the maximum QI.

Some of the rules chosen are subjective but derived from the experience of other centers.

The statistical evaluation of the impact of AMV in the CNMCA NWP system was performed for the same period of the impact of aircraft data (05 January 2004 – 21 February 2004). The ME and RMSE vertical profiles of temperature and wind for EURO-

HRM forecasts (T+12h, +24h, +36h and +48h) from analysis without (green lines) or with (blue lines) the ingestion of AMV data are plotted in the same figures (Fig. 4.16-4.19) considered for the aircraft data impact study. From the inspection of these figures, it is evident that the ingestion of AMV data in the CNMCA NWP system has a similar impact to that of the aircraft data. Minor differences are found in the temperature RMSE around 250 – 300 hPa and in the wind vector RMSE in the layer 200 – 500 hPa, where AMV data seems to have a very slight improvement compared to the aircraft data. On the other hand the wind speed bias of forecasts from analysis with the assimilation of AMV data at T+48h is slightly increased in the 300 – 500 layer and in the stratosphere compared with that of forecasts from analysis with the ingestion of aircraft data.

Similar results to that obtained for aircraft data are found for the surface parameter verification (Fig. 4.20-4.21). AMV data have a slight improvement in the mean sea level pressure bias compared with aircraft data.

From these results it can be argued that aircraft and AMV data have a very similar impact on forecast skill in the Euro-Atlantic area.

In this experiment AMVs are considered unbiased data, but it is well known that AMVs have long exhibited considerable speed biases against model data or other observations (Bormann, Kelly and Thepaut, 2002). The geographical characteristics are well established, such as a slow bias (about 1-5 m/s) above 400 hPa in the extra tropics and a fast bias (1-3 m/s) at 700-400 hPa in the tropics. While some seasonality is observed with a stronger extra-tropical bias for winter, the general zonal pattern is fairly constant. The slow speed bias is not accompanied by a similarly significant directional bias.

The bias and standard deviation evaluation of the wind speed innovation increments (observation minus background) was also performed in this experiment and the results are plotted in Fig. 4.24. These results show the typical slow bias in the higher levels found in the extra tropics. Currently, the origin of the speed bias is not well understood. The most commonly suspected reasons are: problems in the height assignment, clouds that are not acting as passive tracers, or deficiencies in the observation operator. A bias correction scheme based on known characteristics of the AMVs is necessary for an optimal use of these data.

A simple bias correction scheme has been implemented the CNMCA 3DVar data assimilation system. A description of this scheme and its results are provided in the AMV Data Assimilation with Bias Correction section.

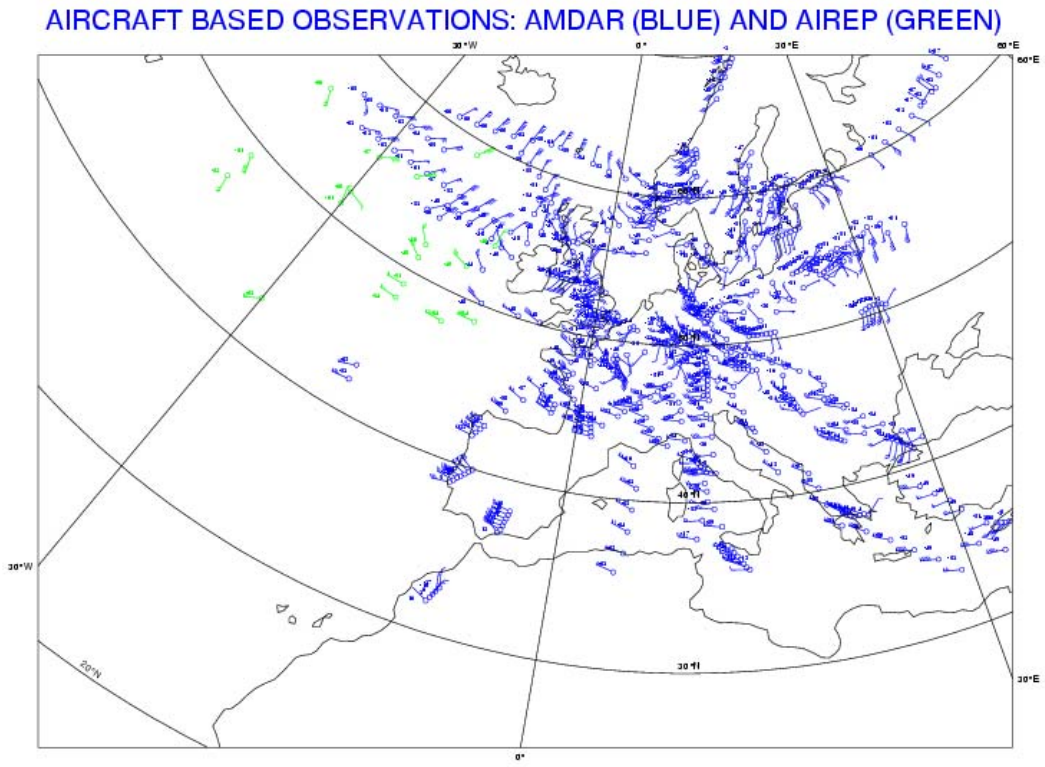

Figure 4.15 Typical coverage of aircraft based observations in 11-13 UTC time window: AMDAR (blue) and AIREP (green).

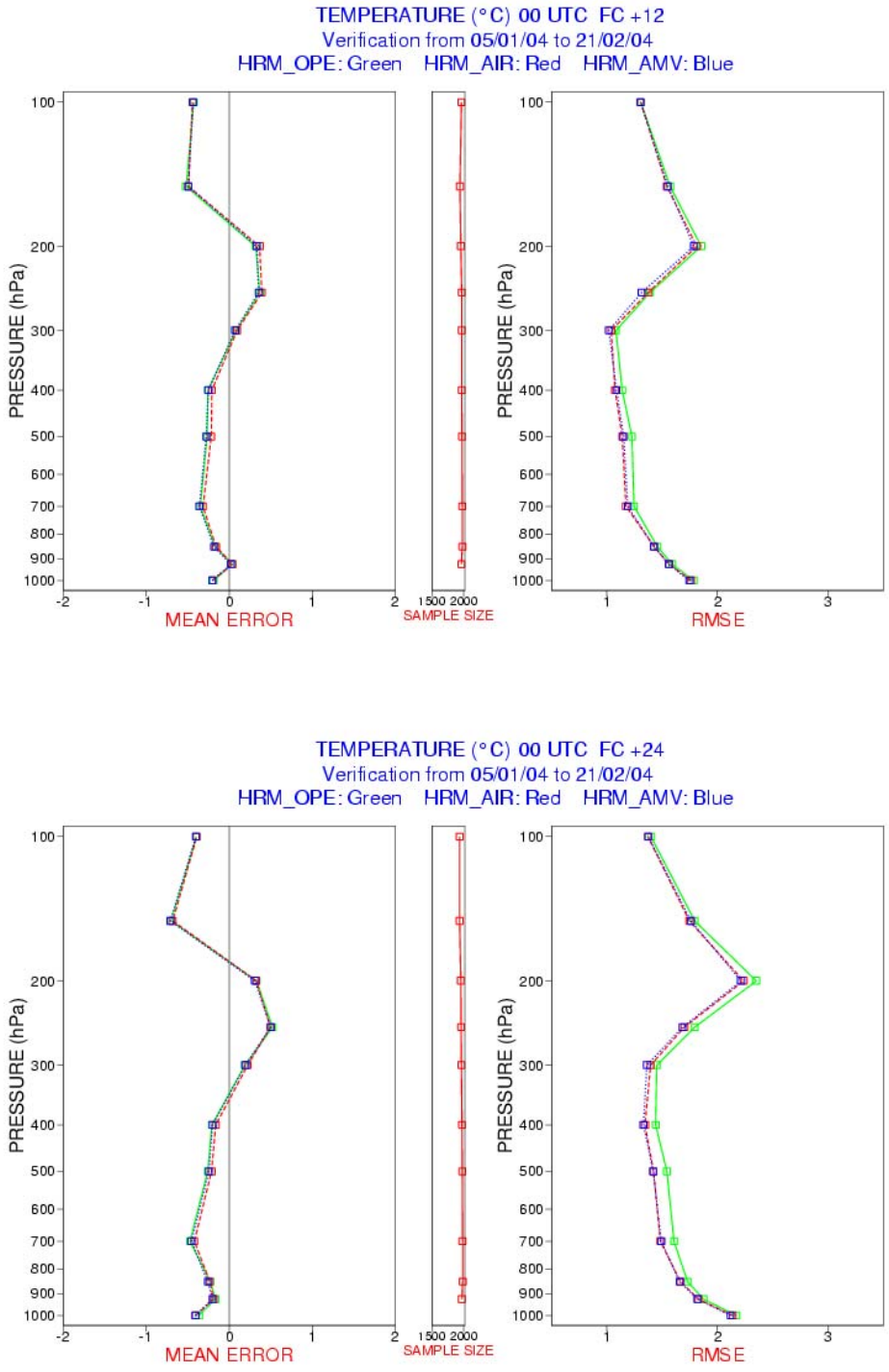

Figure 4.16 Temperature ME and RMSE of EUROHRM forecasts from CNMCA 3DVar analysis without (green) and with the ingestion of aircraft (red) or AMV (blue) data verified against radiosoundings: T+12h (top) and T+24h (bottom).

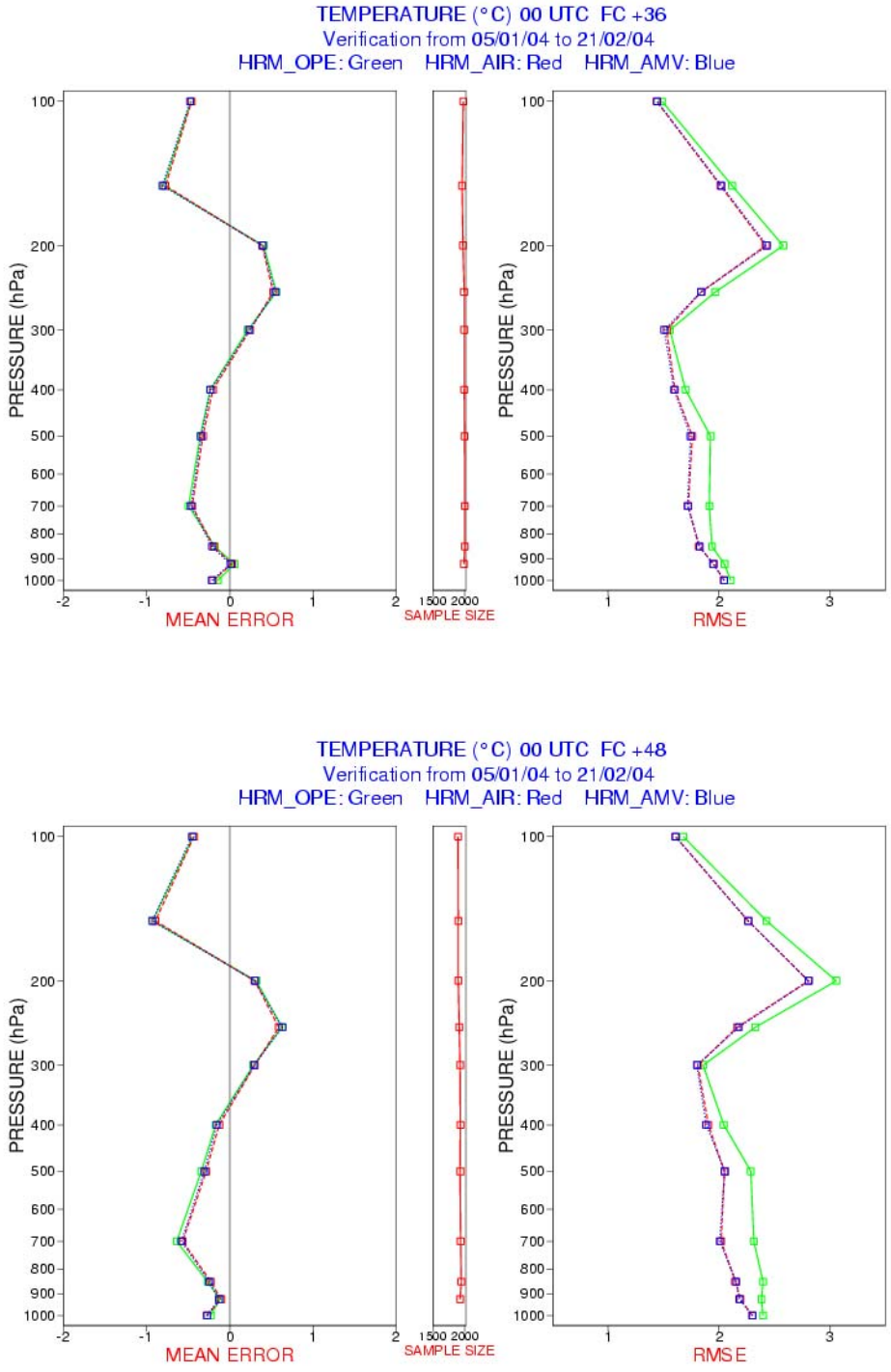

Figure 4.17 Temperature ME and RMSE of EUROHRM forecasts from CNMCA 3DVar analysis without (green) and with the ingestion of aircraft (red) or AMV (blue) data verified against radiosoundings: T+36h (top) and T+48h (bottom).

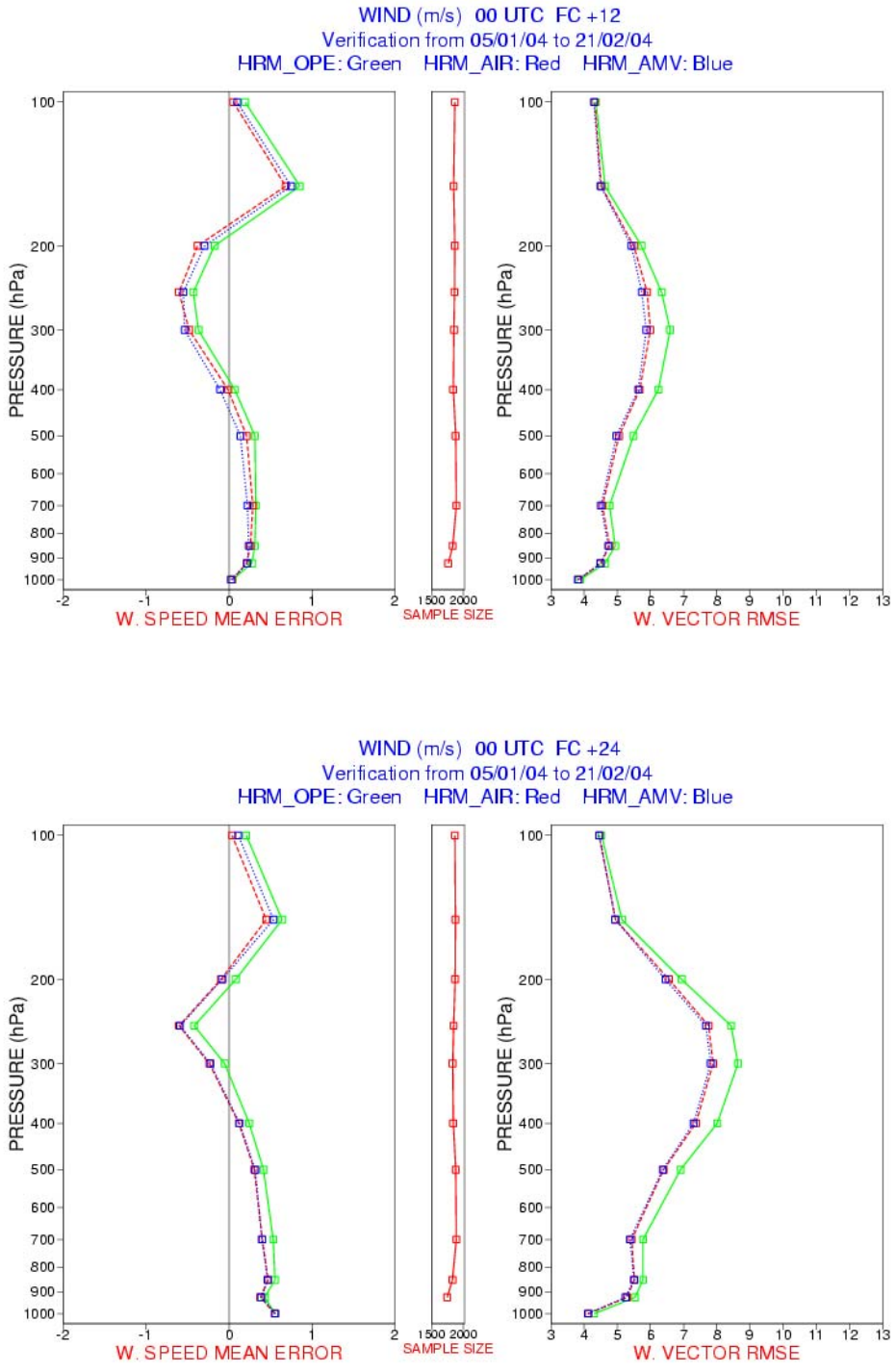

Figure 4.18 Wind speed ME and wind vector RMSE of EUROHRM forecasts from CNMCA 3DVar analysis without (green) and with the ingestion of aircraft (red) or AMV (blue) data verified against radiosoundings: T+12h (top) and T+24h (bottom).

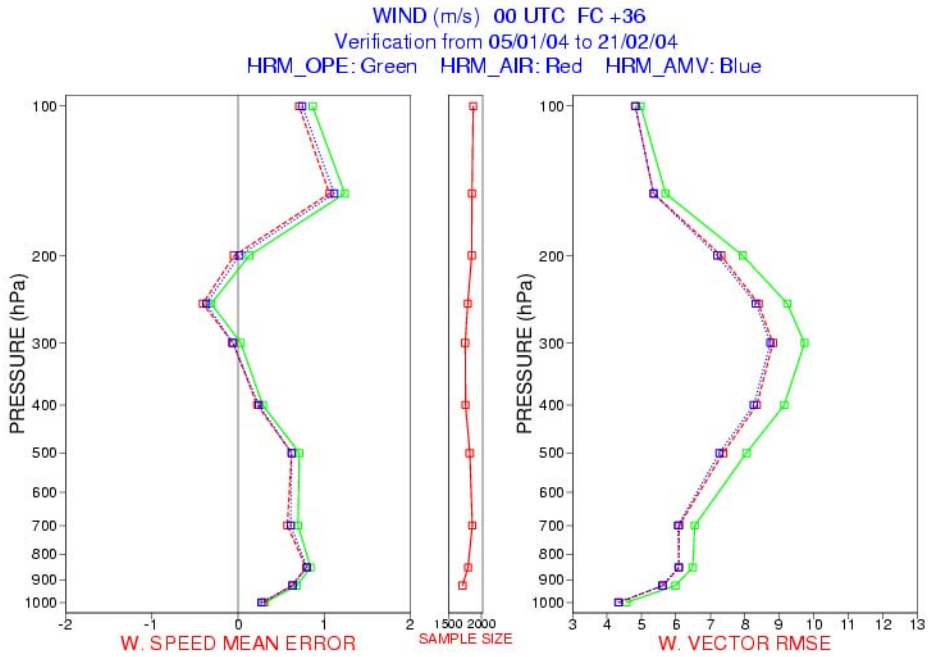

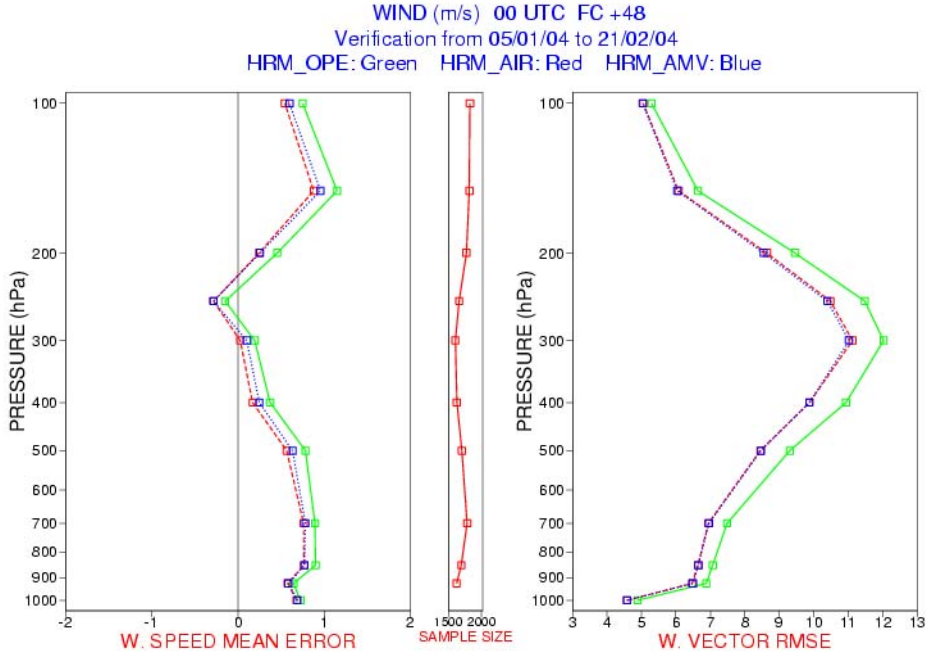

Figure 4.19 Wind speed ME and wind vector RMSE of EUROHRM forecasts from CNMCA 3DVar analysis without (green) and with the ingestion of aircraft (red) or AMV (blue) data verified against radiosoundings: T+36h (top) and T+48h (bottom).

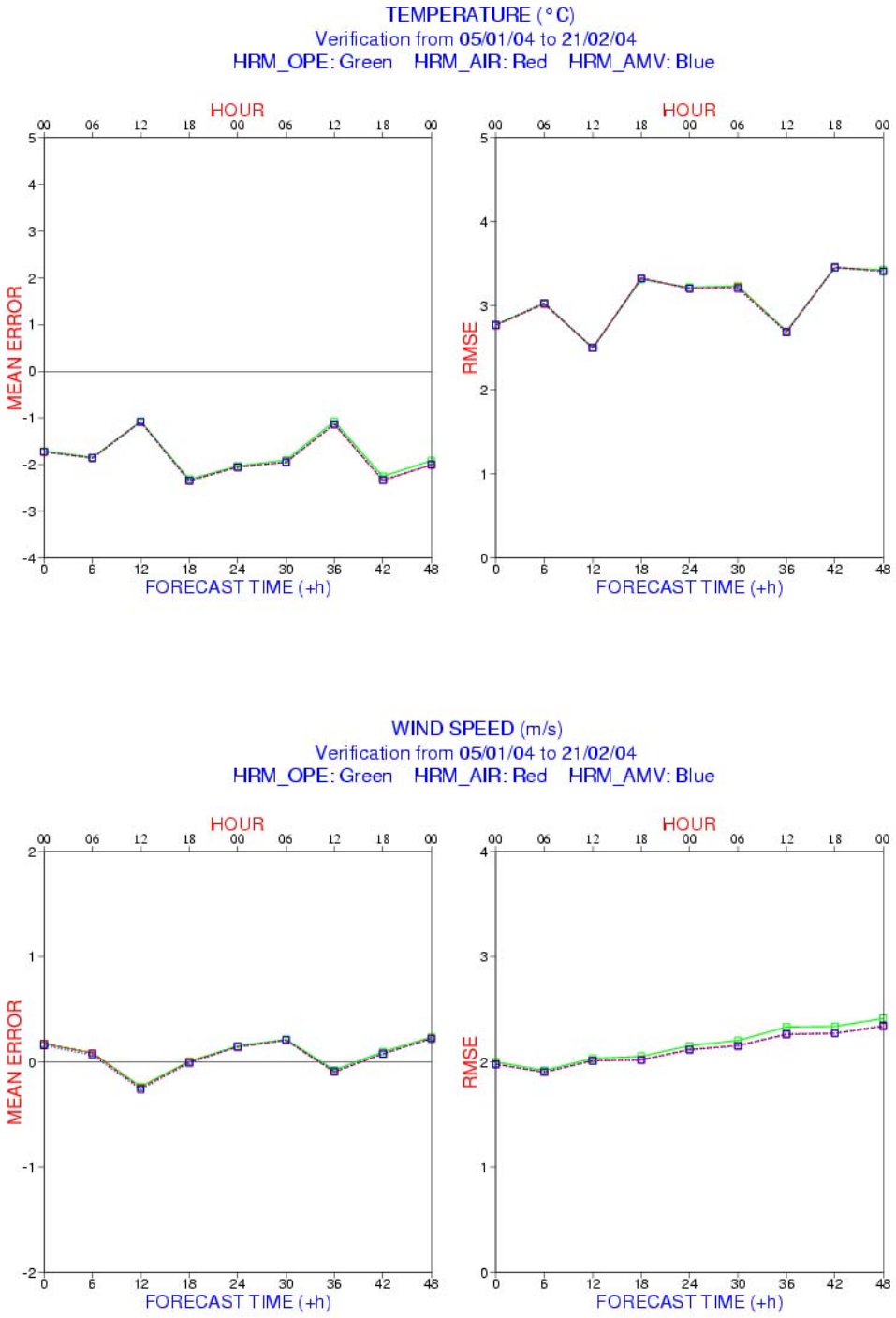

Figure 4.20 ME and RMSE of EUROHRM forecasts from CNMCA 3DVar analysis without (green) and with the ingestion of aircraft (red) or AMV (blue) data observations verified against lowland SYNOP observations: 2m temperature and 10m wind speed.

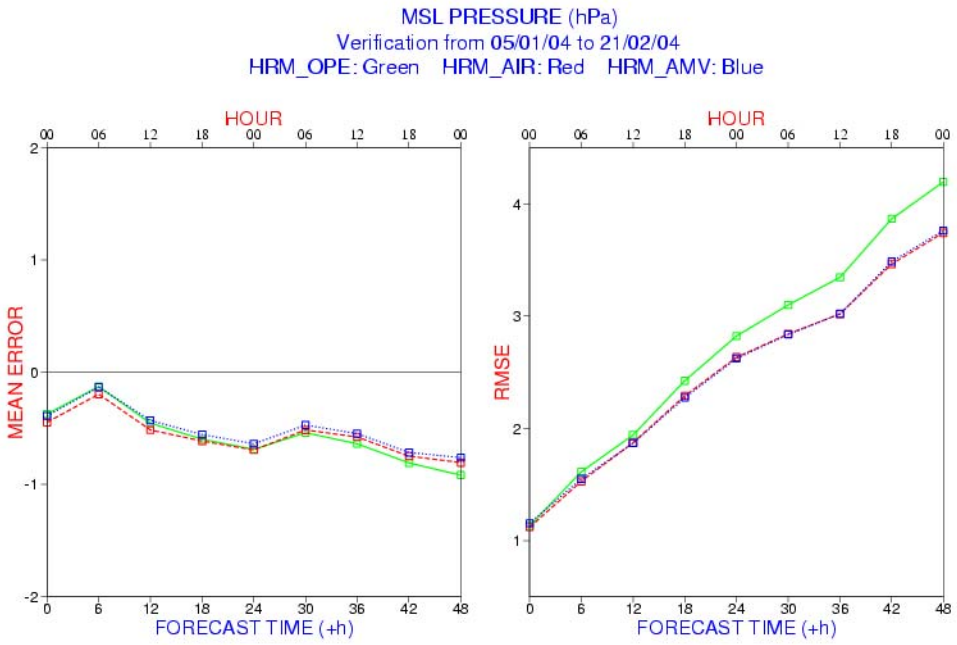

Figure 4.21 Mean sea level pressure ME and RMSE of EUROHRM forecasts from CNMCA 3DVar analysis without (green) and with the ingestion of aircraft (red) or AMV (blue) data verified against lowland SYNOP observations.

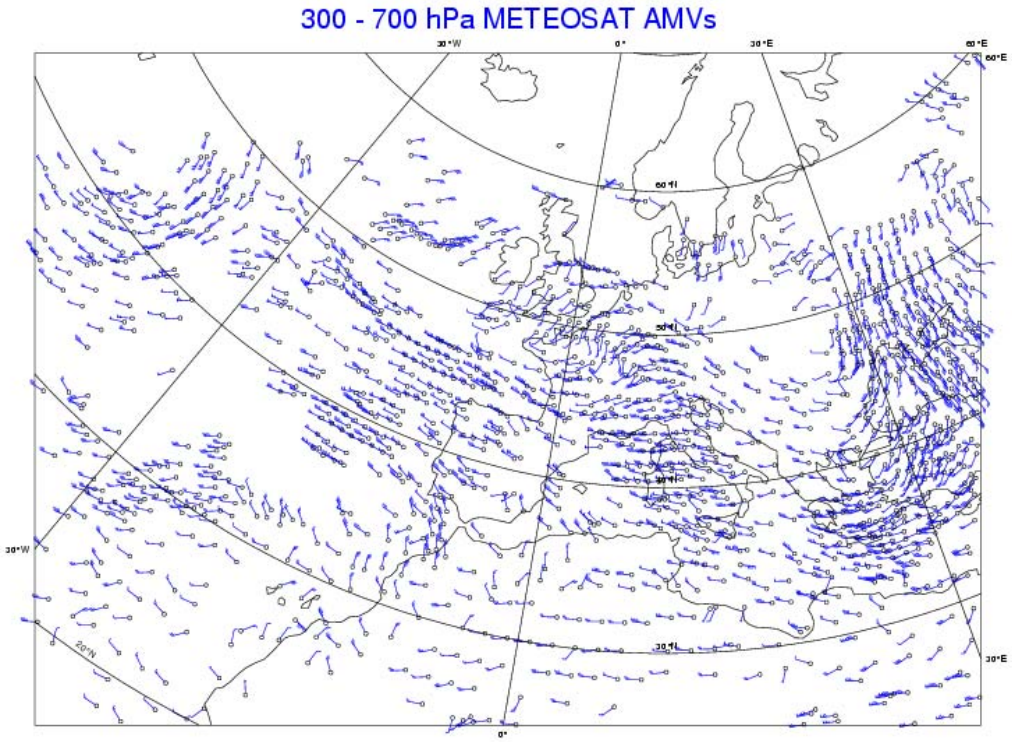

Figure 4.22 Example of the coverage of 300-700 hPa Meteosat AMVs at 12 UTC.

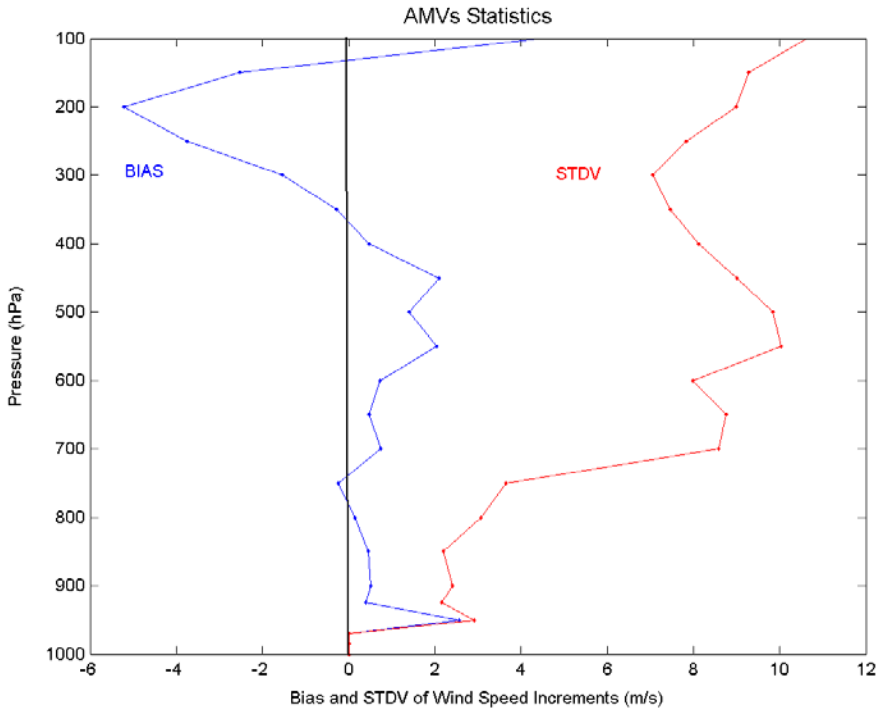

Figure 4.23 Wind speed bias and standard deviation for AMV observation increments.

5. Aircraft and AMV Data Assimilation

The statistical evaluation of the impact of AMV in a CNMCA NWP system assimilating also aircraft observations was performed in the period 21 February 2004 – 14 March 2004. The ME and RMSE vertical profiles of temperature and wind for EURO-HRM forecasts (T+12h, +24h, +36h and +48h) from analysis without (blue lines) or with (red lines) the ingestion of AMV data are plotted in figures Fig. 4.24-4.27. From the inspection of these figures, it is evident that the ingestion of AMV data in the CNMCA NWP system using also aircraft data has a positive impact in the layer 150-925 hPa. The wind speed bias of forecasts from analysis with the assimilation of AMV data at T+36-48h is slightly increased in the 250 – 850 layer. No significant differences are found for the 2m temperature and 10m wind speed (Fig. 4.28). AMV data determine a slight improvement in the mean sea level pressure RMSE after T+18h (Fig. 4.29).

It is clear from this experiment, that the CNMCA NWP system has a considerable improvement in the forecast skill from the ingestion of new observations, such as AMVs and aircraft data. The operational assimilation of these observations can be switched on, even if an increase of computational time has to be taken into account.

6. AMV Data Assimilation with Bias Correction

In the CNMCA 3DVar analysis algorithm the AMV observation operator used for the previous experiments has been an interpolation to the assigned pressure level and horizontal position. To account for the correction of the bias described in the AMV Data Assimilation section, a revised observation operator formulation has been necessary.

It is well known that the main error source in the AMV observations lies in the height assignment algorithm of the derived wind vectors. In order to tackle this difficulty and to try to correct the considerable bias with respect to the model first guess (see Fig. 4.23), the AMV observed height is corrected by a simple yet effective method.

A new observation height (in a range of 80 hPa centered on the reported AMV height) is derived by minimizing the cost function J, which measures the discrepancy between the AMV data and the model first guess corresponding values:

$$J = \left(\frac{u_0 - u_{fg}}{\Delta u} \right)^2 + \left(\frac{v_0 - v_{fg}}{\Delta v} \right)^2 + \left(\frac{p_0 - p_{fg}}{\Delta p} \right)^2 \qquad (4.4)$$

where $\Delta u = \Delta v = 3$m/s, $\Delta p = 60$hPa and $u_{o/fg}$,$v_{o/fg}$ and $p_{o/fg}$ are the observed/first-guess values of wind components and pressure.

The impact of this new AMV observation operator on the CNMCA 3DVar assimilation system using conventional, aircraft and AMV data was evaluated for the period 28 March 2004 – 16 April 2004. This experiment has resulted in a considerable decrease in the observation increments bias in the upper and lower levels (Fig.4.30) and in a measurable improvement in forecast skill as can be seen in Fig. 4.31-4.36. Blue and red lines represent scores for runs without and with the AMV bias correction scheme, respectively. The greatest positive impact is obviously on the wind field (Fig. 4.33-4.34), but a slight improvement is observed for the temperature (Fig. 4.31-4.32) and for the mean sea level pressure (Fig. 4.36).

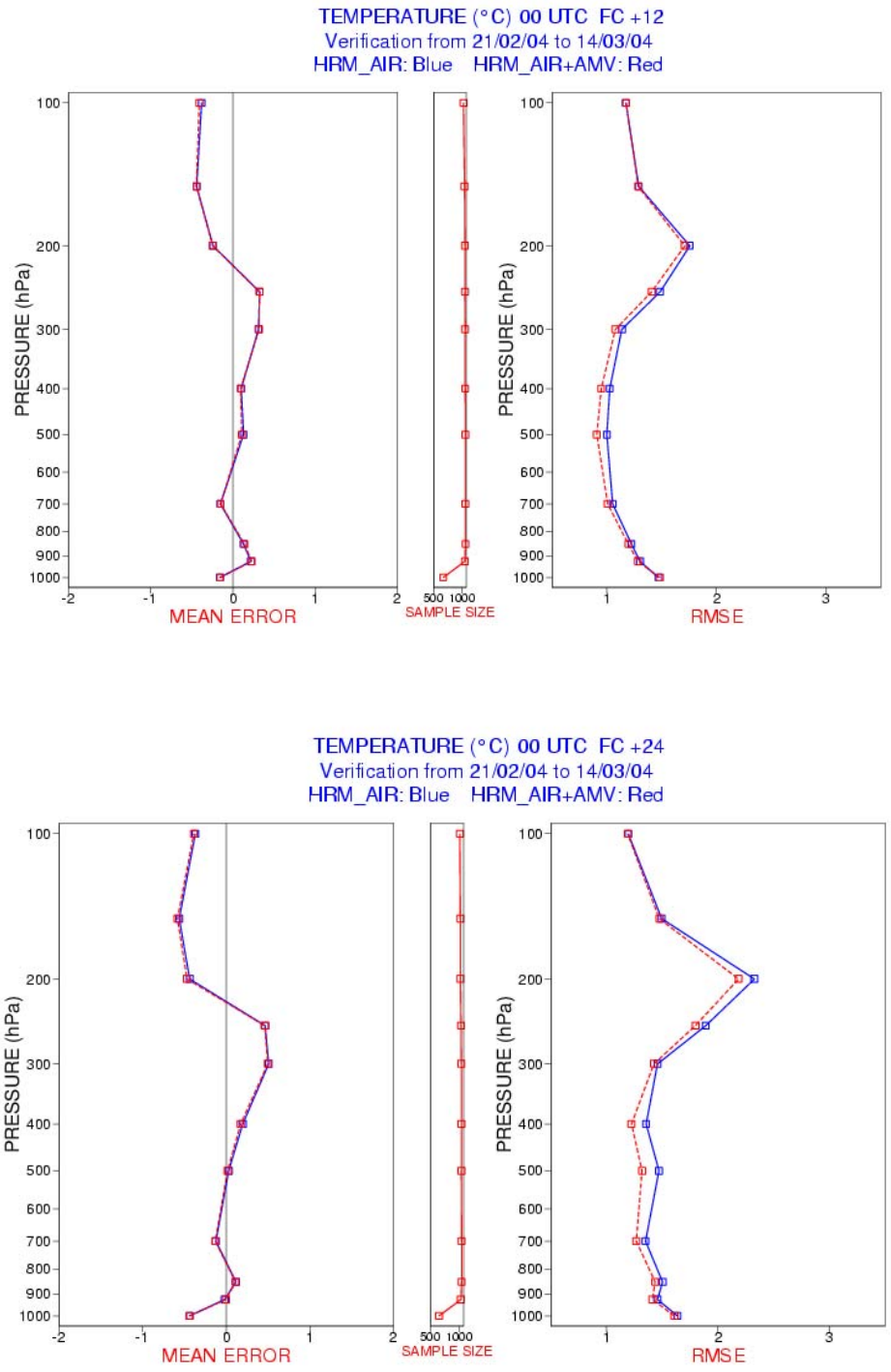

Figure 4.24 Temperature ME and RMSE of EUROHRM forecasts from CNMCA 3DVar analysis using aircraft observations with (red) and without (blue) the ingestion of AMV data verified against radiosoundings: T+12h (top) and T+24h (bottom).

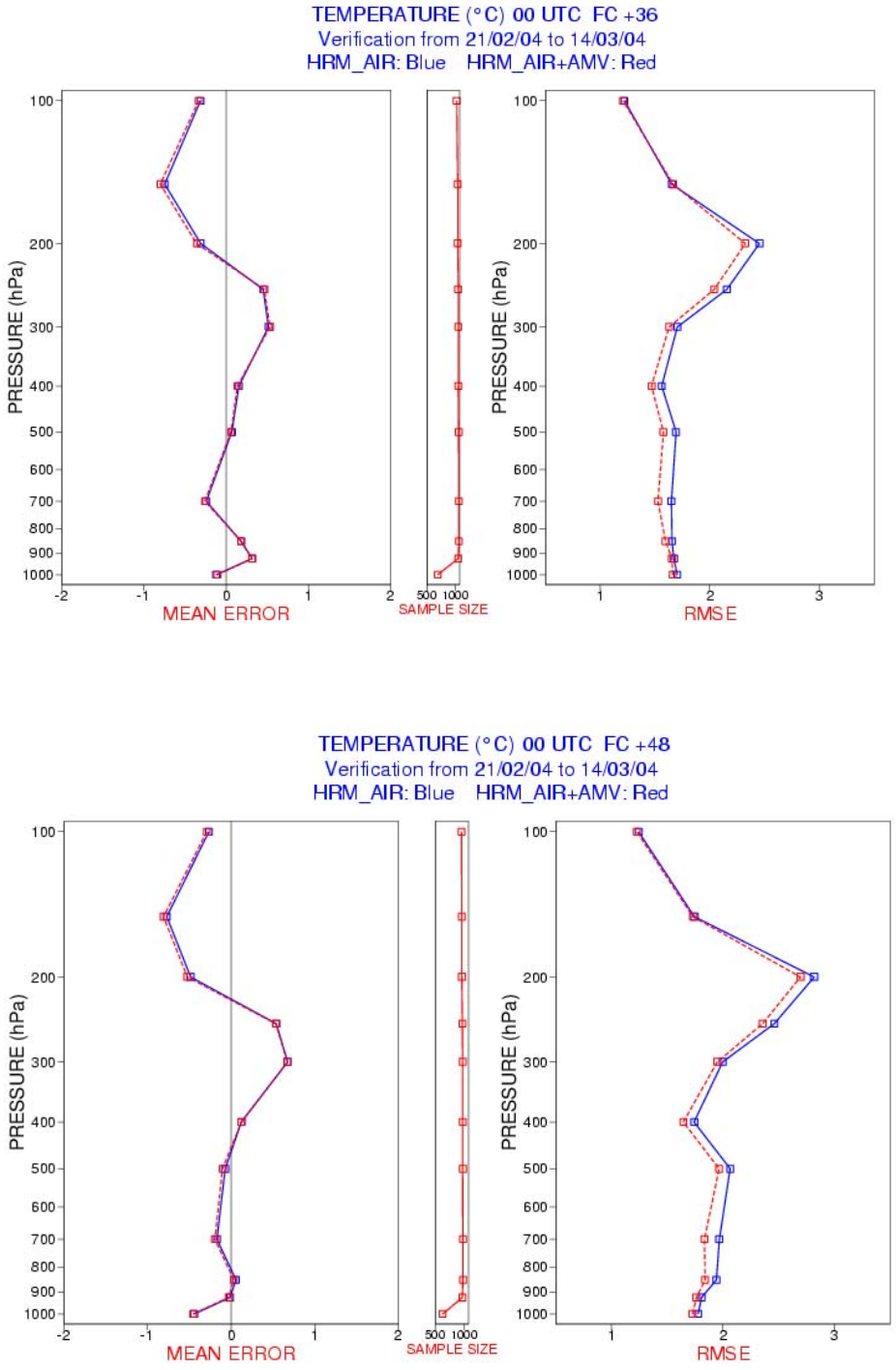

Figure 4.25 Temperature ME and RMSE of EUROHRM forecasts from CNMCA 3DVar analysis using aircraft observations with (red) and without (blue) the ingestion of AMV data verified against radiosoundings: T+36h (top) and T+48h (bottom).

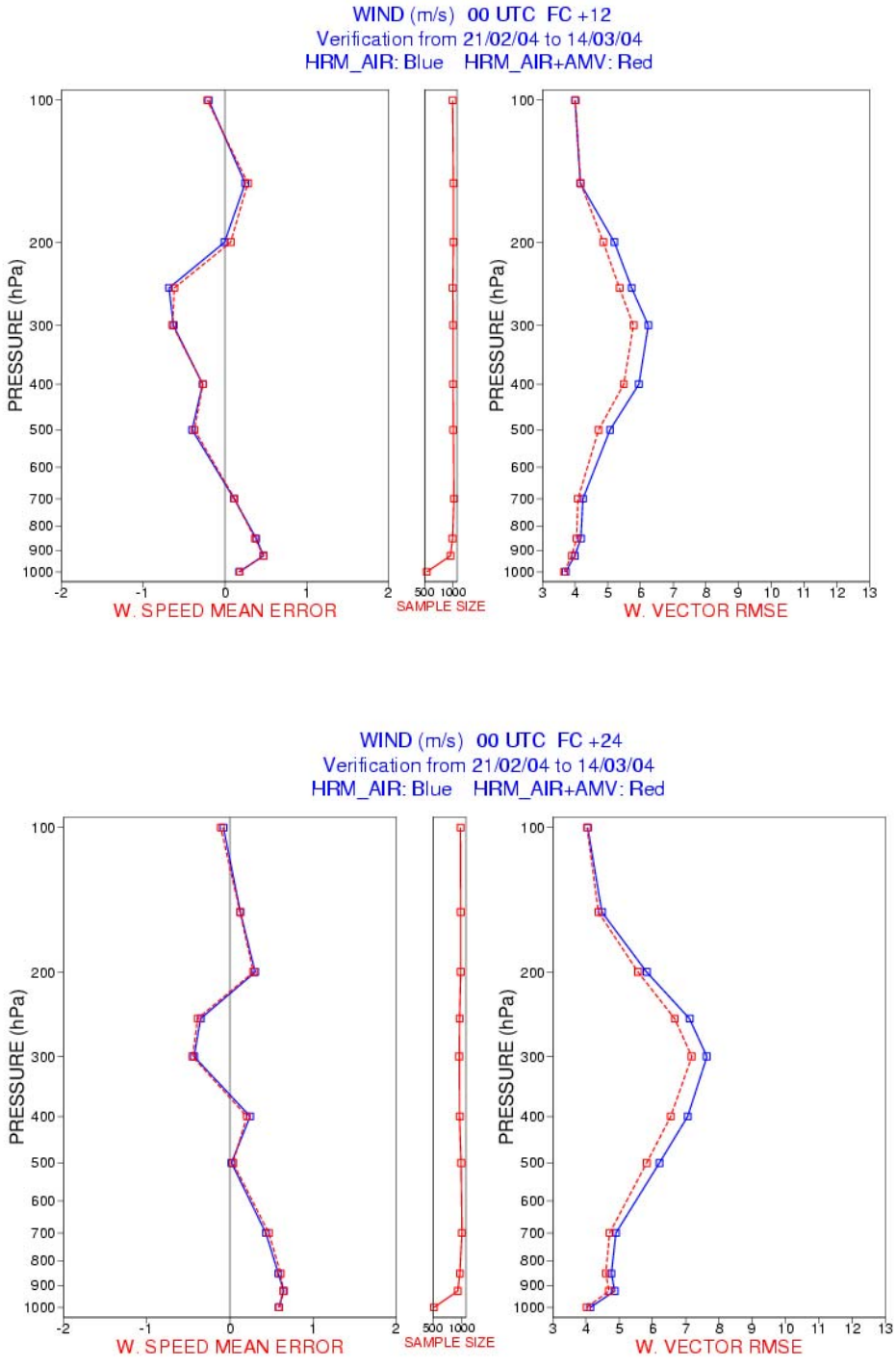

Figure 4.26 Wind speed ME and wind vector RMSE of EUROHRM forecasts from CNMCA 3DVar analysis using aircraft observations with (red) and without (blue) the ingestion of AMV data verified against radiosoundings: T+12h (top) and T+24h (bottom).

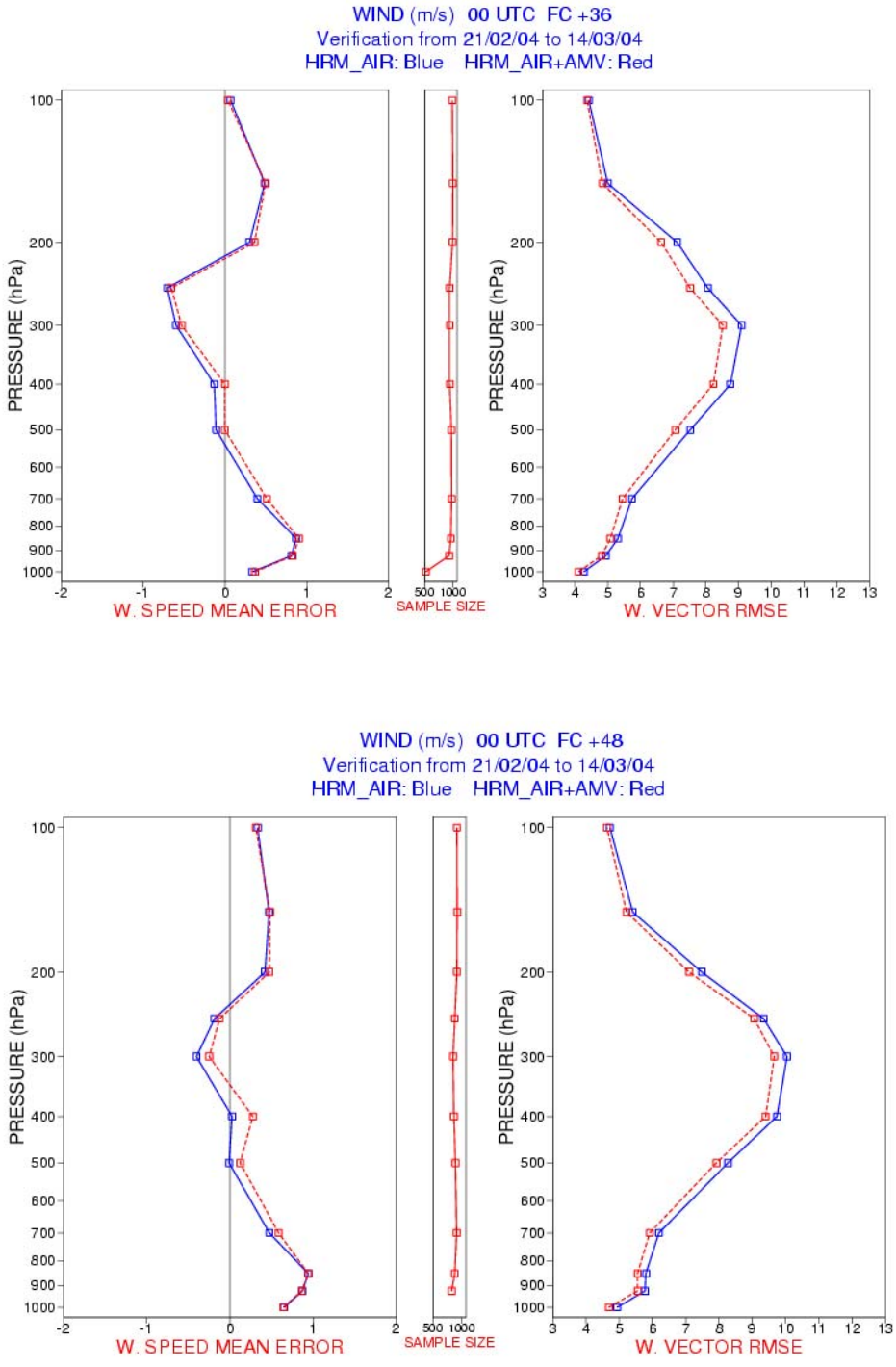

Figure 4.27 Wind speed ME and wind vector RMSE of EUROHRM forecasts from CNMCA 3DVar analysis using aircraft observations with (red) and without (blue) the ingestion of AMV data verified against radiosoundings: T+36h (top) and T+48h (bottom).

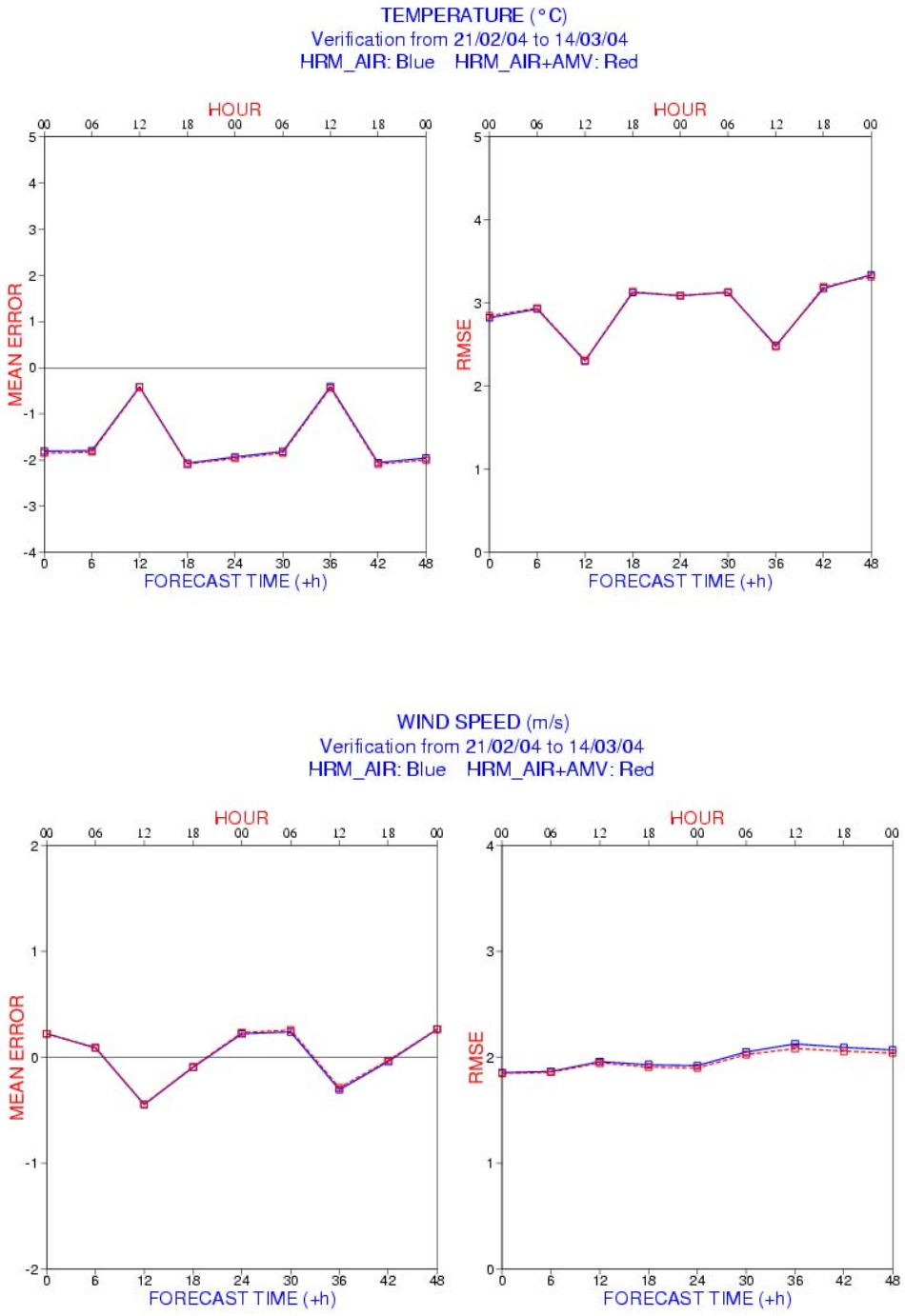

Figure 4.28 ME and RMSE of EUROHRM forecasts from CNMCA 3DVar analysis using aircraft observations with (red) and without (blue) the ingestion of AMV data verified against lowland SYNOP observations: 2m temperature (top) and 10m wind speed (bottom).

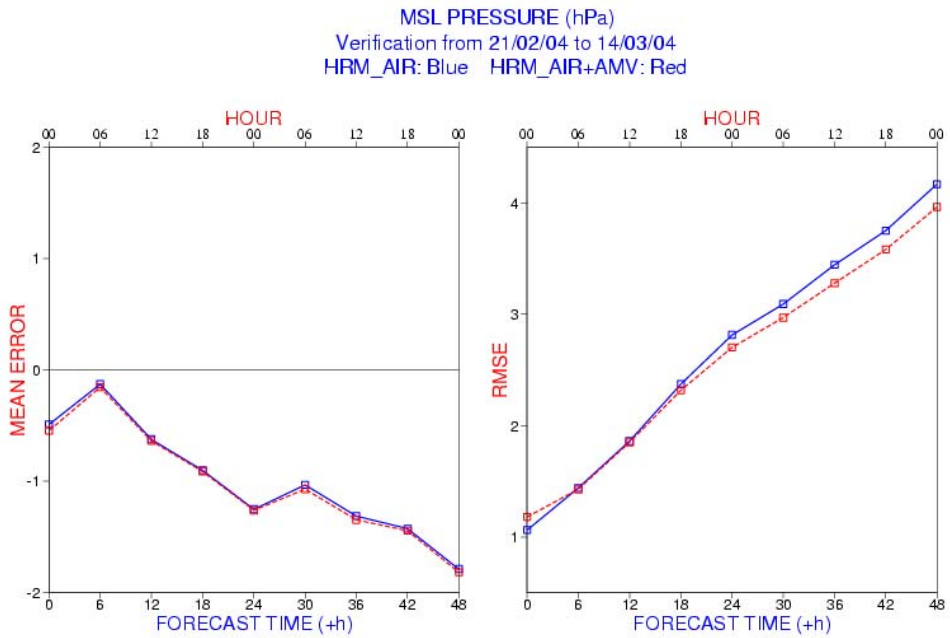

Figure 4.29 Mean sea level pressure ME and RMSE of EUROHRM forecasts from CNMCA 3DVar analysis using aircraft observations with (red) and without (blue) the ingestion of AMV data verified against lowland SYNOPs.

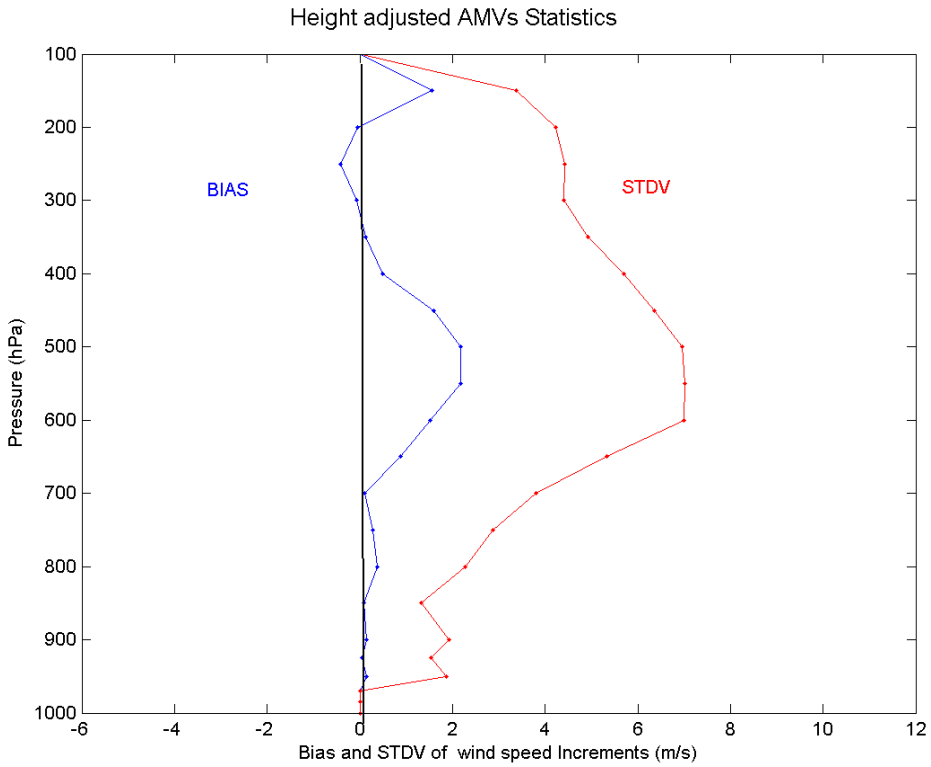

Figure 4.30 Wind speed bias and standard deviation for AMV observation increments using a bias correction scheme.

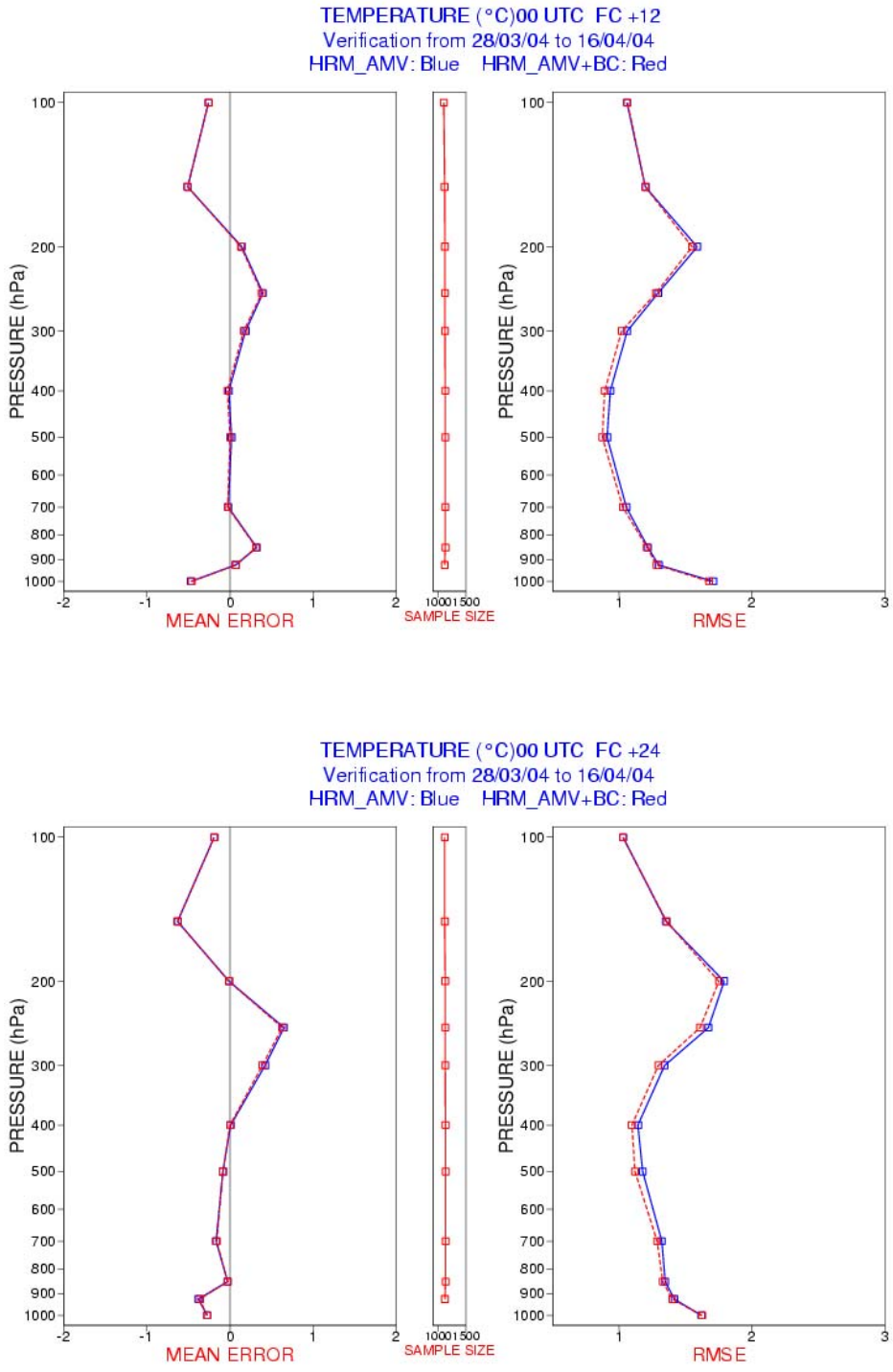

Figure 4.31 Temperature ME and RMSE of EUROHRM forecasts from CNMCA 3DVar analysis without (blue) and with (red) AMV bias correction scheme verified against radiosoundings: T+12h (top) and T+24h (bottom).

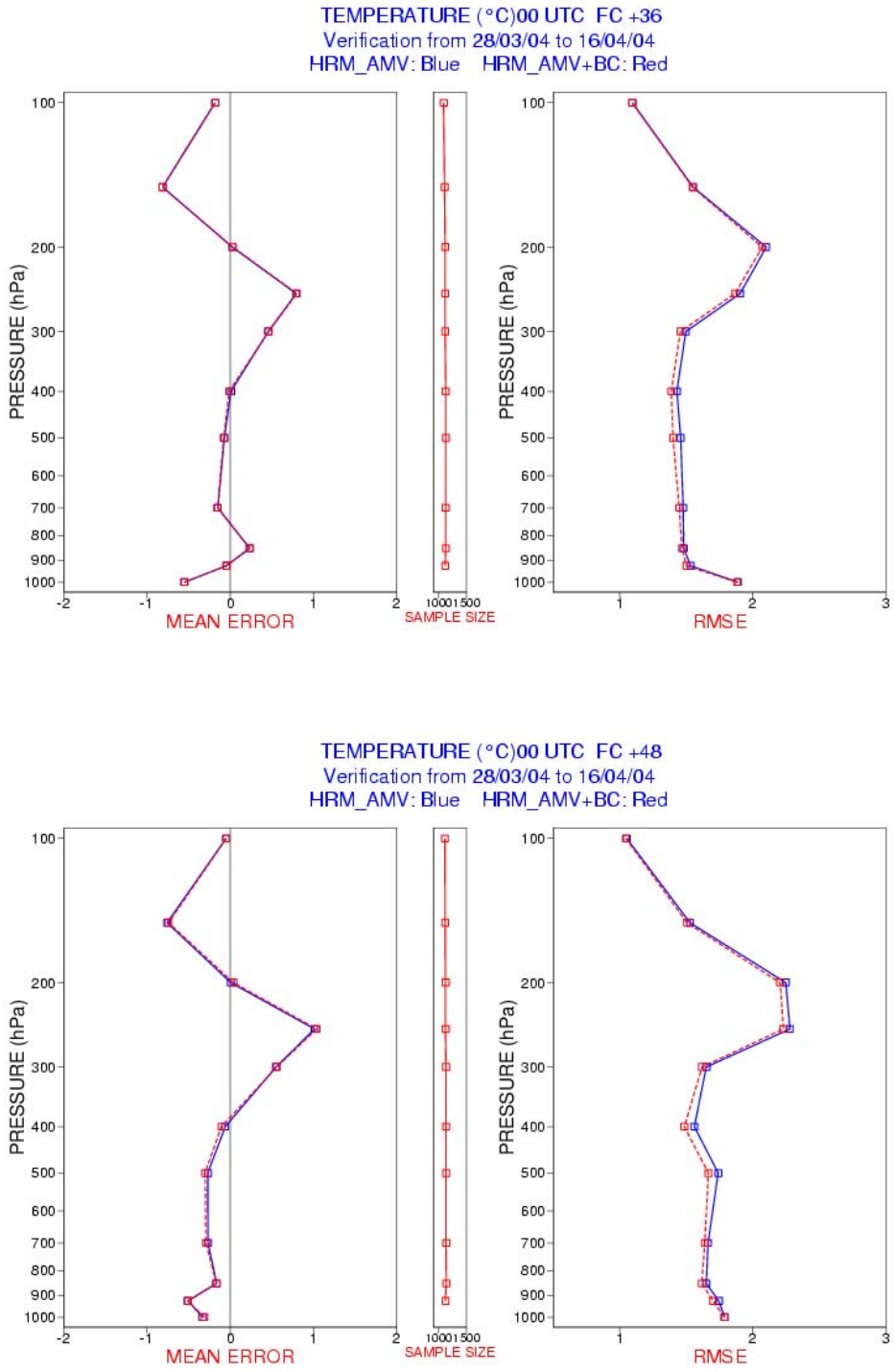

Figure 4.32 Temperature ME and RMSE of EUROHRM forecasts from CNMCA 3DVar analysis without (blue) and with (red) AMV bias correction scheme verified against radiosoundings: T+36h (top) and T+48h (bottom).

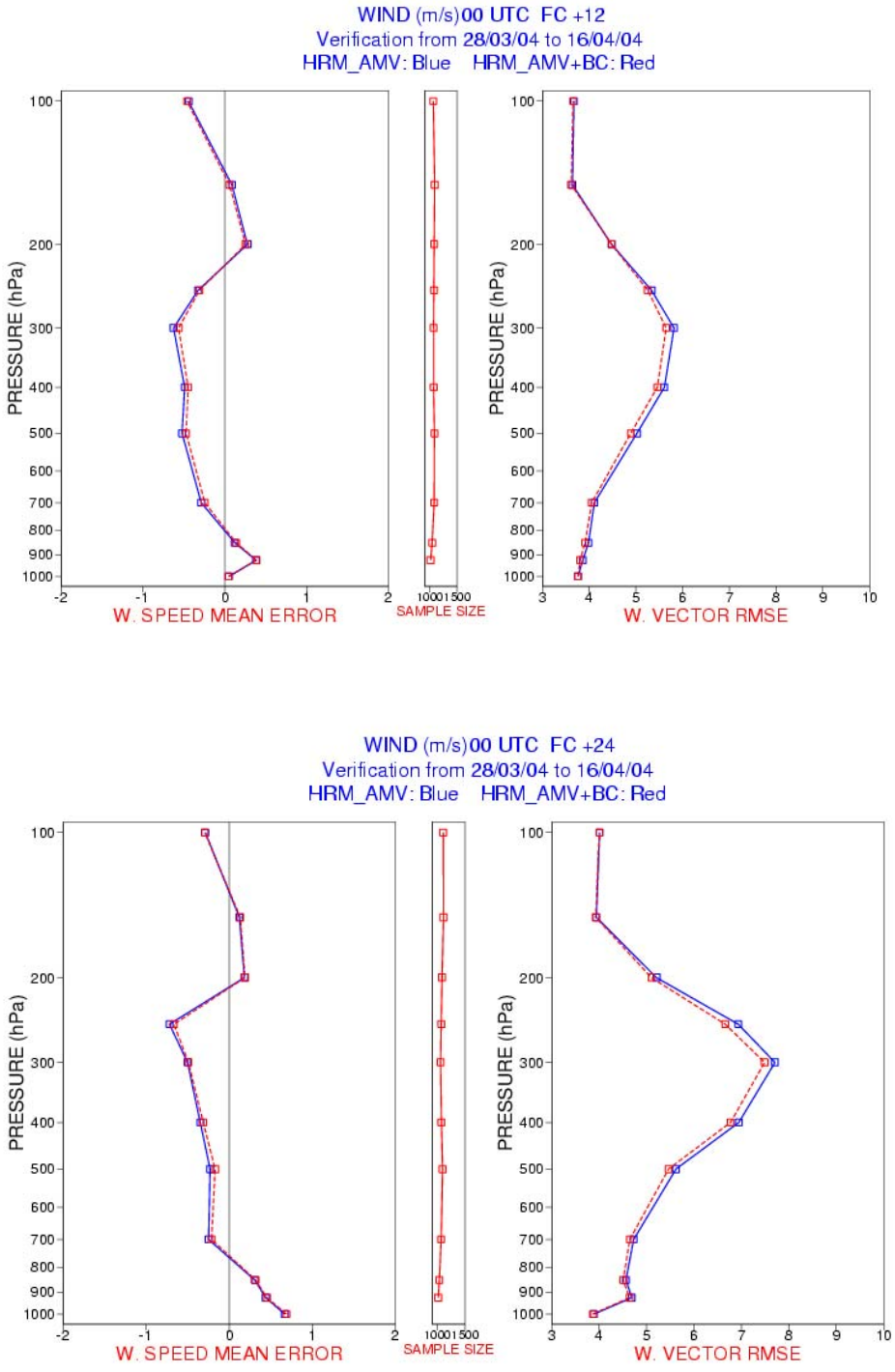

Figure 4.33 Wind speed ME and wind vector RMSE of EUROHRM from CNMCA 3DVar analysis without (blue) and with (red) AMV bias correction scheme verified against radiosoundings: T+36h (top) and T+48h (bottom).

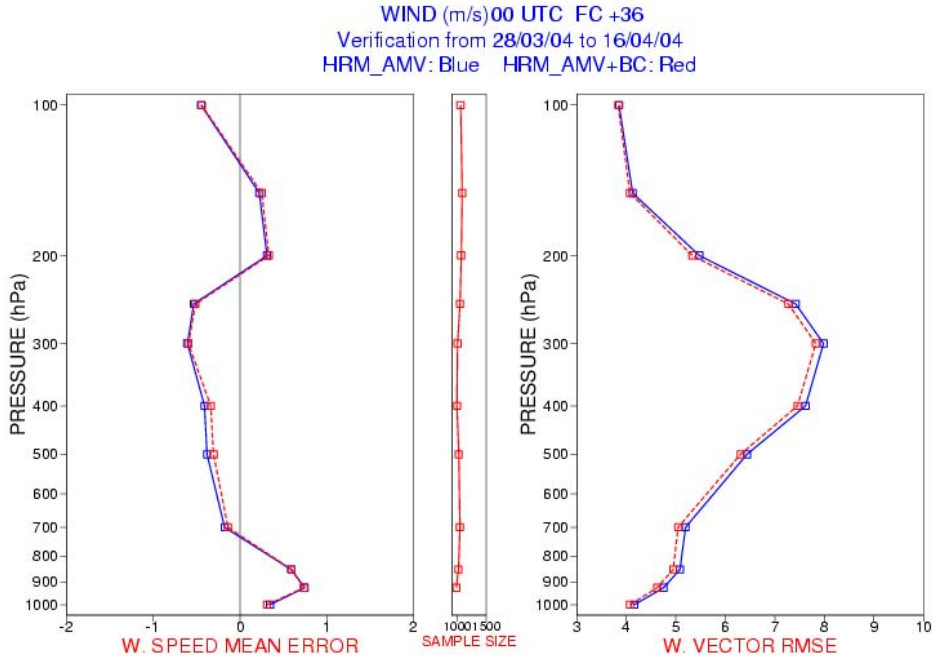

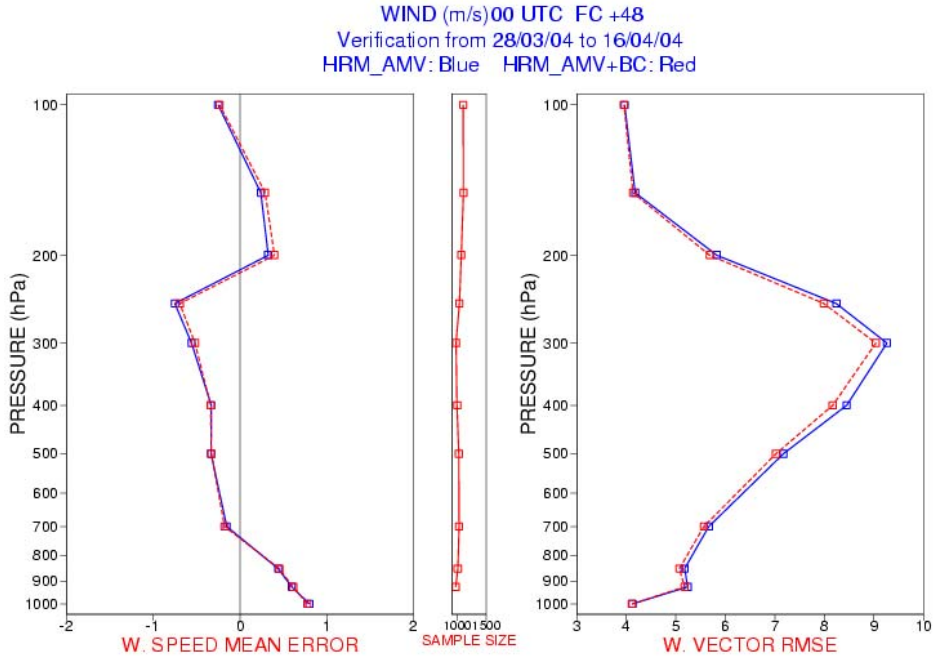

Figure 4.34 Wind speed ME and wind vector RMSE of EUROHRM from CNMCA 3DVar analysis without (blue) and with (red) AMV bias correction scheme verified against radiosoundings: T+36h (top) and T+48h (bottom).

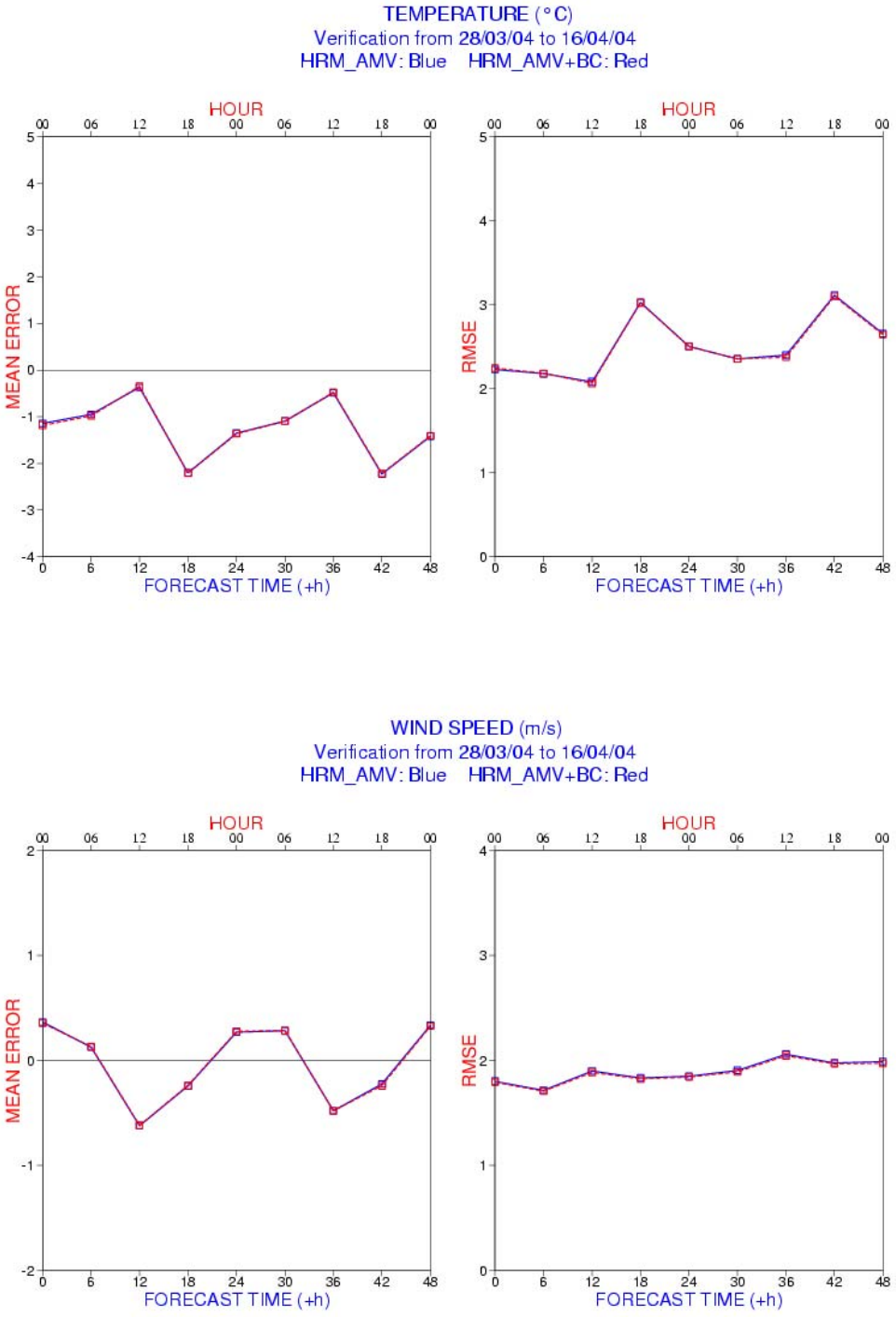

Figure 4.35 ME and RMSE of EUROHRM forecasts from CNMCA 3DVar analysis with (blue) and without (blue) AMV bias correction scheme verified against lowland SYNOP observations: 2m temperature (top) and 10m wind speed (bottom).

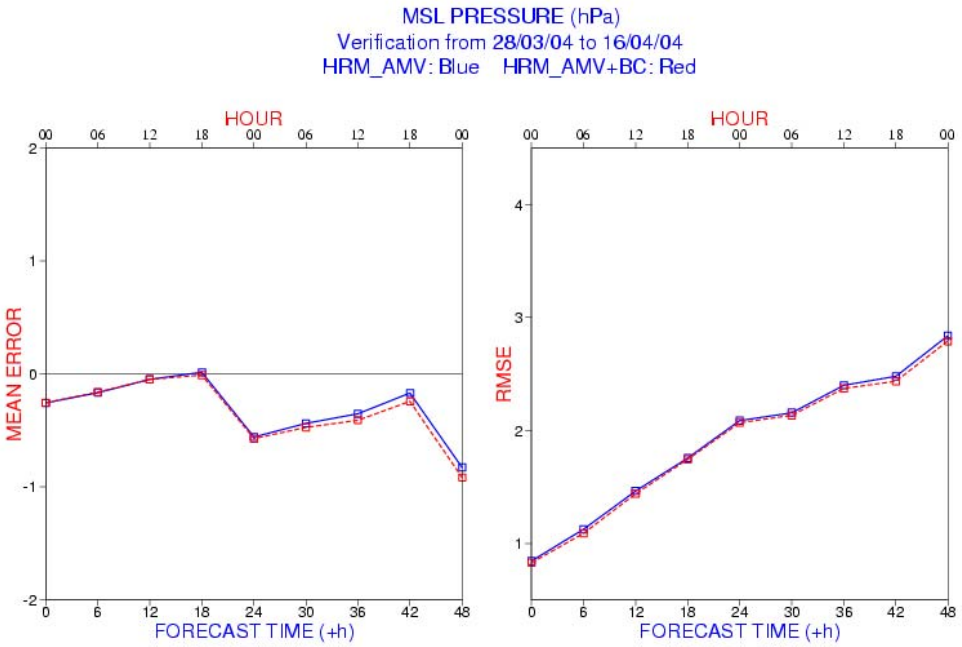

Figure 4.36 Mean sea level pressure ME and RMSE of EUROHRM forecasts from CNMCA 3DVar analysis with (blue) and without (blue) AMV bias correction scheme verified against lowland SYNOP observations.

THIS PAGE INTENTIONALLY LEFT BLANK

V. CONCLUSIONS AND SUGGESTIONS FOR FURTHER DEVELOPMENT

In this work some observing system experiments (OSEs) have been performed in order to gauge the relative impact of some non-conventional observations on CNMCA NWP system. The following data were used: Quikscat surface winds, aircraft based observations and Meteosat AMVs. Moreover, the impact of the increased resolution of the prognostic model has been investigated. Objective verification results have showed a positive impact for each OSE and for the increased resolution experiment. AMV and aircraft data are found to have a significant and largely independent positive impact on forecast skill of comparable magnitude. In addition, a simple bias correction scheme has been implemented to reduce the typical bias in the AMV data. Consequently, the experimental version of the CNMCA NWP system used in this study is ready to become operational.

At this point, the development effort will concentrate mainly on the following areas, which are deemed to be the most urgent requirements for a further improvement of the CNMCA NWP system:

1. The assimilation of MODIS derived winds over the polar region and ATOV retrieved temperature profiles over the Atlantic Ocean. These data are expected to have a significant impact on the forecast quality of the CNMCA NWP system, since they are collocated in data sparse regions. In addition, the assimilation of retrieved temperature profiles from the MIPAS on the ENVISAT satellite is expected to make an improvement in the upper troposphere and in the stratosphere.

2. The use of observations not linearly related to the state variables. This work will be started for SSM/I retrieved surface winds, GPS and SSM/I column precipitable water observations and NOAA and Meteosat satellite radiances. The direct assimilation of satellite radiances is a long term goal whose main value is not expected to be so much in improving the current

analyses over the present analysis domain as in the experience to be gained in view of the future availability of much improved observations from satellite hyperspectral sounders.

3. The implementation of an effective buddy check algorithm for the screening of marginal observations. Approximations to modern methods following Daley and Barker (2000) are being investigated.

LIST OF REFERENCES

Balay, S., Grapp, W.D., McInnes L.C. and B.F. Smith, 2002: "PETSc user manual", Argonne National Laboratory, available at http://www.mcs.anl.gov/petsc - May 2004.

Bergman, K. H., 1979: "Multivariate Analysis of Temperatures and Winds Using Optimum Interpolation", *Mon. Weath. Rev.*, Vol. **107**:1423-1444.

Bonavita, M. and L. Torrisi, 2002: "Il Nuovo Ciclo di Assimilazione Dati del CNMCA: Caratteristiche e Risultati Preliminari**"**, *Rivista di Meteorol. Aeron*. , Vol. **62**, n.2, 4-14**.**

Bonavita, M. and L. Torrisi, 2004: "Impact of a Variational Objective Analysis Scheme on a Regional Area Numerical Model: The Italian Air Force Weather Service Experience", *Meteor. and Atmos. Physics*, to be published.

Bormann, N., Kelly, G. and J.N. Thepaut, 2002: "Characterising and correcting speed biases in atmospherics motion vectors within the ECMWF system", *Proc. of Sixth Int. Winds Workshop*, Madison, Wisconsin, USA, 113-120.

Bormann, N., Saarinen, S., Thepaut, J.N. and G. Kelly, 2002: "The spatial structure of observation errors in atmospheric vectors", *Proc. of Sixth Int. Winds Workshop*, Madison, Wisconsin, USA, 129-136.

Bouttier, F., and G. Kelly, 2001: "Observing system experiments in the ECMWF 4Dvar data assimilation system", *Quart. J. R. Meteor. Soc*., 127, 1469-1488.

Buhler, Y. and K. Holmlund, 1993: "The CMW extraction algorithm for MTP/MPEF", *Proc. Second Int. Winds Workshop*, Tokio, Japan, 205-217.

Burridge, D. M., 1975: "A split semi-implicit reformulation of the Bushby-Timpson 10-Level model". *Quart. J. Roy. Meteor. Soc.*, 101, 430, 777-792.

Cohn, S. E., Da Silva, A., Guo, J., Sienkiewicz, M. and D. Lamich, 1998: "Assessing the Effects of Data Selection with the DAO Physical-Space Statistical Analysis System". *Mon. Wea. Rev*., Vol. 126, 2913-26.

Daley, R., 1991: "Atmospheric Data Analysis". Cambridge University Press, 458 pp.

Daley, R. and Barker, E., 2000: "NAVDAS Source Book 2000". NRL Publication, NRL/PU/7530-00-418. Naval Research Laboratory, Marine Meteorology Division, Monterey, California, USA.

Davies, H. C., 1976: "A lateral boundary formulation for multi-level prediction models". *Quart. J. Roy. Meteor. Soc.*, 102, 432, 405-418.

Doms, G. and Schättler, U., 2003: "The nonhydrostatic limited-area model LM of DWD. Part1: Scientific documentation". Deutscher Wetterdienst, Offenbach, Germany.

Dumelow, R., 2003: "Overview of observing system experiments". *ECMWF Seminar Proceedings on recent developments in data assimilation for atmosphere and ocean*, Reading, UK, 97pp.

Eyre, J. R., 2000: "Planet earth seen from space: basic concepts". *ECMWF Seminar Proceedings on exploitation of the new generation of satellite instruments for NWP*, Reading, UK, 5pp.

Gaspari, G. and S. Cohn, 1999: "Construction of Correlation Functions in Two and Three Dimensions". *Quart. J. Roy. Meteor. Soc.,* 125, 723-57.

Golub, G. and H. van Loan, 1996: "Matrix Computations, third edition". The John Hopkins University Press, 694 pp.

Haltiner, G. and Williams, R.T., 1980: "Numerical Prediction and Dynamic Meteorology". J. Wiley & Sons, 477pp.

Hasler, A. F., W. C. Skillman and W. E. Shenk, 1979: "In situ aircraft verification of the quality of satellite cloud winds over oceanic regions". *J. Appl. Meteor*., 18, 1481-1489.

Hoffman, J., 1990: "The use of spatial coherence method for cloud motion wind retrieval". *Proc. 8th Meteosat Scientific users meeting*, Norroping, Sweden, EUMETSAT EUM P05, 97-100.

Hollingsworth, A., and P. Lonnberg, 1986: "The Statistical Structure of Short-range Forecast Errors as Determined from Radiosonde Data. Part I: The Wind Field." *Tellus*, **38A**, 111-136.

Holmlund, K., 1998: "The utilization of statistical properties of satellite-derived atmospheric motion vectors to derive quality indicators", *Wea. Forecasting*, 13, 1093-1104.

Holmlund, K., 2002: "Current status of the Eumetsat operational and future AMV extraction facilities*", Proc. of Sixth Int. Winds Workshop*, Madison, Wisconsin, USA, 45-52.

Jacobson, I. and E. Heise, 1982: "A new economic method for the computation of the surface temperature in numerical models". *Beitr. Phys. Atm*., 55, 128-141.

Jarvinen, H., and P. Unden, 1997: "Observation screening and background quality control in the ECMWF 3DVar data assimilation system". *ECMWF Technical*

Memorandum 236, Reading, UK.

JPL, 2001: "Quikscat science data product user's manual", version 2.2. Jet Propulsion Laboratory D-12985, pp. 89.

Leidner, M., Hoffman, R. and J. Augenbaum, 2000: "SeaWinds scatterometer real time BUFR geophysical data product", version 2.2.0. NOAA/NESDIS.

Lorenc, A., 1981: "A global three-dimensional multivariate statistical interpolation scheme". *Mon. Wea. Rev*., Vol. **109**: 701-21.

Lorenc, A., 1986: "Analysis Methods for Numerical Weather Prediction". *Quart. J. Roy. Meteor. Soc*., 112, 1177-94.

Lorenc, A., 1988: "Optimal Nonlinear Objective Analysis". *Quart. J. Roy. Meteor. Soc.,* 114, 205-240.

Louis, J. F., 1979: "A Parametric Model of Vertical Eddy Fluxes in the Atmosphere". *Bound.-Layer Meteor.,* Vol. 17, 187-202

Majewski, D., 2003: "HRM User's Guide", available from the author (detlev.majewski@dwd.de)

Mellor, G.L. and T. Yamada, 1974: "A Hierarchy of Turbulence Closure Models for Planetary Boundary Layers", *J. Atmos. Sci*., Vol. 31, 1791-1806.

Nieman, S. J., J. Schmetz and W. P. Menzel, 1993: "A comparison of several techniques to assign heights to cloud tracers". *J. Appl. Meteor*., 32, 1559-1568.

Norris, B., 1990: "Pre-processing - General Data Checking and Validation". *ECMWF Meteorological Bulletin*, M1.4/3.

Nuret, M., and J. Schmetz,, 1988: "Production of cloud motion winds Meteosat Imagery". *Proc. Seventh Meteosat Scientific Users' Meeting*, Madrid, EUMETSAT, EUM P04, 19-22.

Portabella, M., 2002: "Wind field retrieval from satellite radar systems". Doctoral Thesis in Physics. University of Barcelona.

Portabella, M. and A. Stoffelen, 2004: "A probabilistic approach for SeaWinds data assimilation". *Quart. J. Roy. Meteor. Soc.,* 130, 127-152.

Ritter, B., and J.-F. Geleyn, 1992: "A Comprehensive Radiation Scheme for Numerical Weather Prediction Models with Potential Applications in Climate Simulations". *Mon. Wea. Rev.*, Vol. 120, 303-325.

Rohn, M., Kelly G. and R. Saunders, 1998: "Experiments with AMVs at ECMWF", Proc. of Fourth Int. Winds Workshop, Saanenmöser, Switzerland, 139-146.

Rutherford, I. D., 1972: "Data Assimilation by Statistical Interpolation of Forecast Errors". *J.Atmos. Sci.*, Vol. 29, 809.

Schmetz, J., Holmlund, K., Hoffman, J., Strauss, B., Mason, B., Gartner, V., Koch, A. and L. Van de Berg, 1993: "Operational cloud-motion winds from Meteosat infrared images", *J. Appl. Meteor.*, 32, 1206-1225.

Simmons, A. J. and D. M. Burridge, 1981: "An energy and angular-momentum conserving vertical finite-difference scheme and hybrid vertical coordinates". *Mon. Wea. Rev*., 109, 758-766.

Simmons, A., 2000: "Assimilation of satellite data for NWP: Basic importance, concepts and issues". *ECMWF Seminar Proceedings on exploitation of the new generation of satellite instruments for NWP*, 21pp.

Spencer, M. W., Wu, C. and D. G. Long, 1997: "Tradeoffs in the design of a spaceborn scanning pencil beam scatterometer: application to SeaWinds". *IEEE Trans. Geosci. Rem. Sens.*, 35, 1, 115-126.

Stoffelen, A., Voorips A. and J. de Vries, 2000: "Towards the real time use of Quikscat winds", Final Report Beleidscomissie Remote Sensing, The Netherland (available at http://www.knmi.nl/scatterometer/seawinds - May 2004).

Stickland, J., 2001: "Aircraft data for NWP". *Proc. of 8th ECMWF Workshop on Meteological Operational Systems*, Reading, UK.

Temperton, C. and M. Roch, 1991: "Implicit Normal Mode Initialization for an Operational Regional Model". *Mon. Wea. Rev*, Vol. 109, 758-766.

Thepaut, J. N., 2003: "Satellite data assimilation in NWP: an overview". *ECMWF Seminar Proceedings on recent developments in data assimilation for atmosphere and ocean*, 75pp.

Thiebaux, H.J., Mitchell, H.L. and D.W. Shantz, 1986: "Horizontal Structure of Hemispheric Forecast Error Correlations for Geopotential and Temperature". *Mon. Wea. Rev*, Vol. 114, 1048-1066.

Thiebaux, H.J., Morone, L.L. and R.L. Wobus, 1990: "Global Forecast Error Correlation. Part 1: Isobaric Wind and Geopotential". *Mon. Wea. Rev.*, Vol. 118, 2117-2137.

Tiedtke, M., 1989: "A Comprehensive Mass Flux Scheme for Cumulus Parameterization

in Large-Scale Models". *Mon. Wea. Rev*., Vol. 117, 1779-1800.

Tillman, G., 1999: "Correlations Functions for Atmospheric Data Analysis". *Q. J. R. Meteorol. Soc*., Vol. 125, 2449-2464.

Vocino, A., 2002: "The diagnostic Component of the CNMCA Numerical Prediction System: Characteristics, Performance and Future Developments of the New Data Assimilation System" Thesis, 32nd Meteorology and Atmospheric Physics Course, CNMCA, Pratica di Mare, Italy, 90pp. (In Italian, available fro the author, vocino@meteoam.it)

Wentz, F. J. and D. K. Smith, 1999: "A model function for ocean normalized radar cross section at 14 GHz derived from NSCAT observations", *J. Geophys. Res*., 104 (C5), 11499-11514.

Wilkes, D.S., 1995: "Statistical methods in the atmospheric sciences: An introduction." Academic Press, 467 pp.

WMO, 1996: "Guide to meteorological instruments and methods of observation". WMO-no.8, Geneva, Switzerland.

WMO, 2003: "AMDAR Reference Manual". WMO-no.958, Geneva, Switzerland.

THIS PAGE INTENTIONALLY LEFT BLANK

INITIAL DISTRIBUTION LIST

1. Defense Technical Information Center
   Ft. Belvoir, Virginia

2. Dudley Knox Library
   Naval Postgraduate School
   Monterey, California

3. Prof. Roger T. Williams
   Naval Postgraduate School
   Monterey, California

4. Prof. Carlyle H. Wash
   Naval Postgraduate School
   Monterey, California

5. Gen. Roberto Sorani
   Ufficio Generale per la Meteorologia
   Aeroporto Centocelle, Rome, Italy

6. Col. Massimo Capaldo
   CNMCA
   Aeroporto De Bernardi, Pratica di Mare, Pomezia (RM), Italy

7. Col. Giuseppe Tarantino
   CNMCA
   Aeroporto De Bernardi, Pratica di Mare, Pomezia (RM), Italy

8. Ten.Col. Massimo Ferri
   Ufficio Generale per la Meteorologia
   Aeroporto Centocelle, Rome, Italy

9. Ten.Col. Casimiro Ciotti
   CNMCA
   Aeroporto De Bernardi, Pratica di Mare, Pomezia (RM), Italy

10. Ms Annamaria Munno
    Office of Defense Cooperation, US Embassy in Italy
    Rome, Italy

11. Cap. Lucio Torrisi
    CNMCA
    Aeroporto De Bernardi, Pratica di Mare, Pomezia (RM), Italy